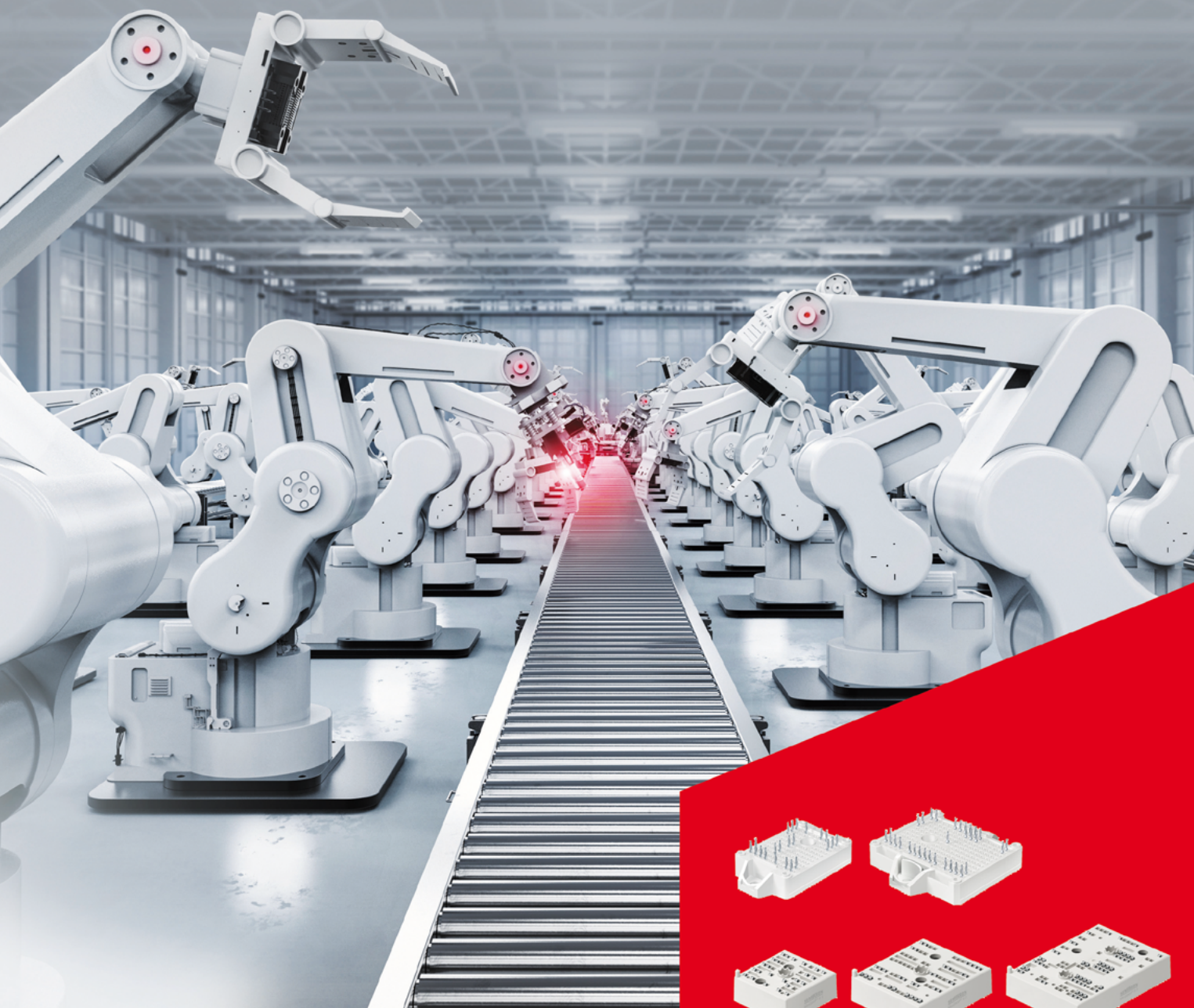


Bodo's Power Systems®

Electronics in Motion and Conversion

May 2023

Partnering for the Safe Supply of Industrial Power Modules





POWER CHOKE TESTER DPG10/20 SERIES

Inductance measurement from 0.1 A to 10 kA

KEY FEATURES

Measurement of the

- Incremental inductance $L_{inc}(i)$ and $L_{inc}(\int U dt)$
- Secant inductance $L_{sec}(i)$ and $L_{sec}(\int U dt)$
- Flux linkage $\psi(i)$
- Magnetic co-energy $W_{co}(i)$
- Flux density $B(i)$
- DC resistance

Also suitable for 3-phase inductors

APPLICATIONS

Suitable for all inductive components from small SMD inductors to very large power reactors in the MVA range

- Development, research and quality inspection
- Routine tests of small batch series and mass production

KEY BENEFITS

- Very easy and fast measurement
- Lightweight, small and affordable price-point despite of the high measuring current up to 10000A
- High sample rate and very wide pulse width range => suitable for all core materials

AVAILABLE MODELS

Model	max. test current	max. pulse energy
DPG10-100B	0.1 to 100A	1350J
DPG10-1000B	1 to 1000A	1350J
DPG10-2000B	2 to 2000A	1350J <i>new model</i>
DPG10-2000B/E	2 to 2000A	2750J <i>new model</i>
DPG10-3000B/E	3 to 3000A	2750J
DPG10-4000B/F	4 to 4000A	8000J
DPG20-10000B/G	10 to 10000A	15000J

5PT Series



Smaller Than
a Paperclip!

Specifically designed to meet

High Current Carrying Requirements Of Resonant Power Circuits

- ✓ Cost Effective
- ✓ Minimum inductance, lower impedance and ESR
- ✓ Direct plug-in spade lugs

Contact ECI Today! sales@ecicaps.com | sales@ecicaps.ie

www.ecicaps.com

Content

Viewpoint 4	Measurement 52 - 54
Again Back in Nuremberg!	Minimize Current Consumption While achieving high accuracy with Current Sensors <i>By WangSam Jang, President, J&D Electronics</i>
Events 4	Power Modules 56 - 58
News 6 - 12	Package for the Highest Voltage Classes Si IGBTs and SiC MOSFETs <i>By Virgiliu Botan, Roman Ehrbar, Antoni Ruiz, Andreas Baschnagel, and Lluis Santolaria, Hitachi Energy Semiconductors, Lenzburg, Switzerland</i>
Product of the Month 14 - 15	Power Management 60 - 63
Reliable Temperature Measurement of Converters	Helping Power Solutions Keep Up with Moore's Law <i>By Steve Roberts, Innovation Manager, RECOM Power</i>
Guest Editorial 16 - 17	Wide Bandgap 64 - 67
embedded world 2023: Busy Halls and Happy Smiles <i>By Roland R. Ackermann, Correspondent Editor, Bodo's Power Systems</i>	Power ICs Enable High-Efficiency and High-Power-Density 140 W, PD3.1 Adapter Designs <i>By Tom Ribarich, Sr. Director Strategic Marketing, and Xiucheng Huang, Sr. Applications Engineering Director, Navitas Semiconductor</i>
Blue Product of the Month 18	MOSFETs 68 - 71
Win a CryptoAuth Trust Platform Development Kit	Contribution to the Turn-On Losses Won of a 600V MOSFET Caused by the FWD's Storage Charge Qrr <i>By J. Ranneberg, Professor, HTW Berlin</i>
Guest Editorial 20 - 21	eMobility 72 - 73
10 th ECPE SiC & GaN User Forum: Potential of Wide Bandgap Semiconductors in Power Electronic Applications <i>By Andreas Lindemann, Otto-von-Guericke-University at Magdeburg, Chair for Power Electronics</i>	How to Design an Intelligent Battery Junction Box for Advanced EV Battery Management Systems <i>By Issac Hsu, Product Marketing Engineer, Brushless DC Motor Drivers, Texas Instruments</i>
Cover Story 22 - 27	Battery 74 - 75
Partnering for the Safe Supply of Industrial Power Modules <i>By Paul Drexhage, Technical Marketing Manager, Semikron Danfoss</i>	Ionic Mineral Technologies: Unearthing the Nano-Silicon Solution <i>By Andre Zeitoun, CEO and Founder, and Dr Jake Entwistle, Director of Battery Materials, Ionic MT</i>
Wide Bandgap 28 - 30	Power Quality 76 - 82
Test-to-Fail Methodology for Accurate Reliability and Lifetime Evaluation of eGaN Devices in Solar Applications <i>By Shengke Zhang, Ricardo Garcia, and Siddhesh Gajare, Efficient Power Conversion (EPC)</i>	Power Quality Monitoring Part 2: Design Considerations for a Standards Compliant Power Quality Meter <i>By Jose Mendia, Senior Engineer, Product Applications, Analog Devices</i>
Motion Control 32 - 34	Power Modules 84
Get More Out of Your Heat Pump <i>By Michele Portico, Senior Product Marketing Manager, Vincotech</i>	Mission Critical Power Electronics <i>By Ron Yurko, Chief Operating Officer, Powerex</i>
DC/DC Converter 36 - 38	New Products 86 - 88
DC/DC Converters For Industrial Applications <i>By Mitch Van Ochten, Application Engineer, Rohm Semiconductor</i>	
Design and Simulation 40 - 42	
Advanced Inductor Circuit Models <i>By Dr. Ray Ridley and Art Nace, Ridley Engineering</i>	
Wide Bandgap 48 - 50	
Extending Output Power of Unified, AC-Input Light Industrial Applications Through Low RDS(ON) SiC MOSFETs <i>By Simon Kim and Kwok Wai Ma, Infineon Technologies</i>	

Supporters & Friends



P
O

WÜRTH ELEKTRONIK MORE THAN YOU EXPECT

REDEXPERT

The world's most accurate AC loss Model



© ei50s



WE meet @ PCIM

Hall 6-217

REDEXPERT.

Würth Elektronik's online platform for simple component selection and performance simulation:

www.we-online.com/redexpert

New Thermal Analysis

- The world's most accurate AC loss model
- Filter settings for over 20 electrical and mechanical parameters
- Inductor simulation and selection for DC/DC converters
- Online platform based on measured values
- Ability to compare inductance/current and temperature rise/DC current using interactive measurement curves
- No login required
- Order free samples directly
- Direct access to product datasheets
- Available in seven languages

A Media

Katzbek 17a
24235 Laboe, Germany
Phone: +49 4343 42 17 90
Fax: +49 4343 42 17 89
info@bodospower.com
www.bodospower.com

Publisher

Bodo Arlt, Dipl.-Ing.
editor@bodospower.com

Editor

Holger Moscheik
Phone + 49 4343 428 5017
holger@bodospower.com

Correspondent Editor Bavaria

Roland R. Ackermann
roland@bodospower.com

Editor China

Min Xu
Phone: +86 156 18860853
xumin@i2imedia.net

US Support

Rusty Dodge
Phone +1 360 920 7825
rusty@eetech.com

Creative Direction & Production

Bianka Gehlert
b.gehlert@t-online.de

Free Subscription to qualified readers
Bodo's Power Systems is available for
the following subscription charges:
Annual charge (12 issues) is
150 € world wide · Single issue is 18 €
subscription@bodospower.com

**Printing by:**

Westdeutsche Verlags- und Druckerei
GmbH; 64546 Mörfelden-Walldorf
Germany

A Media and Bodos Power Systems

assume and hereby disclaim any
liability to any person for any loss or
damage by errors or omissions in the
material contained herein regardless
of whether such errors result from
negligence accident or any other
cause whatsoever.

Again Back in Nuremberg!

Dear Friends

It is about 30 years since we first met at PCIM in Nuremberg. Our podium discussions have become a tradition - like having a good meal with asparagus. The asparagus is still a good choice and there is no limitation on how many pieces you can eat. Unfortunately, the presenters' seats on my podiums are limited to six people only, by the Mesago administration. This creates a problem, as I am unable to include all my industry friends. As I turn 70 this year, I am still having fun running my own activities. I was told by Mesago, just before I became 67, that I was no longer good for the conference advisory board, after a quarter of a century supporting PCIM. So, I turned my full strength to my own magazine's activities, the quarterly "Tech Talk" and my annual Wide Bandgap Conference, which started back in December 2017. By doing so, all my Industry partners get a solid platform to present their wide bandgap developments in a proper way. Nevertheless, I am looking forward to seeing you all at my podium discussions at PCIM:

May 10th Wednesday 13:05 we start with GaN and 14:10 with SiC - Hall 7 Booth 480.

Also, Our booth will be in Hall 6 Booth 270, where my team will be there to support the industry and my readers. Stop by for a chat, we will be happy to see you.

SiC and GaN will be the future of power semiconductors. Currently we have GaN serving up to line voltage applications while SiC is the choice for higher voltages. Bringing Vertical GaN in the arena may be a game changer but, at the moment, there is a limited number of companies working on this. There could be more activity happening behind closed doors that people are not ready to share.



We will definitely find out more over time and will share any news with you.

Bodo's magazine is delivered by postal service to all places in the world. It is the only magazine that spreads technical information on power electronics globally. We have EETech as a partner serving our clients in North America. If you speak the language, or just want to have a look, don't miss our Chinese version at www.bodospowerchina.com. An archive of my magazine with every single issue is available for free at my website www.bodospower.com.

My Green Power Tip for the Month:

Charge your electric car from your photovoltaic panels during daylight. That is the best way for us to be independent from the power grid.

Looking forward to seeing you all in Nuremberg.

Kindest regards,

Events

PCIM Europe 2023

Nuremberg, Germany May 9 – 11
www.pcim-exhibition.com

Sensor + Test 2023

Nuremberg, Germany May 9 – 11
www.sensor-test.de

SMTconnect 2023

Nuremberg, Germany May 9 – 11
www.smtconnect.com

ICPE 2023 – ECCE Asia

Jeju, Korea May 22 – 25
<https://icpe-conf.org>

CWIEME Berlin 2023

Berlin, Germany May 23 – 25
<https://berlin.cwiemeevents.com>

SEMICON Southeast Asia 2023

Penang, Malaysia May 23 – 25
www.semiconsea.org

The Battery Show Europe 2023

Stuttgart, Germany May 23 – 25
www.thebatteryshow.eu

IEEE ISPSD 2023

Hong Kong May 28 – June 1
<https://ispsd2023.com>

WPTCE 2023

San Diego, CA, USA June 4 – 8
<https://ieee-wptce.org>



A breath of fresh air in power electronics

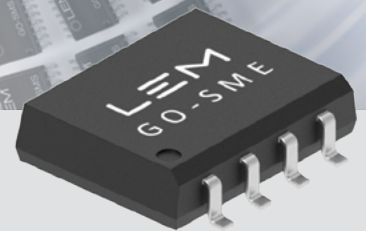
GO series

Cost-effective and accurate, miniature isolated current sensor GO speeds your drives applications.

A unique sensor with an integrated primary conductor achieves optimum temperature accuracy, measuring from -40 to +125 °C in a surface mounted SO8 or SO16 package.

www.lem.com

- 10-30 A nominal current
- Better than 1.3 % accuracy @ +25°C
- Differential Hall principle measurement: very robust against external fields
- 2 µs response time
- Up to 3 kV RMS isolation
- Double Over-Current Detection outputs for short circuit and over-load protection (SO16 version)



LEM

Life Energy Motion

Celebrating 75,000,000 GaN Power Shipments

Navitas Semiconductor announced a milestone of over 75 million high-voltage GaN units shipped. GaN is a next-generation technology that is a significant upgrade over conventional high-voltage legacy silicon power semiconductors, that reduces the energy and physical space needed to deliver that performance. It runs up to 20x faster and can also enable up to three times more power handling or three times faster charging capability, in half the size and weight.

Navitas was founded in 2014, and pioneered a revolution in power electronics, beginning with the mass production release of GaN-Fast™ power ICs in 2018. GaNFast ICs monolithically-integrate GaN power and GaN drive, plus control and protection. Next, GaN-Sense™ power ICs added autonomous sensing and fast control, with single and half-bridge portfolios. Now, GaN-Sense Control ICs combine high-voltage GaN power ICs with high-speed, low-voltage silicon system controllers for even higher integration, ease-of-use and system performance. Navitas is addressing a 2 billion unit per year mobile fast, and now ultra-fast charging market opportunity, with over 240 end-customer chargers reaching production. All of the top 10 mobile OEMs are in production or development with



Navitas, including Dell, Samsung, Lenovo, LG, Xiaomi, Asus and OPPO, plus a broad range of aftermarket companies such as Anker, Belkin, Baseus and many more. As smartphone power demand has increased – driven by larger screens, bigger batteries, and 5G functionality – users have insisted on faster charging and ultra-portability.

www.navitassemi.com

Silicon Chip for Patented AC Direct DC Power Delivery Technology

Amber Semiconductor announced that it completed the first silicon tapeout and entered the manufacturing and integration phase for one of its three core patented technologies – the AC Direct DC Enabler™, a silicon solution that extracts DC directly from AC Mains without the use of transformers, rectifier bridges, or filtering. This



technology represents a massive global opportunity to revolutionize the way power is delivered to every electrical endpoint on earth.

AmberSemi's AC Direct DC Enabler silicon chip enables dynamic delivery of DC power on demand, and it requires only half the components of today's standard, comparable systems. The impact of coupling dynamic power capabilities with its much smaller system size is transformative, enabling significantly more capabilities and features to be added into electrical endpoints without altering the standard footprints of products. AmberSemi's AC Direct DC Enabler is ideally suited for integration into a broad range of electrical products, including smoke detectors, doorbell cameras, thermostats, smart products, appliances, intelligent HVACR, and more; virtually any electronic device that uses DC and is powered by the AC mains will benefit from this breakthrough technology. In addition, this technology can be paired with key semiconductor devices like microcontrollers and wireless radios for unique AC Direct semiconductor systems, that enable both housekeeping power plus outside sensor power provisioning from the single AC Direct system.

www.ambersi.com

Bare Die SiC Chosen for Line of Power Modules

ROHM Semiconductor announced that precision power analog company Apex Microtechnology is adopting ROHM's silicon carbide (SiC) MOSFETs and SiC Schottky Barrier Diode (SBD) for a line of power modules. This product family currently includes the three-phase SA310 module, ideal for driving high-voltage BLDC (brushless DC) motors, as well as two half-bridge devices, SA110 and SA111, ideal for a wide range of high-voltage applications.

ROHM's 1200V S4101 SiC MOSFETs and 650V S6203 SiC SBD are supplied in bare die form, enabling Apex to save space and increase the performance and reliability of

its modules. In addition to the SiC devices, Apex's new line of power modules use



ROHM's tightly-matched BM60212FV-C gate drivers in bare die format, contributing to high-efficiency operation of high-voltage motors and power supplies. By using these parts in bare die form, Apex has been able to increase the levels of integration offered by these power modules. According to a study commissioned by the company, such modules are usually 67% smaller than discrete solutions developed by customers. Apex is often able to include not only MOSFETs, gate drivers and SBDs, but also bootstrap supply and bypass capacitors with compact surface mount form factors.

www.rohm.com

pcim
EUROPE

VISIT US:
HALL 9
BOOTH 310

ROHM
SEMICONDUCTOR



POWER THE FUTURE ROHM'S GEN 4 SiC POWER DEVICES

As a technology leader ROHM is contributing to the realization of a sustainable society by focusing on the development of low carbon technologies for automotive and industrial applications through power solutions centered on SiC Technology. With an in-house vertically integrated manufacturing system, ROHM provides high quality products and stable supply to the market. Take the next development step with our Generation 4 SiC power device solutions.

Industry-leading low ON resistance

Reduced ON resistance by 40% compared to previous generation without sacrificing short-circuit ruggedness.

Minimizes switching loss

50% lower switching loss over previous generation by significantly reducing the gate-drain capacitance.

Supports 15V Gate-Source voltage

A more flexible gate voltage range 15 -18V, enabling to design a gate drive circuit that can also be used for IGBTs.

www.rohm.com

MJC
ELEKTROTECHNIK

Components for Power Electronics

Visit us at the PCIM:
Hall 7 · Booth 127

MJC Elektrotechnik GmbH
www.mjc-elektrotechnik.de

Report on GaN Reliability

EPC announces the publication of its "Phase-15 Reliability Report", documenting continued work using test-to-fail methodology and adding specific reliability metrics and predictions for real world applications including solar optimizers, lidar sensors, and DC-DC converters.



This report presents the results of testing eGaN devices to the point of failure, which provides the information to identify intrinsic failure mechanisms of the devices. By identifying these intrinsic failure mechanisms, physics-based models that accurately project the safe operating life of a product over a more general set of operating conditions are developed. This is applied to information from real-world experience to determine mission robustness for specific applications.

This report is divided into eight sections, each dealing with a different failure mechanism or application case. According to Dr. Alex Lidow, CEO and co-founder of EPC, "The release of EPC's Phase-15 reliability report examines information from real-world experience that either confirms the laboratory-derived data or opens new questions about mission robustness that leads to a deeper understanding of the behavior of GaN devices over a wide range of stress conditions."

www.epc-co.com

Combined Technology Designed to Replace Analog Controls in GaN Power Supplies

Wise-integration and Powernet announced an agreement to build compact and energy-efficient technology for power-supply applications that are currently limited to analog control. The memorandum of understanding addresses the needs of OEMs that require compact, digitally controlled power-supply systems for faster, smaller and more energy-efficient electronic equipment in products ranging from USB PD fast chargers to monitors, TV sets and electric vehicles. The system will combine Wise-integration's WiseWare® digital controller and Wisegan®, a 650V enhancement-mode GaN-on-silicon IC for power applications from 30W to 3kW, with Powernet's switched mode power supply (SMPS) technology that efficiently converts electrical power.

"We expect our collaboration to be the start of a new era in the power-supply industry by combining Powernet's well-established experience in productizing power supplies and Wise-integration's GaN IC and digital-control technologies," said Lee Don Ju, CEO of Powernet, which is a supplier to Korea's semiconductor industry. "This combination will deliver a much higher level of energy efficiency to mass-market products, while reducing their environmental impact."



"This partnership, guided by our long-term business and development roadmap, will bring Wise-integration's unique GaN IC and digital-control technologies to global markets and enable Powernet to increase the power density and reduce the size of its SMPS products," said Thierry Bouchet, CEO of Wise-integration. "We will jointly deliver the high-level of compactness and superior performance required for the mass-market applications."

www.wise-integration.com

RECOMMENDED
BY
CAPTAIN
ELECTRON

INCREDIBLE

**SUPER
POWER**



High Voltage IGBT, Hybrid & SiC MOS
High density • Low loss • High cycling
Efficient • Effective • Enabled



pdd@hitachi-eu.com



+44 1628 585151



pdd.hitachi.eu

Division for Industrial Applications to Operate Under the Name Green Industrial Power



Infinion Technologies has changed the name of its Industrial Power Control (IPC) Division to Green Industrial Power (GIP). The semiconductor manufacturer is thus highlighting its consistent alignment with the Decarbonization and Digitalization trends. For the newly named Division, green energies are key growth drivers for the business.

"Infineon is making green, cost-efficient electrical energy possible. We have a leading position in the fields of wind energy and solar power, with our power semiconductors setting the standard for higher efficiency levels throughout the entire energy conversion

chain. This represents an enormous amount of growth potential, and we're putting a name on that potential by rebranding our Division", says Dr. Peter Wawer, President of the Green Industrial Power Division. "The focus on industrial business has made us highly successful. This field will continue to grow in the future. At the same time the decarbonization of energy supplies and mobility will additionally accelerate the growth of renewable energies, grid expansion and charging infrastructures. Our extensive product portfolio, technologies, leading-edge expertise in power semiconductors, software and services, together with our highly experienced, global team all mean we are in a perfect position to shape the green transformation of our society."

www.infineon.com

Innovation to Serve the Customer

Enabling innovation and growth – these are the main objectives of Würth Elektronik's High-tech Innovation Center (HIC), officially opened in Munich-Freiham on April 3, 2023. The new high-technology site focuses on partnership with customers, research institutions, start-ups, and semiconductor manufacturers.

A successful entrepreneur for 73 years, with almost EUR 20 billion in sales at the Würth Group in 2022: Prof. Dr. h. c. mult. Reinhold Würth, Chairman of the Supervisory Board of the Würth Group's Family Trusts, could actually sit back and relax. But anyone familiar with the 87-year-old knows that he is still a visionary who is interested in the future like nothing else.

Because part of this future is now being driven in Munich-Freiham, the prominent Baden-Württemberg entrepreneur traveled to the Freiham-Süd Industrial Park for the inauguration of the High-tech Innovation Center. Albert Füracker, Minister of State for Finance and Home Affairs, was there as a representative of the Bavarian State Government. "We are impressed by what has been created here," praised Würth at the ceremony. "I'm looking to provide a workplace for employees that is defined by friendliness and optimism."



Reinhold Würth always sees the customer in focus, however: "I'm a salesman with all my heart and know that customers have enabled our success," Prof. Dr. h. c. mult. Reinhold Würth affirmed and emphasized that success was built upon the trust earned from customers. Modesty, predictability and honesty are at the core of corporate culture.

www.we-online.com

POWER TRANSFORMERS for HIGH FREQUENCY CONVERTERS

15 ÷ 25 kW

10 ÷ 16 kW

9 ÷ 13 kW

6 ÷ 12 kW

4 ÷ 8 kW

2 ÷ 5 kW

FULLY AUTOMATED JUST-IN-TIME PRODUCTION - MADE IN EUROPE

INDUCTIVE COMPONENTS
FOR HF INDUSTRIAL APPLICATIONS

SIRIO ELETTRONICA S.r.l.
Via Selve, 2 - 35037 TEOLO (PD) - ITALY
Phone: 0039 049 9901090
Fax: 0039 049 9901868
E-mail: postoffice@sirio-ic.com
www.sirio-ic.com

45th ANNIVERSARY

For standard components visit
www.sirio-ic.com



High Power next Core (HPnC)

with Fuji Electric's X series - 7G IGBT and SiC



MAIN FEATURES

for traction & industrial applications

▶ Latest chip technology

- Fuji Electric's X series IGBT and FWD with low losses

▶ SiC – MOSFET: Super low switching loss energies

▶ High reliability

- CTI>600 for higher anti-tracking
- High thermal cycling capability with ultra sonic welded terminals
- MgSiC base plate for traction version
- Improvement of delta T_j power cycle capability by using 7G Package Technology

▶ RoHS compliance

- Ultrasonic welded terminals
- RoHs compliant solder material

▶ Over temperature protection

- Thermal sensor installed

▶ Easy paralleling

- HPnC module has a minimized current imbalance
- Easy scalability

SiC E-Mobility Module Powers Geely Auto EV's

Hitachi Energy has won a multi-year order via its partner Jiansan, from VREMT Geely Auto, China's largest privately owned auto manufacturer and one of the world's largest makers of electric cars. Hi-



tachi Energy will supply its RoadPak™ power semiconductor module for Geely's ZEEKR, a premium all-electric brand of long-range luxury cars.

In independent tests, RoadPak has performed more than four million start-stop cycles giving flawless operational reliability over the vehicle's lifetime. RoadPak is available in the 750-volt and 1,200-volt ranges, making it ideal for all types of electric vehicles – regular and luxury cars, commercial vehicles, buses, agricultural EVs, heavy-duty trucks, and even high-performance racing cars.

"We are delighted to have won this order for our groundbreaking RoadPak semiconductor technology from one of the world's leading automakers and EV innovators," says Niklas Persson, Managing Director of Hitachi Energy's Grid Integration business. "The electrification of transportation is a key element of a sustainable energy future, an ambition that RoadPak advances by enhancing the performance of electric vehicles."

www.hitachienergy.com

First Stop on the Biden Administration's 'Invest in America' Tour

Wolfspeed hosted the first stop of President Joe Biden's 'Invest in America' tour at the company's Durham, N.C. headquarters. The President highlighted initiatives designed to boost American manufacturing, rebuild the nation's infrastructure and strengthen supply chains. U.S. Secretary of Commerce Gina Raimondo and North Carolina Governor Roy Cooper were also in attendance at the event.

As an American company at the forefront of the transition from silicon to Silicon Carbide to enhance technology efficiency and energy savings, Wolfspeed is committed to shaping the future of the semiconductor markets. Initiatives like the CHIPS & Science Act that are investing in and advancing the semiconductor industry will help propel the transition to electric vehicles, the move to faster 5G networks, the evolution of renewable energy and energy storage, and the advancement of industrial applications.

"We're honored to have been the first stop on the President's 'Invest in America' tour and to be recognized for our commitment to growing U.S. manufacturing and making a name for North Carolina in the tech space," said Wolfspeed President and CEO, Gregg Lowe. "Silicon Carbide is at the heart of what we do -- it's essential to accelerating the adoption of EVs, delivering energy savings to con-



sumers, and meeting global emission reduction targets. Wolfspeed is proud to play a critical role in fulfilling the objectives of the CHIPS & Science Act and the Inflation Reduction Act, and to reinforce U.S. leadership in the energy transition and the semiconductor industry."

www.wolfspeed.com



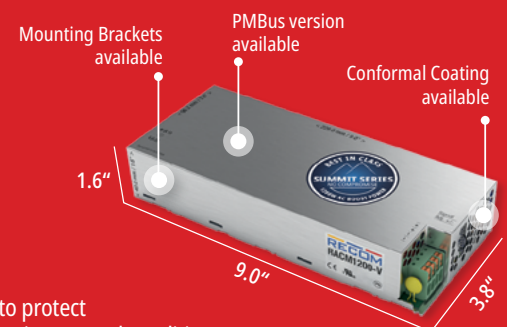
THE NEW COOL: 1200 WATT AC/DC POWER WITHOUT FAN

RACM1200-V THE MAINTENANCE-FREE AC POWER SUPPLY WITH CONTACT COOLING FOR MEDICAL APPLICATIONS

- DC Output voltage: 24, 36, and 48VDC
- Analog and digital control and monitoring
- 5VSB AUX and adjustable 5-12VDC fan output
- Built-in class B EMI filter & Parallel operation
- 2MOPP insulation system, BF ready
- Medical, industrial, and ITE safety certified
- Lighting standards certified, IEC61347-1 & UL8750 (48V Version)

OPTIONAL:

- PMBus version
- Custom Variants
- Mounting Brackets
- Conformal Coating - to protect the unit from harsh environmental conditions



Japanese precision since 1935

HIOKI

Your power inverter's efficiency is more than 100%?



If your **power inverter measurements** show an efficiency of more than 100% or if the measured values simply sound too good to be true then the reason is very likely a **measurement error caused by phase shift**.

Every current sensor produces a gradually increasing phase error in the high-frequency region which can make precise measurements on SiC & GaN based applications quite difficult.

HIOKI products can compensate this phase error because we make both **power analyzers** as well as the **specially designed current sensors**. This ensures that your power measurements at high currents and high frequencies are as **precise as you can expect them to be**.

Check our website to find out more about **phase error compensation** with **HIOKI power analyzers** and **current sensors**. Or simply contact us:

hioki@hioki.eu
www.hioki.eu



Reliable Temperature Measurement of Converters

Temperature is a key parameter that affects the operation and reliability of power electronic systems. Therefore, there is a growing need for more accurate measurement methods. Temperature measurement of fiber optic sensors can have a unique added value in predicting remaining life and in unlocking new revenue streams in applications with advanced condition-based monitoring requirements such as remote asset health monitoring/life prognostic services.

The technology

Opsens Solutions fiber optic temperature sensing technology for power electronics is based on a simple but robust spectrophotometric technique. This technique relies on the temperature dependency of the bandgap of GaAs semiconductor crystal. GaAs crystal is opaque for wavelengths below its bandgap and transparent for wavelengths above. The transition region, i.e. the bandgap spectral position, is a function of the temperature.

The schematic of the GaAs technology is shown in Figure 1. The FO temperature sensor is made of a miniature GaAs crystal bonded to the tip of an optical fiber. Light injected from the signal conditioner into the optical fiber is delivered to the GaAs crystal. The later absorbs light with wavelengths below the bandgap spectral position and reflects back to the signal conditioner wavelengths above the bandgap.

Light reflected goes into a miniature Optical Spectrum Analyser that spatially decomposes the light into its wavelength constituents. A linear CCD array detector measures the intensity versus wavelengths with each pixel corresponding to a specific calibrated wavelength. Therefore, the whole detector array provides the spectral intensity distribution of the light reflected by the GaAs crystal.

Applications of FO sensors in power electronics

Power cycling and mission profiling applications

Accurate Junction Temperature is critical and essential for thermal characteristics extraction of IGBT, elaboration of lifetime laws and study of stability of power dies. Ageing and failure modes of power modules have been elaborated through these processes. These measurements are usually done in controlled conditions over relatively short period of time. Sensors are rarely fixed permanently to the die or the wire, allowing reuse. Figure 2 list the advantages of FO sensors for power cycling applications.

Integrated permanent condition monitoring

Active monitoring has the objective to predict end of life or potential problems on power modules hard to reach or integrated in critical systems such as:

- Offshore power generator
- Dangerous environment (radiated zone)
- Complex converters (high power density multichip modules)
- Critical infrastructures (high speed train)

Unlike Power Cycling, Active Monitoring is done with fixed sensors to avoid unwanted movement and guarantee long-term stability. Figure 3 presents the benefits vs challenges of such instrumentation.

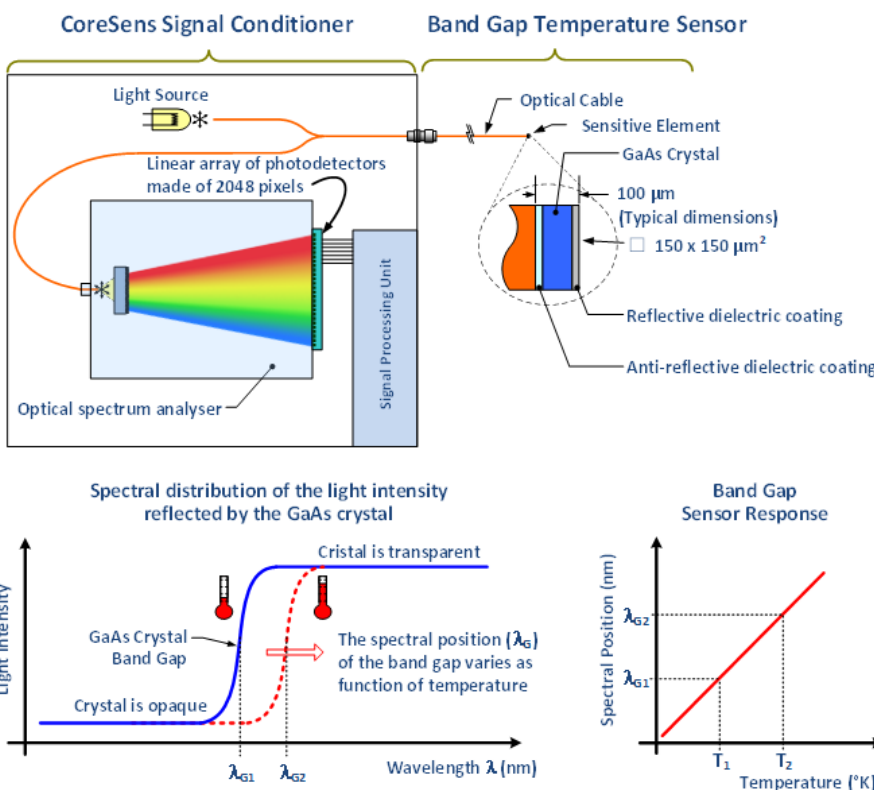


Figure 1: Opsens Solutions GaAs technology overview

Summary of benefits
Fast response time (in the millisecond range)
Immune to Electromagnetic interferences & High voltage
Non invasive (very low thermal mass)
Miniature – sensor head as small as 150x150 µm
Limited intrusiveness for easier deployment
Temperature range -200 to 350 °C
Simple design – easy to adapt
No maintenance required

Why using optical sensors for condition Monitoring

It was reported that the IGBT module is a top ranked subsystem contributing to the overall failure rate and downtime of wind turbines. Owing to a rising concern over the long-term reliability of wind turbines, there have been significant interests in developing online health monitoring technologies for major wind turbine subsystems. Therefore, to ensure the safe operation and reduce the

maintenance cost via condition-based maintenance for wind turbines, it is critical to monitor online the aging of the IGBTs used in wind turbine power converters [1]

[1] Z. Wang, B. Tian, W. Qiao and L. Qu, "Real-Time Aging Monitoring for IGBT Modules Using Case Temperature," in IEEE Transactions on Industrial Electronics, vol. 63, no. 2, pp. 1168-1178, Feb. 2016, doi: 10.1109/TIE.2015.2497665.

Challenges of Power Cycling	Advantages of fiber optic sensors
Power modules having silicon gel hard to evaluate	Sensor could be packaged for module with AND without gel
Getting temperature reading on specific & precise location on power dies	Miniature rigid head could be placed precisely with micromanipulators
Fast temperature variations during cycles	Response time in the ms with 1000 Hz sampling rate
Risks related to high voltage equipment	No risk to technicians (no energy to be transferred)

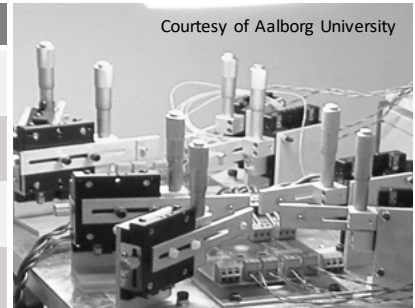


Figure 2: Advantages vs challenges of Power Cycling

Challenges of Condition Monitoring	Advantages of fiber optic sensors
Sensors should not require any maintenance after installation.	Plug & Forget technology - no drift of results over time
Limited modifications of the converter design and package	Only a small hole per fiber is required after installation of sensors
Must operate in real operating conditions after instrumentation	Fully dielectric technology not affected by EMI or high voltage
Cost must be lower than simple redundancy of power converters	Cost per system could be significantly cheaper than redundancy

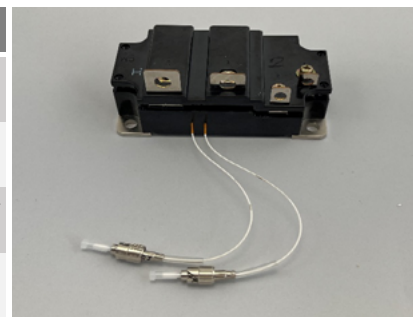


Figure 3: Advantages vs challenges of Condition Monitoring

www.opsens-solutions.com

Enlightenment through smart measurements

Reliable junction temperature with fiber optic sensors

WHEN RELIABILITY IS NOT AN OPTION

opsens-solutions.com

Multiple chips

Condition monitoring

Gel-filled module

opsens-solutions.com

Come and meet us at PCIM 2023 - our Stand #410 at Hall 9

embedded world 2023: Busy Halls and Happy Smiles

Impressive increase in visitors of over 50 percent

By Roland R. Ackermann, Correspondent Editor, Bodo's Power Systems

Mid March, the Exhibition Center Nuremberg was the hotspot for the international embedded community. Over 950 exhibitors from 44 countries presented their product innovations and solutions at the embedded world Exhibition&Conference. Organizers and exhibitors alike were overwhelmed by the number of visitors: Almost 27,000, which is over 50 percent more than last year, flooded the exhibition halls during the three days, including over 40 percent from abroad.



embedded world and electronic displays conferences

The top-class lecture program of the two conferences, which were held in tandem, attracted 1659 participants and speakers from 46 countries. The classes and sessions as well as the three keynotes – including a presentation on AI Ethics by Prof. Ali Hessami – were exceptionally well attended” confirmed chairman Axel Sikora.

embedded award 2023:

A power solution among the winners

A top-class jury has evaluated a record 98 submissions for the 19th embedded award in eight categories. “I was impressed this year by the continuingly high level of innovation in the industry and by the extremely wide scope of the submissions,” emphasized jury chairman Prof. Dr.-Ing. Axel Sikora.

The first price in the startup category was awarded to Linköping, Sweden, based Epishine for its product OneCell, active in the field of Energy Harvesting to solve the issue of disposable batteries. Epishine OneCell was developed as an organic solar cell tuned to indoor light with world leading light energy harvesting performance, efficiently converting light to electricity even at very low illumination. The OneCell is a sustainable method for powering small wireless electronics. With a flexible design that can be adapted to intricate and customized layouts to meet specific surface finishes of the product, for example, soft touch plastics, leather, brushed etc.

Two examples of power-related innovations on show

Although not in its naming, power and power handling played an important role in the exhibition. We have selected two characteristic examples:

Keysight’s battery emulation and profiling solution for IoT devices

Keysight Technologies presented its E36731A Battery Emulator and Profiler, a complete emulation solution that identifies the impact

of variables affecting the battery drain of IoT devices to enable development engineers to improve their device designs. The solution speeds and simplifies battery life testing with automation and integrated emulation and profiling capabilities, allowing engineers to achieve longer battery run time and reduce device size while shortening time-to-market

As the name implies, the instrument addresses the battery testing needs of IoT device designers by giving them an integrated electronic load and power supply that can be used to emulate battery performance. By testing with an emulated battery, engineers can quickly assess the effect of design or software changes on battery life by instantly transitioning the battery’s charge state.



E36731A-Battery-Emulator-and-Profiler

The device works with the Keysight PathWave BenchVue Advanced Battery Test and Emulation Software to provide a complete solution that:

- **generates battery profiles** – to establish known, good references with consistent properties that can be used over and over to simulate battery drain. Profiles can be linked to factors such as age and temperature.
- **increases battery profile accuracy** – By using the simulated current drain of a device to generate battery profiles, engineers can enhance the accuracy of profiles.
- **speeds testing with battery emulation** – so engineers can instantly transition a battery’s charge state and gain real-time insight into current drain to optimize designs for longer run time.
- **automates battery run-down and cycle testing**
- **offers flexibility** – providing power up to 200W, 30V, 20A and a wide dynamic measurement range from microamps to amps.

Battery Management System from Texas Instruments

TI’s battery management system (BMS) reference board spotlighted its comprehensive portfolio for vehicle electrification. This includes several devices for precise battery monitoring and high-accuracy current and voltage sensing, as well as connectivity devices, solid-state relays, isolated power supply components and more. Also demonstrated by TI was a complete hardware and software BMS solution connected to a Comemso hardware-in-the-loop simulator to replicate a real battery pack with a stand-alone system.

Moreover, TI demonstrated a battery energy storage system based on a precision battery monitor and balancer, a voltage and cur-

rent sensor, and an isolated switch driver. The system enables highly accurate monitoring of multi-module battery cells, providing precise voltage and temperature readings of individual cells and statements about total current. In this way, the state of charge and operation can be estimated more accurately, and higher system reliability is achieved.

embedded world goes West

Following the premiere of embedded world China in Shanghai from 14 to 16 June 2023, the North American edition will be the second international offshoot of this successful exhibition from 8 to 10

October 2024 in the “Silicon Hills”, Austin, Texas. The concentration of major industry players such as AMD, Apple, Dell, Google, Hewlett-Packard, IBM, Oracle and Wincor Nixdorf makes Austin the perfect venue for the first embedded world North America, which will be held at the Austin Convention Center.

Save the date

The next embedded world Exhibition&Conference in Nuremberg will be held April 9-11, 2024.

www.embedded-world.de

TRACO POWER

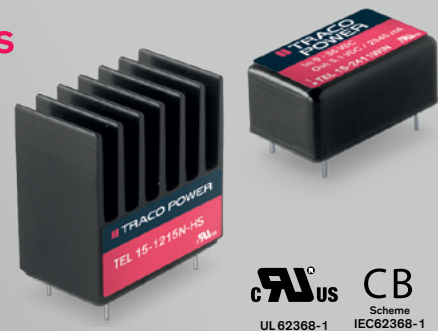
Reliable. Available. Now.

www.tracopower.com

TEL 15(WI)N and TEL 15(WI)N-HS Series

Ultra compact 15 Watt DC/DC converters (DIP-16) for industrial applications

- Ultra compact 15 Watt converter in DIP-16 metal casing
- Highest power density of 4.51 W/cm³
- Available in standard or heatsink package
- 6-side shielded metal case with insulated baseplate
- Wide 2:1 and 4:1 input voltage ranges
- High efficiency (up to 87 %) for low thermal loss



Series	Rated Power	Package Style	Temp. range	Input	Output voltage	Size (in mm)
TEL 15N	15 Watt	DIP-16	-40 to +55°C w/o derating	2:1	5.1, 12, 15, 24, ±12, ±15 VDC	23.8 × 13.7 × 10.2
TEL 15N-HS	15 Watt	DIP-16, heatsink case	-40 to +70°C w/o derating	2:1	5.1, 12, 15, 24, ±12, ±15 VDC	24.4 × 14.3 × 24.4
TEL 15WIN	15 Watt	DIP-16	-40 to +55°C w/o derating	4:1	5.1, 12, 15, 24, ±12, ±15 VDC	23.8 × 13.7 × 10.2
TEL 15WIN-HS	15 Watt	DIP-16, heatsink case	-40 to +70°C w/o derating	4:1	5.1, 12, 15, 24, ±12, ±15 VDC	24.4 × 14.3 × 24.4

TEST FASTER

The fastest, most powerful production line testers for power SiC, GaN, MOS, IGBT and bipolar devices.



See our latest Mostrak high power testers in action:

PCIM
Nuremberg
Hall 7
Stand 475

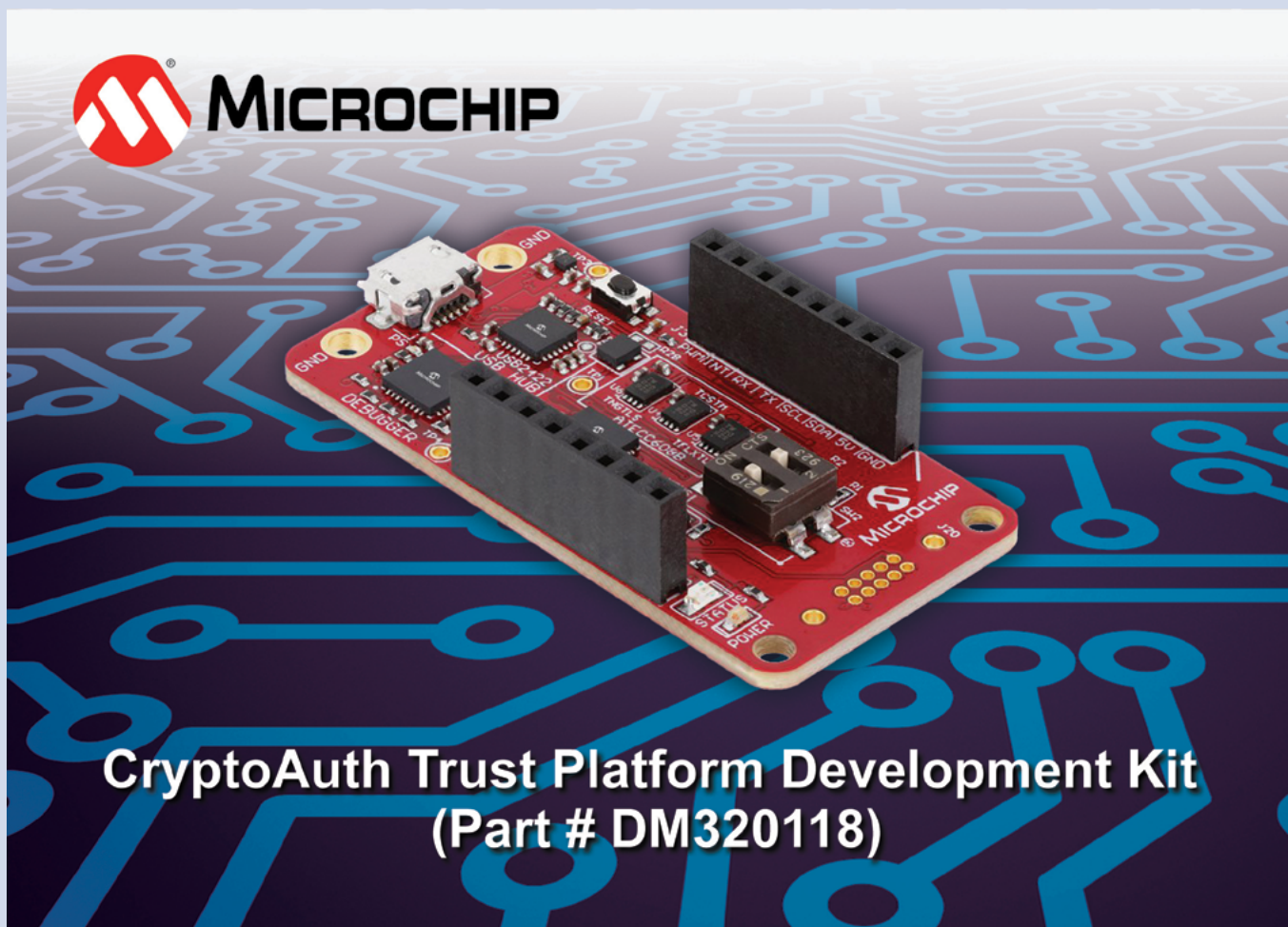


iptest.com



Win a CryptoAuth Trust Platform Development Kit

Win a Microchip CryptoAuth Trust Platform Development Kit (DM320118) from Bodo's Power and if you don't win, receive a 15% off coupon for this board, plus free shipping.



CryptoAuth Trust Platform Development Kit (Part # DM320118)

The CryptoAuth Trust Platform is a compact hardware evaluation kit that can be used with the Trust Platform Development Suite (TPDS) and other software tools. This kit is used for exploring and implementing solutions for the IoT space with a pre-provisioned ATECC608B Trust&GO, pre-configured ATECC608B TrustFLEX and fully customizable ATECC608B TrustCUSTOM products. The Trust&GO and TrustFLEX products have been developed to allow for an easy way to add hardware security to IoT Cloud solutions, accessory authentication, IP Protection, and firmware verification.

Using these kits with the Microchip development tools and Microchip provisioning systems allows for even low volume projects to easily implement secure authentication into their application. The user guide provides a physical overview of connections, components and switch settings implemented on the board.

The CryptoAuth Trust Platform consists of ATSAM21E18A that is the main MCU which comes pre-programmed with Microchip's Secure Product Group (SPG) kit protocol. A low-power, high-performance Microchip's ARM® Cortex®-M0+ based Flash micro-

controller, the ATSAM21E18 is ideal for a wide range of home automation, consumer, metering, and industrial applications. This protocol takes care of the communication between the CryptoAuthentication™ devices and the host MCU over the USB HID interface. The data transfer between the secure elements and the host MCU is indicated by the Status LED.

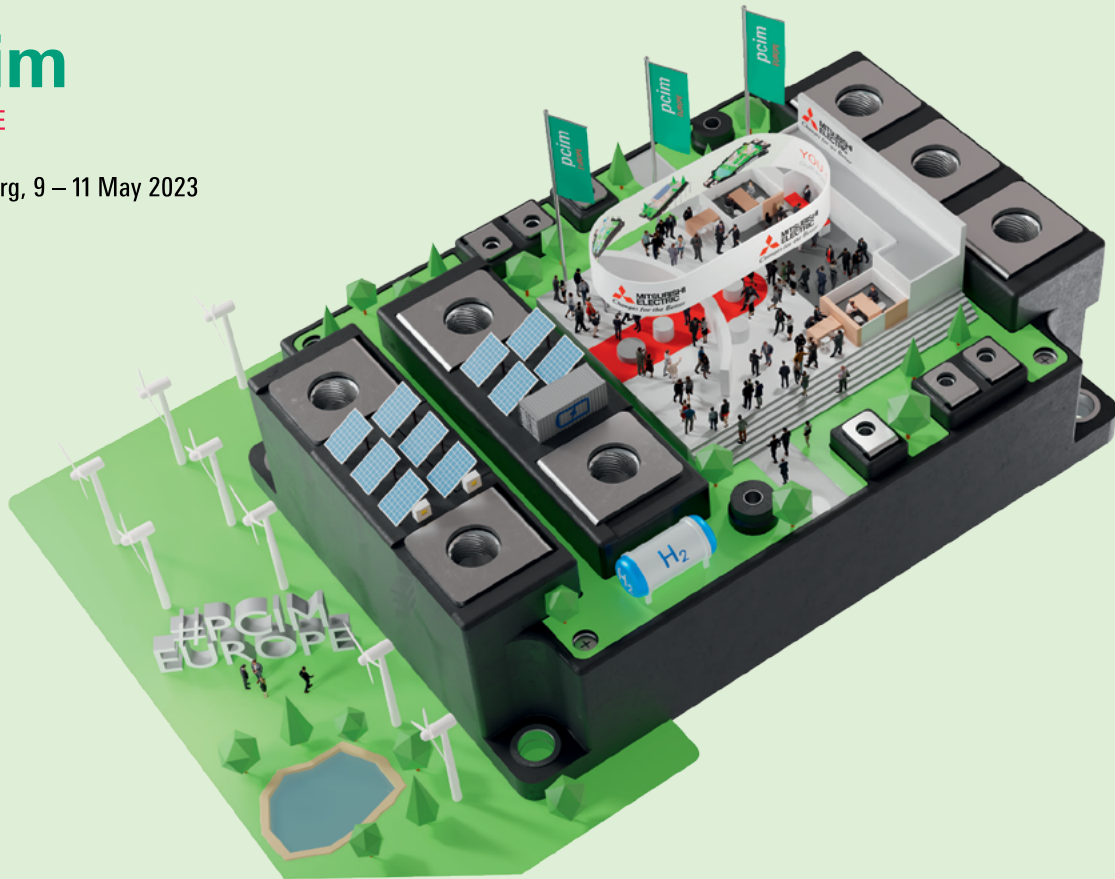
The kit supports mikroBUSTM for easy connection to MikroElektronika add-on boards such as the EV92R58A Development board, which is an accessory board for evaluating the ECC204, a new member of the CryptoAuthentication product family. The device is targeted for disposable and ecosystem control applications and is intended to be used as a companion device with Microchip or other vendors' microcontrollers.

For your chance to win a CryptoAuth Trust Platform Development Kit or receive a 15% off coupon for this board, plus free shipping, visit <https://page.microchip.com/Bodo-Crypto.html> and enter your details in the online entry form.

www.microchip.com

pcim
EUROPE

Nuremberg, 9 – 11 May 2023



YOU CAN
BUILD ON IT.

OUR POWER MODULES –
YOUR GREEN DEAL.

Save the Date:

PCIM EUROPE

Nuremberg, 9 – 11 May 2023

We look forward to seeing
you in Hall 7, Booth 419

7th Generation Industrial IGBT Modules in LV100 Package

- // New standardised package for high power applications
- // 1200V, 1700V and new 2000V class as optimised solution for 1500V_{DC} 2-level inverters
- // Highest power density
- // Latest 7th Gen. IGBT and Diode chips
- // Thermal cycle failure free SLC package technology
- // Easy paralleling providing scalable solutions
- // Simplified inverter design
- // Advanced layout provides low stray inductance and symmetrical current sharing

More Information:

semis.info@meg.mee.com

www.meu-semiconductor.eu

10th ECPE SiC & GaN User Forum

Potential of Wide Bandgap Semiconductors in Power Electronic Applications

— Report of Conclusions —

By Andreas Lindemann, Otto-von-Guericke-University at Magdeburg, Chair for Power Electronics



FAKULTÄT FÜR
ELEKTROTECHNIK UND
INFORMATIONSTECHNIK

Overview

The biannual ECPE Wide Bandgap User Forum is dedicated to report state of the art and prospects of SiC and GaN devices in power electronic systems and to foster an exchange between system, circuit and device designers. This year the tenth User Forum could be marked. It has been conducted as a hybrid event with the vast majority of the international participants and speakers being on-site at Erding/Munich.

The programme comprised an overview as well as detailed presentations about GaN devices and related systems on the first day and SiC devices and systems on the second. These have been complemented by common topics — such as reliability and passive components — and an outlook. Some main findings are summarised in the following:

State of the Art and Trends

The GaN power devices available today are usually horizontal transistors with voltage ratings up to 650V. Different versions need to be distinguished, in particular the high electron mobility transistors (HEMTs) which can be normally-on and — with p-GaN gate — normally-off; gate injection transistors (GITs) provide normally-off behaviour as well. Their operating principles and thus their properties are partially different which is important for a deeper understanding. Normally-on transistors can be combined with an enhancement-mode silicon MOSFET to constitute a normally-off component — either as a cascode circuit where the switching state is solely controlled via the MOSFET gate, or in a way that the MOSFET is only turned on once to afterwards directly switch the HEMTs via their gates. The unipolar devices are not avalanche-rated but usually provide a high safety margin between rated maximum voltage and breakdown voltage. Most devices would conduct a very high short-circuit current leading to fast failure; to prevent this, drivers integrated in the component or even in the chip itself are capable to turn-off quickly within some 100ns after the short-circuit occurs. Such drivers can also safely hamper cross-conduction through integrated phaselegs and thus overcome issues frequently faced in circuits built with discrete components. Packages are mostly surface-mountable with the option to parallel multiple chips in bigger, integrated assemblies. This allows to use GaN transistors in a vast range of applications: It is already known that they are suitable e.g. for single-phase off-grid power supplies with high switching frequency; in spite of their low switching losses it may be advantageous to operate them in resonant mode. On the other hand, they also become increasingly attractive for high current applications such as traction drives of electric vehicles with a battery voltage up to some 400V.

Although undesirable dynamic R_{Dson} and current collapse are still subject to current work on GaN transistors, these profit from the use of the same material for RF components, leading to a comparably high maturity of the relatively new devices. The aforementioned integrated solutions may also help to increase reliability due to their low part count. Research is among others dedicated to vertical devices where higher voltage ratings can be achieved with increased thickness instead of increased area; this would basically be cost efficient but requires to identify and process suitable substrates which is a topic of current research and development. This also applies to multi-channel devices, while a release of a new bidirectional HEMT has already been announced: It basically consists of two anti-serial normally-off or -on HEMTs with two source and gate terminals, using the same area between the gates as drain-to-gate path for both polarities. This saves chip area, minimising the length of the current path and thus the conduction losses. Such devices are suitable as bipolar, bidirectional switches for known circuits such as T-type three-level converters or Vienna rectifiers; in addition they allow to explore new circuits and also series connections to achieve higher blocking voltages.

SiC components have been introduced in power electronics about two decades ago. They have since matured and experienced a tremendous growth. Diodes had been the first commercially available SiC devices and are well established. Several types of transistors followed. The user forum focused on the most advanced devices, i. e., normally-off SiC MOSFETs with blocking voltages between 650V and 3300V and corresponding JFETs. Today these are manufactured predominantly on 6 inch substrates with 8 inch already being introduced and ramping up; additionally new substrate technologies are investigated. Chip sizes are moderate, usually up to about 25mm² to achieve maximum yield. Parallel connection allows higher current capability; it is achieved either by paralleling multiple discrete devices or multiple chips in a module. Such solutions are to a large extent applied in converters for electric vehicles: Automotive charging and traction converters belong to the volume applications, especially because the higher achievable efficiency is beneficial for the driving range of the car, this way offering benefits on system level. Correspondingly, also railway traction and auxiliary power supplies profit from SiC devices which allow to build converters with higher power density, simplified cooling and significantly increased efficiency also on system level. Those applications obviously are demanding regarding robustness and reliability. Recent work on this topic refers to stability issues, in particular with reference to trapping effects, threshold voltage drift and edge termination, where considerable electric fields have to be handled, and short-circuit capability which is achievable for about 1 μ s.

Packaging technology is advanced in parallel, in particular to achieve modules with low parasitic inductance, highly reliably interconnects and optimised cooling. Of course, standardisation with respect to the qualification of SiC devices is advancing as well. While SiC and GaN devices are commercially available and continuously improved, in parallel new wide bandgap materials are explored. As examples, Ga₂O₃ has been presented as a base material for Schottky diodes and prospectively MOSFETs, and even more basic research on AlN substrates. Last but not least, besides the semiconductor devices and their packaging the passive components strongly influence the performance of a converter. Consequently a presentation has been dedicated to different types of advanced capacitors with particularly low equivalent series inductance.

Conclusion and Outlook

The findings as briefly summarised above illustrate the fast development of wide bandgap power semiconductors and their successful use in industry, driven by their advantages in key applications and the exploration of new areas. Engineers in research and development of devices, components, circuits and power electronic systems have achieved impressive results: For example, they allow an increase in energy efficiency, optimisation of the usage of renewable sources for electric energy supply and they are a key for the introduction of e-mobility.

Research and development in power electronics are ongoing. The European Center for Power Electronics (ECPE) is a stakeholder in this area, bringing together industrial partners and research institutions. After the broad interest of far more than 250 international participants in this year, ECPE will announce the next SiC & GaN User Forum in 2025. There will be the occasion to report the progress achieved since today and pave the way to proceed even further.

www.ecpe.org
www.uni-magdeburg.de/ilge

Designed for High Voltage Applications

- Diodes
- Optocouplers
- Power Supplies
- SMD Multipliers
- Bridges
- Rectifiers

VMI
VOLTAGE MULTIPLIERS INC.

SOLUTIONS. PERFORMANCE. RESULTS.

voltage-multipliers.com ▪ vmi.protec-semi.de

TAMURA

High Power Magnetics | Low Power Magnetics | Gate Drivers Module | Current Sensor | Electronic Chemicals FA Systems

YOUR ONE AND ONLY COMPANY

We look forward to having you join us!

pcim EUROPE 9-11 May 2023, Nuereberg, Germany, **Visit Us! Hall 7 Booth No.7-521**

DATA CENTER WORLD 8-11 May 2023, Austin Convention Center, Austin TX U.S.A., **Visit Us! Booth No.8330**

Web **Linked In**

Partnering for the Safe Supply of Industrial Power Modules

Power semiconductor users are painfully aware of the challenges faced in recent years due to an uncertain supply chain. Therefore, “multiple sourcing” has always been a desire when designing a power converter. Semikron Danfoss, as the largest chip-independent power module manufacturer, is in a unique position to address this. Together with our long-time partner ROHM Semiconductor, we add a fully compatible new source of 1200V IGBT to our low power module offering. This will further help to mitigate power module delivery shortages and secure the supply chain.

By Paul Drexhage, Technical Marketing Manager, Semikron Danfoss

The worldwide growth in electrification technologies has created unprecedented demand for power modules. Often, it is the chip supply that limits power module availability. Despite ongoing investments in production capacity by the chip manufacturers, the supply situation remains tight. It is against this backdrop that ROHM has introduced the new 1200V RGA IGBT, targeted as an alternative to the latest Generation 7 IGBT devices in industrial applications. For years, ROHM has been a trusted partner to Semikron Danfoss for the supply of silicon carbide devices. ROHM is now expanding their silicon bare die offering to Semikron Danfoss, positioning themselves as an advanced alternative to traditional chip suppliers.

The RGA is a newly designed, light punch through, trench gate IGBT with $T_{j,max} = 175^{\circ}\text{C}$. The conduction, switching, and thermal characteristics are optimized for new industrial drive applications in the low to medium power range. At the same time, the RGA is intended to remain compatible with existing IGBT solutions, enabling a multiple source approach. The following discussion shows this with a comparison of basic device characteristics between two otherwise identical modules. The 1200V RGA IGBT has been tested in the baseplate-less MiniSKiiP package. A Generation 7-equipped SKiiP24AC12T7V1 ($I_{Cnom} = 35\text{A}$) is used as the reference. In both test modules, the circuits are identical and use the Semikron Danfoss CAL4F freewheeling diode.

Static behavior

The RGA’s modern trench gate design and selected carrier profile are designed to give a low on-state voltage drop. As with all mod-

ern silicon IGBTs, the RGA exhibits a positive temperature coefficient (PTC) for forward voltage drop over the higher end of the current range. While this PTC characteristic is stronger in the RGA than the Generation 7 IGBT, the slightly higher resulting forward voltage drop at high temperatures is partially helped by a lower voltage drop at room temperature (Figure 1). The result is similar forward voltage drops for both IGBTs at rated current, with the RGA device being with $\pm 4\%$ of the Generation 7 device over the given temperature range. Overall, like the Generation 7 IGBT, the RGA demonstrates a much lower forward voltage drop than previous chip generations.

The high current behavior of the RGA IGBT differs from the Generation 7 IGBT. As shown in Figure 2, the RGA IGBT comes out of saturation at a higher current. This allows for better handling of transient currents that occur in applications with frequent overloads such as motor drives. Even with the temperature coefficient impacting behavior at 150°C , the RGA device can still handle peak currents of three times the nominal rating. This potentially allows for modules with a peak repetitive current rating of $I_{CRM} = 3 \times I_{Cnom}$, which is suitable for applications with expected step overloads.

For additional overload capability, the RGA IGBT equipped power modules allow for the same high temperature operation as Generation 7 chipsets: periodic operation up to the maximum chip rating of 175°C is permitted. Details of the allowed temperature profile are given in section 2.3 of [1]. For continuous operation, the RGA IGBT-equipped power modules follow the same guideline as existing devices: 25K margin from the absolute maximum junction (i.e. $T_{j,op}=150^{\circ}\text{C}$).

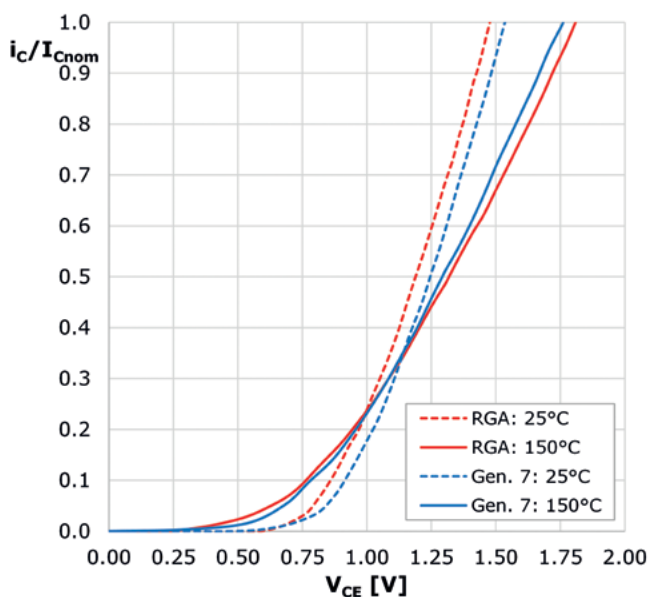


Figure 1: Forward characteristics (chip level), scaled to nominal current

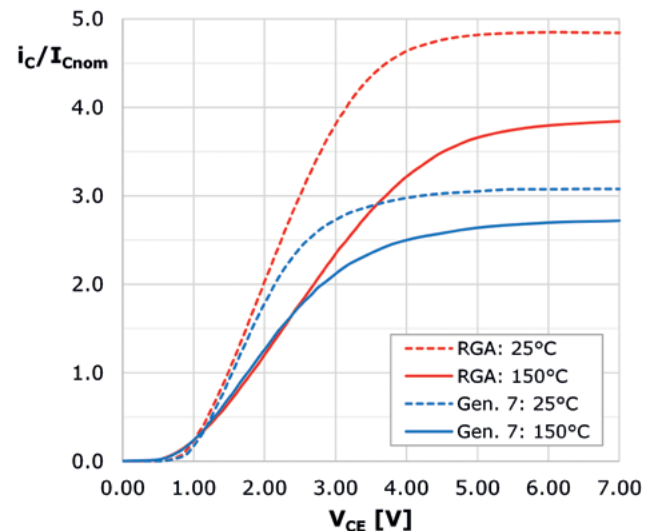


Figure 2: High current forward characteristics (chip level), scaled to nominal current

„WHERE INNOVATION GOES IN SERIES: GVA”

Our Development, Production and Quality departments are separated by one floor and two flights of stairs – nothing else. Because all GVA experts share the same systemic understanding and the latest know-how. That´s why we are able to mass-produce innovative developments in the shortest possible time. With guaranteed quality – and gladly also for you!



Your GVA expert:
Jürgen Kolasinski
+49 (0)621 / 78992-22
j.kolasinski@gva-power.de



Gate characteristics

Generation 7 IGBT employs a striped trench gate structure to achieve a very small IGBT cell pitch and high electrical conductivity (i.e. low voltage drop). However, a drawback to this structure is that it presents a significantly higher gate capacitance compared to e.g. IGBT 4. This high capacitance results in a high load (current) requirement for the driver circuit when switching. The well-proven, conventional trench gate structure employed in the RGA IGBT gives an 18% smaller gate charge than the equivalent Generation 7 IGBT device. At the same time, the gate threshold voltage, $V_{GE(th)}$, remains similar (e.g. 6.0V) to other modern IGBTs, providing a fair balance between parasitic turn-on resilience and ease-of-driving. The recommended gate drive voltage is also the same as most IGBT devices, with testing having been carried out with $V_{G,on} = 15V$ and $V_{G,off} = -8V$.

Dynamic behavior

Newer generations of IGBT tend to exhibit higher dv/dt levels (e.g. in excess of $7kV/\mu s$) because of the efforts to reduce switching losses through increasing the speed of the turn-on and turn-off processes. The RGA is no different, but like the Generation 7 IGBT, the turn-on dv/dt and di/dt can be controlled by varying the gate resistance. dv/dt levels acceptable to motor drive applications (e.g. $<5kV/\mu s$) are achieved, particularly at higher currents. In general, a higher R_{Gon} value is required for the RGA to meet similar dv/dt and di/dt values to Generation 7 devices (Figure 3).

The effect of this higher speed switching and the role of the gate resistor is apparent when examining the turn-on process of the

RGA and Generation 7 IGBTs under the same conditions and with the same gate resistor ($R_{Gon} = 8.2\Omega$, Figure 4). In this situation, the peak current on the RGA device is approximately 22% higher than on the Generation 7 device. However, the high di/dt , coupled with the fast drop in collector-emitter voltage, mean that the current-voltage product and resulting switching losses are lower. If the high dv/dt can be tolerated, such as in high-speed servo drive applications, the reward is a 25% reduction in turn-on energy when using the RGA IGBT.

Conversely, if switching speeds similar to a Generation 7 IGBT are required, doubling the turn-on gate resistance gives very similar behavior. Figure 5 demonstrates that smooth, nearly overlapping, voltage and current waveforms are achieved with an increased gate resistance ($R_{Gon} = 16\Omega$). The slower switching speed increases losses, but in this example the turn-on energies in the RGA and reference Generation 7 device are nearly identical.

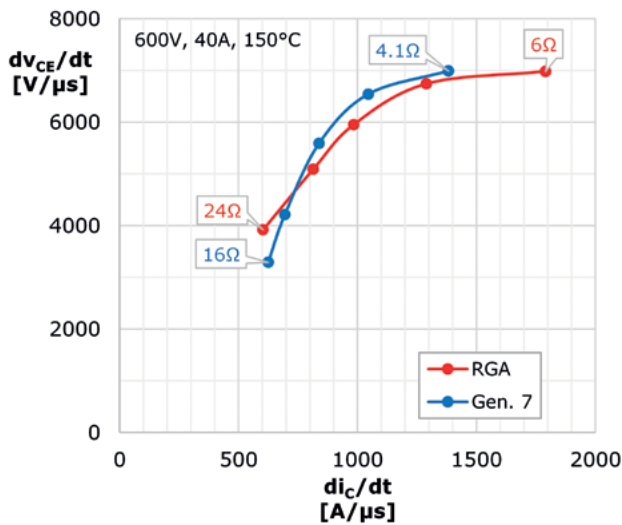


Figure 3: Turn-on dv/dt and di/dt characteristics, with varying R_{Gon}

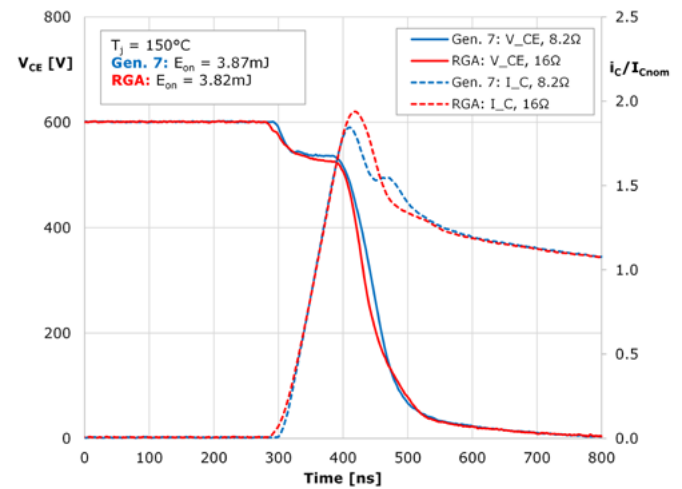


Figure 5: Turn-on behavior with different R_{Gon} current waveforms centered at I_{Cnom}

Generation 7 IGBTs, as with most modern trench-gate IGBT designs, are less responsive to the effect of small changes in the turn-off gate resistance. This is also true for the RGA IGBT, where adjusting the resistor over a $\sim 20\Omega$ range produces little change in the di/dt , dv/dt , and turn-off energy. A side-by-side comparison to the Generation 7 IGBT during turn-off using the same 8.2Ω gate resistance shows nearly identical voltage overshoot despite a rapid rise time (Figure 6). The RGA IGBT exhibits a soft, but long, current “tail” that increases the voltage-current product. However, this effect is partially compensated by the higher dv/dt . The net result is that the turn-off energy in the RGA is only 5% higher than in the reference Generation 7 device.

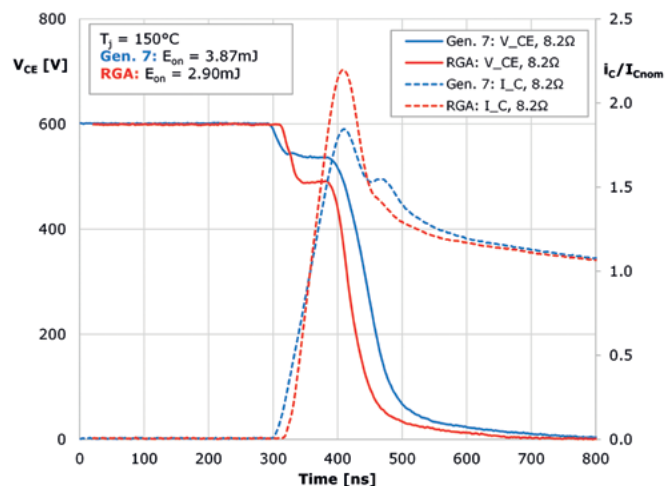


Figure 4: Turn-on behavior with same R_{Gon} current waveforms centered at I_{Cnom}

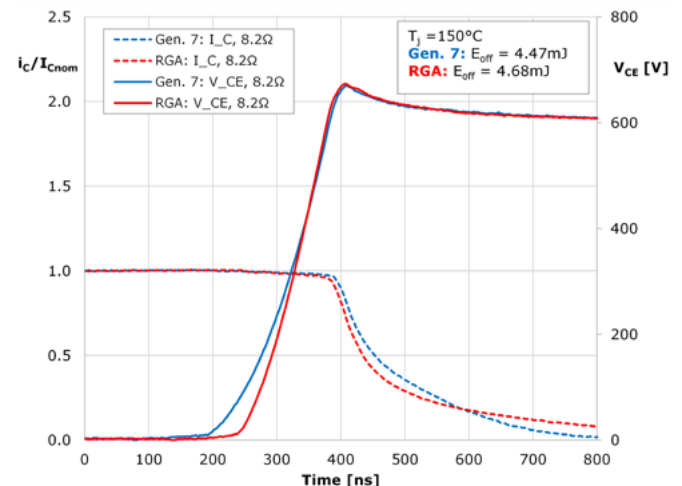


Figure 6: Turn-off behavior with same R_{Gon} current waveforms centered at I_{Cnom}

LH3 Series



FILM CAPACITOR DESIGNED FOR

Next Generation Inverters

FEATURES

✓ ESL 7nH typical

✓ Operating temperature to +105°C

✓ High RMS current capability - greater than 400Arms

✓ Innovative terminal design to reduce inductance

Scan to Learn More!



www.ecicaps.com

Application comparison

The net effect of conduction losses, switching losses, and thermal performance is best indicated by calculating the resulting junction temperature for a given application conditions. In this case, a three-phase, 2-level voltage source inverter circuit is considered with a sixpack MiniSKiiP module and the application parameters given in Table 1. Two modules with a nominal current rating of 35A are selected for comparison. This size of module would be suitable for an industrial motor drive in the 5.5-11kW range, depending on the considered overload profile.

DC Voltage, V_{DC}	650V
Line-Line Voltage, V_{out}	400V
Power Factor, $\cos(\phi)$	0.85
Fundamental Frequency, f_{out}	50Hz
Output Current, I_{out}	25.9A _{rms} ($P_{out} = 15.3kW$)
Switching Frequency, f_{sw}	Variable
PWM	Sine-Triangle
Junction Temperature, T_j	Variable
$R_{th(s-a)}$	0.1K/W
Ambient Temperature, T_a	45°C
Junction-Sink Thermal Resistance, $R_{th(j-s)IGBT}$	0.80K/W (RGA)
	0.93K/W (Gen. 7)
R_{Gon}	16.4Ω (RGA)
	8.2Ω (Gen. 7)
R_{Goff}	13.7Ω (RGA)
	8.2Ω (Gen. 7)

Table 1: Parameters for example thermal calculation

For this comparison, Semikron Danfoss' proven SemiSel calculation tool, now in its fifth generation, is used. A single MiniSKiiP module is mounted using High Performance Thermal Paste (HPTP) onto a hypothetical, forced air-cooled heatsink with 45°C air. The junction temperature is calculated with the inverter circuit operating under the parameters given in Table 1. Based on the earlier discussion, a higher turn-on gate resistor is chosen for the RGA IGBT to give a similar dv/dt behavior as the Generation 7 IGBT. A current is selected that gives a junction of 125°C junction temperature for the highest chosen switching frequency. This temperature is considered a typical continuous limit for sizing modules in motor drive applications due to power cycling lifetime concerns. The resulting junction temperature and efficiency versus frequency are plotted in Figure 7.

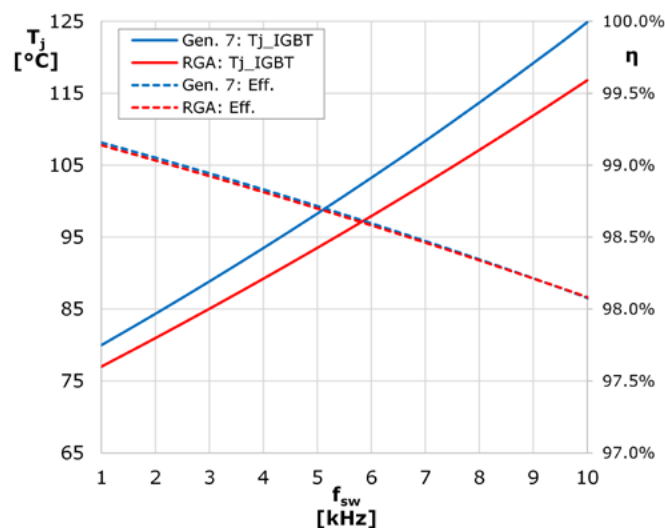


Figure 7: Calculated junction temperature and efficiency for a fixed output current

Under the same operating conditions, the calculated RGA IGBT junction temperature is, on average, 6K lower than that of the Generation 7 IGBT (solid lines in Figure 7). This is primarily the result of the optimized chip size of the RGA IGBT which results in a 14% lower thermal resistance from junction to heatsink. A lower junction temperature yields lower thermomechanical stress in the power module and potentially increased power cycling lifetime. If a similar junction temperature is acceptable with the RGA IGBT, reduced cooling effort is required. This could be in the form of a lower cost heatsink or reduced fan speed.

The higher forward voltage drop of the RGA at high temperatures impacts efficiency at low switching frequencies where conduction losses are dominant. Conversely, the reduced turn-on energy of the RGA gives it an edge in efficiency at higher switch frequencies. However, in the given application example the semiconductor efficiencies for the two chips are essentially the same over the range of 1...10kHz (dashed lines in Figure 7).

Alternatively, it might be desirable to use the superior thermal performance of the RGA to achieve more output current in the same package. A separate thermal calculation has shown that the RGA IGBT is capable of 2...9% higher output current than the Generation 7 IGBT in the 1...10kHz range, at the cost of a slightly reduced efficiency.

Short circuit behavior

The general trend towards smaller chip sizes has reduced the thermal capacity of modern IGBT dies and hence the short circuit capability compared to older IGBT chip generations. The 1200V RGA IGBT maintains the present standard of pulsed short circuit withstand time, t_{psc} , of 8μs at 800VDC, 150°C that is also shared by Generation 7 IGBT. The high di/dt of the RGA IGBT means that it also reaches high peak currents during short circuit events, above five times I_{Cnom} . Despite this, the turn-off behavior remains controlled, without any high frequency oscillations.

Humidity robustness

As power converter deployment expands into new applications around the globe, more power semiconductor devices are likely to be subjected to high humidity environments. This, combined with a better understanding of device failure modes has pushed the industry to more stressful qualification tests. In particular, the High Voltage, High Humidity, High Temperature Reverse Bias (HV-H³TRB) test has become the standard for measuring long term humidity robustness. This test stresses the edge termination structure of an IGBT chip by applying 80% of rated blocking voltage (e.g. 960VDC) in a test chamber at 85°C air temperature with 85% relative humidity. Devices are evaluated based on how many hours (e.g. 168/504/1000h) they can withstand this environment without exceeding leakage current limits for a given blocking voltage. Testing by Semikron Danfoss has shown the RGA IGBT can meet the 1000h minimum, which puts it in the same class as Generation 7 IGBT.

Implementation

Semikron Danfoss can offer the 1200V RGA IGBT in a full range of nominal current classes from 10A to 150A. This range, combined with the suitability of the RGA chip for motor drive applications, means that the MiniSKiiP family is the ideal choice for module implementation. The baseplate-less, spring-contact MiniSKiiP is already deeply embedded in the worldwide motor drive market and always equipped with the latest generation IGBTs. Therefore, it is important for this product to have an alternative IGBT source to diversify the supply chain. The uniform-height MiniSKiiP housing family (Figure 8) is also offered on the market as a multiple source package, making an alternative IGBT a valuable option for manufacturers. The first RGA-equipped MiniSKiiPs will be available in sixpack ("AC") and converter-inverter-brake ("NAB") topologies to allow for pin-compatible replacements to Generation 7 IGBT equipped modules. The MiniSKiiP is available with the same pre-applied High Performance Thermal Paste (HPTP) used in the calculated application comparison.

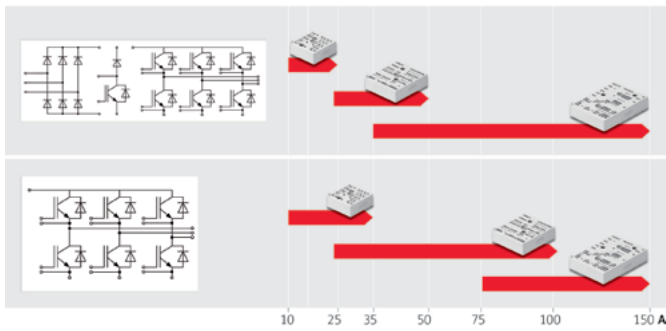


Figure 8: RGA-equipped MiniSKiiP 1/2/3

For press-fit/solder applications, the industry-standard SEMITOP E package will also be available in pin-compatible configurations to existing Generation 7 IGBT module offerings. This housing family (Figure 9) will also offer sixpack (“GD”) and converter-inverter-brake (“DGDL”) circuit configurations. The SEMITOP E package is fully compatible to other industry standard offerings, despite giving an advantage in the form of integrated mounting

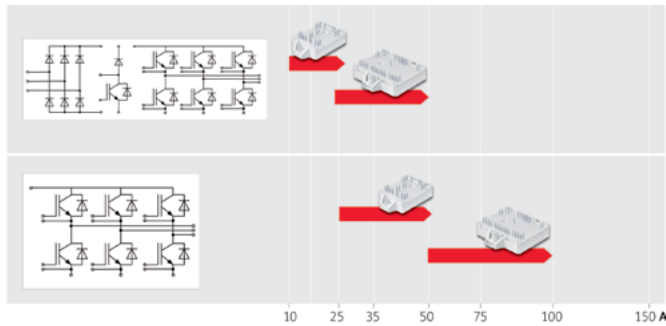


Figure 9: RGA-equipped SEMITOP E1/E2

tabs instead of metal clips. These give increased mounting pressure, resulting in lower thermal resistance. The superior enhanced press-fit pin features an internal strain relief for higher mechanical mounting robustness. The SEMITOP E is available with pre-applied HPTP or the new Semikron Danfoss exclusive pre-applied High Performance Phase Change Material (HP-PCM) for ease-of-handling during assembly. The 1200V RGA IGBT will be indicated by the “12RA” nomenclature in the power module description: e.g. a MiniSKiiP CIB module with a 35A nominal current rating will be named SKiiP 24NAB12RAV1.

Conclusion


The power electronics industry continues to recover and learn lessons from the supply issues in recent years. It’s clear that diversification in both semiconductor chip and module manufacturing is required to generate true “multiple source” power modules. In the case of 1200V Generation 7 IGBTs, a reliable equivalent from a reputable manufacturer is now available to address this issue also in the low power range. The 1200V RGA IGBT from ROHM is a perfect alternative to the Generation 7 IGBT and can be made to behave in a remarkably similar manner with small gate resistor adjustment. Slight differences in conduction losses are completely compensated by improved thermal performance. This makes the 1200V RGA IGBT’s performance in the application fully compatible with the latest Generation 7 IGBTs available in the same power module packages. With humidity, short-circuit, and temperature robustness, the 1200V ROHM RGA IGBT is positioned to be a highly reliable choice when packaged in Semikron Danfoss power modules.

References

Introduction of new IGBT Generation 7 (AN 19-002); <https://www.semikron-danfoss.com/dl/service-support/downloads/download/semikron-application-note-introduction-of-new-igbt-generation-7-en-2019-10-10-rev-01.pdf>

www.semikron-danfoss.com

Your reference for wide-band AC current measurement









Visit us at

pcim

EUROPE


Hall 7 – 116

CWT

For over 25 years, PEM Ltd has been helping customers measure AC currents using our innovative market leading **CWT** range of flexible, clip-around, wide-band Rogowski probes. Whatever your application, we have an unrivalled range of flexible probes to meet your needs, featuring:

- High frequency innovation, with bandwidths up to 50 MHz and patented noise immune shielding
- Accurate gain/phase response from less than 0.1Hz into the MHz range
- Coil geometries to suit the smallest spaces, the largest conductors and the most challenging environments



www.pemuk.com

info@pemuk.com

Test-to-Fail Methodology for Accurate Reliability and Lifetime Evaluation of eGaN Devices in Solar Applications

Modern solar panels are demanding increasingly higher power density and longer operating lifetimes. Solar applications including power optimizers and panels with built-in microinverter are becoming the prevailing trend for an increasing number of solar customers, where low voltage GaN power devices ($V_{DS} < 200$ V) are extensively used.

By Shengke Zhang, Ricardo Garcia, and Siddhesh Gajare, Efficient Power Conversion (EPC)

Greater than 25 years of reliable operation is a typical requirement for solar installations. The test-to-fail methodology stresses devices to failures quickly. By understanding the intrinsic underlying failure mechanisms, physics-based lifetime models can be developed to accurately predict the lifetime under all mission profiles [1-5]. In this report, we use these physical insights and apply them to the unique demands of solar applications.

the device is exposed to high drain-source voltage (V_{DS}). By understanding hot electrons trapping mechanism, a hard switching topology circuit was developed and implemented to accelerate this failure mechanism by providing more hot electrons at maximum rated V_{DS} [2,6-8] and beyond. Using the characterization test results from this development, a physics-based lifetime model was developed to describe the dynamic $R_{DS(on)}$ effects in eGaN FETs under all bias and temperature stress conditions.

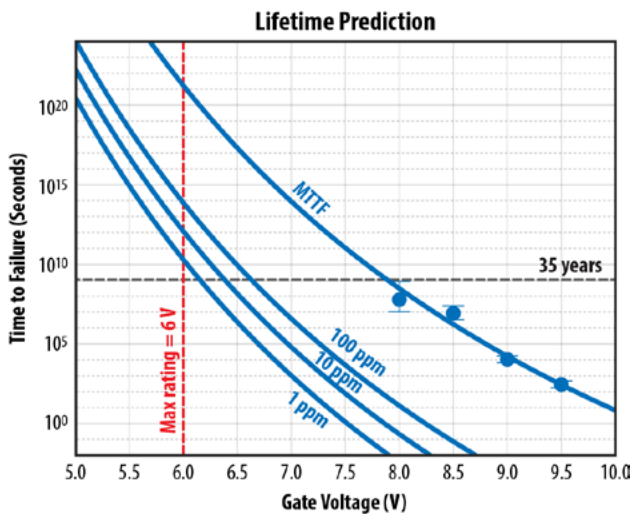


Figure 1: EPC2212 time to failure vs. V_{GS} at 25°C MTF (and error bars) are shown for four different voltage legs.

Gate Stress:

Representative discrete GaN devices (EPC2212) showed excellent long-term gate reliability. Failure analysis was conducted on multiple failures from the study, and a consistent failure mode was found between the gate metal and the metal field plate. By understanding the underlying failure mechanism, a first-principles model was developed to explain all observations. This model can be used to predict the lifetime under different gate biases, temperatures, and duty cycles. The lifetime equation is plotted against the measured accelerated data for EPC2212 in Figure 1. Figure 1 shows that EPC2212 has less than 1 ppm failure rate projected over more than 35 years of lifetime under continuous DC gate bias at the maximum rated gate voltage ($V_{GS} = 6$ V). This projected result is also consistent with EPC's field experience for gate failures.

Drain Stress:

One common concern for GaN is dynamic on-resistance. This is a condition whereby the on-resistance of a transistor increases when

Flyback is one of the most used topologies for the microinverters in solar applications where the EPC2059, a 170 V max V_{DS} rated product, is frequently selected by solar customers for such applications. Figure 2 shows an EPC2059 device that was operated under continuous hard switching at 136 V (80% of the max rated drain bias of 170 V) while the case temperature was modulated at 80°C, where 80°C is considered a nominal operation temperature for solar applications. The measured data and the corresponding model predict the $R_{DS(on)}$ increase due to continuous hard switching in 35 years is expected to be approximately 10%.

Another popular option for solar applications is to use a DC-DC converter in the primary stage (typically a full bridge) of a microinverter. This topology is frequently used in a power optimizer, which has been increasingly adopted by solar providers due to its superior efficiency. GaN devices such as 100 V-rated EPC2218, EPC2088, and EPC2302, among others, are a good fit for this application. Fig-

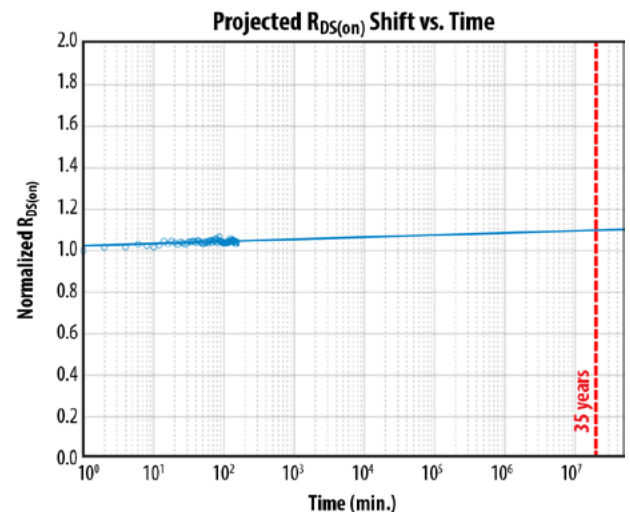


Figure 2: Projected $R_{DS(on)}$ shift of EPC2059, a 170 V rated device, in 35 years of continuous hard-switching operation is expected to be approximately 10%.

Figure 3 shows the projected $R_{DS(on)}$ increase of an EPC2218 device is expected to be 10% in 35 years of continuous hard switching operation at 80 V, ambient temperature.

Therefore, eGaN devices demonstrate good robustness in dynamic on-resistance with more than 25 years of lifetime and beyond.

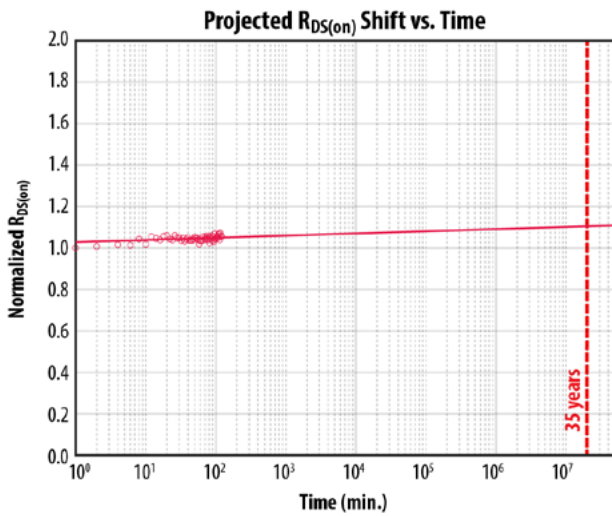


Figure 3: Projected $R_{DS(ON)}$ shift of EPC2218, a 100 V rated device in 35 years of continuous hard-switching operation is expected to be approximately 10%.

Thermo-mechanical stress:

Thermo-mechanical reliability is another critical area of particular interest in solar applications. Solar panels are placed outside and experience significant ambient temperature change. A similar test-to-fail approach was used to study the board level thermo-mechanical reliability of EPC2218A.

Three different combinations of test conditions are studied as shown below.

- TC1 condition without underfill: -40°C to 125°C
- TC2 condition without underfill: -40°C to 105°C.
- TC1 condition with underfill: -40°C to 125°C, where the underfill manufacturer is HENKELS and the part number is ECCOBOND-UF 1173.

All parts were mounted on test coupons consisting of a 2-layer, 1.6 mm thick, FR4 board using SAC305 solder paste, and water-soluble flux. A group of 88 devices was tested for each leg, and all three test legs used similar ramp rate and dwell time at the two temperature extremes. After every temperature cycling interval, electrical

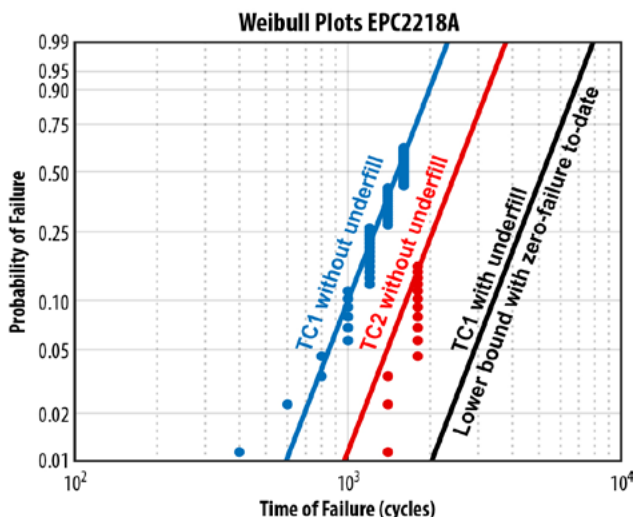


Figure 4: Weibull plots of temperature cycling results for EPC2218A.

PCIM 2023 – Nürnberg
 Visit us in Hall 9, Booth 9-531



**Vertically Integrated
 III-V Manufacturing**

**Delivering the highest grade materials,
 advanced compound semiconductor
 technologies & high reliability, with state-
 of-the-art III-V equipment.**

- Power SiC devices & foundry services
- Power GaN foundry services
- Backend assembly and test services
- Full turnkey manufacturing platform



www.sanan-ic.com

EU: +49 176-62139892

USA: 657-247-0089

HQ: +86-592-6300505

IATF 16949:2016 | ISO 9001:2015 | ISO 27001:2013

@Sanan-IC

screening was performed, where exceeding datasheet limits was used to determine failures. Physical cross-sectioning and SEM inspection followed to further examine the electrical test failures. Solder joint cracking was found to be the single failure mode through-out all failures analyzed.

Figure 4 shows Weibull failure distribution of the temperature cycling results. The failure distribution was analyzed using a 2-parameter Weibull distribution for each temperature cycling leg using maximum likelihood estimation (MLE) [9]. The fits are indicated by solid lines in the graph.

From TC1 (-40°C to 125°C) to TC2 (-40°C to 105°C) without underfill, a strong acceleration was found. Two primary failure mechanisms are responsible for the significant acceleration. First, the difference in ΔT of two testing conditions leads to the acceleration of the solder fatigue failure mechanism [10,11]. However, this failure mechanism alone is insufficient to explain the acceleration observed. A second mechanism, creep solder joint failure mechanism, is introduced. Creep is believed to be the main effect during the dwell period at the hot temperature extreme [11-16].

After 1800 cycles of TC1 (-40°C to 125°C) with underfill, no failures have been found to-date. This shows that applying proper underfill material can significantly improve the thermo-mechanical capability of the chip-scale package devices. Based on the test results, a more general TC lifetime model was developed.

$$N = A \cdot f^{-\alpha} \cdot \Delta T^{-\beta} \cdot \exp\left(\frac{E_a}{kT_{Max}}\right) \quad \text{equation (1)}$$

Where N is the number of cycles to fail, f is the cycling frequency and α is the frequency exponent, at $-1/3$ [12-17]. This frequency term is to describe the frequency of usage. ΔT is the range of temperature change and β is the temperature exponent. Since SAC305 solder is used, β is 2.0 [12-17]. The last variable is an Arrhenius term that models the creep failure mechanism, where E_a is the activation energy, k is the Boltzmann constant, and T_{max} is the maximum temperature in Kelvin units (°K). By comparing the mean-time-to-fail between TC1 and TC2 without underfill, the E_a was calculated to be 0.2 eV.

In real world application, solar panels experience varying temperature profiles. As a result, a more general lifetime model is warranted to include all mission profiles. An empirical equation is therefore developed in equation 2.

$$\frac{1}{N_{Total}} = \frac{a}{N_{\Delta T_a}} + \frac{b}{N_{\Delta T_b}} + \dots + \frac{i}{N_{\Delta T_i}} \quad \text{equation (2)}$$

Where N_{Total} is the total calculated lifetime of number of cycles, $N_{\Delta T_i}$ corresponds to cycles-to-failure for the condition of ΔT_i and i is the fraction of time the device was operational under ΔT_i .

Now let's examine a real-world example to estimate the lifetime by applying different mission profiles. The first assumption is that the solar panels are installed in Phoenix, Arizona, where solar is well-suited for the climate that has long sun exposure, but also demands stringent thermo-mechanical requirements. Using the year 2023 forecast as an example [18] and then adding 30 °C of device self-heating on top of each ambient mission profile, the projected lifetime of EPC2218A with underfill material at 0.1% failure rate is estimated to be approximately 42 years due to temperature cycling stress.

Conclusions:

Based on the discussions above, making use of EPC's 100 V rated generation 5 product family with underfill for real-world solar application vastly reduces thermal cycling reliability risk while giving excellent lifetimes that significantly exceed the expected 25 years.

References:

- Lidow, A., "GaN Transistors for Efficient Power Conversion, Third Edition", John Wiley & Sons, 2019
- Lidow, A., "GaN Power Devices and Applications", 2021
- Meneghini, M., et al. "GaN-based power devices: Physics, reliability, and perspectives", J. Appl. Phys. 130, 181101, 2021
- De Santi, C. et al, "Review on the degradation of GaN-based lateral power transistors", Advances in Electrical Engineering, Electronics and Energy, Vol. 1, 100018, 2021
- Stockman, A. et al, "Gate Conduction Mechanisms and Lifetime Modeling of p-Gate AlGaIn/GaN High-Electron-Mobility Transistors", IEEE Transactions on Electron Devices, PP(99):1-8, 2018
- Lidow, A et al., "Intrinsic Failure Mechanisms in GaN-on-Si Power Transistors", IEEE Power Electronics Magazine, vol. 7, no. 4, pp. 28-35, 2020
- Zhang, S. et al, "GaN Reliability and Lifetime Projections", CIPS 2022; 12th International Conference on Integrated Power Electronics Systems, pp. 1-7, 2022
- Brazzini, T., et al., "Mechanism of hot electron electroluminescence in GaN-based transistors," J. Phys. D: Appl. Phys. 49, 435101, 2016
- Cramér, H., "Mathematical methods of statistics", Princeton Univ. Press (1946)
- JEDEC Standard, "Temperature Cycling", Test Method JESD22-A104F, November 2020
- Automotive Electronics Council, "FAILURE MECHANISM BASED STRESS TEST QUALIFICATION FOR DISCRETE SEMICONDUCTORS IN AUTOMOTIVE APPLICATIONS", AEC-Q101-Rev E, March 2021
- Norris, K. C., & Landzberg, A. H., "Reliability of Controlled Collapse Interconnections", IBM Journal of Research and Development, 13(3), pp. 266-271, 1969
- Vasudevan, V., and Fan, X., "An Acceleration Model for Lead-Free (SAC) Solder Joint Reliability Under Thermal Cycling," ECTC, pp. 139-145, 2008
- Sun, F.Q., Liu, J.C., Cao, Z.Q. et al. "Modified Norris-Landzberg Model and Optimum Design of Temperature Cycling Alt." Strength Mater 48, pp. 135-145, 2016
- Lall, P., Shirgaokar, A., and Arunachalam, D. "Norris-Landzberg Acceleration Factors and Goldmann Constants for SAC305 Lead-Free Electronics." ASME. J. Electron. Packag., 134(3), 031008, 2012
- Deshpande, A., Jiang, Q., Dasgupta, A., and Becker, U., "Fatigue Life of Joint-Scale SAC305 Solder Specimens in Tensile and Shear Mode," 18th IEEE Intersociety Conference on Thermal and Thermomechanical Phenomena in Electronic Systems (ITHERM), Las Vegas, NV, USA, pp. 1026-1029, 2019
- Cui, H., "Accelerated Temperature Cycle Test and Coffin-Manson Model for Electronic Packaging", RAMS, pp. 556-560, 2005
- "MSN weather", <https://www.msn.com/en-us/weather/monthlyforecast>, January 2023

Need to include thermal aspects in your converter simulation?



Download PLECS semiconductor loss models from leading manufacturers

Get More Out of Your Heat Pump

High functional integration and power density are at the foundation of our energy-efficient, cost-effective power modules for motor drives tailored to the needs of advanced heat pump solutions.

By Michele Portico, Senior Product Marketing Manager, Vincotech

Heat pumps are in the spotlight these days, for good reasons. They dramatically increase the energy efficiency of indoor heating, cooling, and hot water production. This allows them to contribute to meeting growing demand for renewable energy sources and curb global CO₂ emissions. And, thanks to their high efficiency and the availability of government subsidies promoting sustainable heating and cooling technologies, they have become a smart investment that pays for itself.

It's no wonder that heat pumps are already the most popular form of heating in Europe's residential buildings, accounting for almost 80% of renewable energy systems deployed on the continent. Around the world, they are finding their way into the heating infrastructure of shopping centers, logistics centers, and other commercial buildings, driven, for instance, by the Chinese government's "Coal to Electricity" program, promoting a shift from coal-based to electrical heating systems in the colder parts of China.

Efficiency gains that add up over a lifetime

Unlike conventional heating systems that produce heat through combustion, heat pumps work by extracting heat from a source – the outdoor air, or underground – and transferring it to a desired destination. To do so, they rely on several mechanical components. These include a compressor, a condenser, an expansion valve, and an evaporator.

Operating continuously throughout the system's lifetime, the compressor makes up for most of the system's power demand. As a result, even small improvements to its efficiency add up, resulting in considerable energy emissions savings. Fortunately, there continue to be underexploited avenues that promise efficiency gains by the compressor.

For one, heat pumps require reliable power modules that convert all the power they receive into performance. This makes active power factor correction an indispensable feature in these applications. Additionally, drives for heat pumps require a motor inverter capable of controlling their output to maximize both efficiency and comfort. Vincotech has been leading the market for products that integrate both of these functionalities into one module for the past 15 years.

Delivering high functional integration and power density

Vincotech solutions are designed to deliver high functional integration and power density, enabling the design of cost-effective embedded systems. Their high level of integration lets system engineers take advantage of a proven combination of power components and gate drive circuits to develop more compact final products. And because Vincotech's modules integrate multiple functionalities into a single package, they cut the development time of new drives, dramatically reducing costs at a system level and time to market.

Drawing on our vast experience and know-how in developing power modules with power factor correction and a motor inverter, Vincotech has developed a power-efficient, cost-effective product portfolio specifically tailored to the needs of today's heat pump applications. Designed around key constraints identified by the customers, the modules offer an optimal solution combining multiple innovative technologies that all aim to increase the degree of integration:

- Thick-film technology for intelligent power modules
- Power-integrated modules with integrated power factor correction circuits
- Thin ceramic for improved thermal performance.

At the same time, Vincotech has been spearheading the trend towards the integration of other key features such as shunt systems, on-board capacitors, and

interleaved power factor correction topology that support the complex electrical and thermal design of motor drives.

The unique features of our 600V flowPIM + PFC family

As we've seen, one of the main goals in the design of heat pump systems is to increase their power density, simply defined as the ratio between the power output and the volume of the system. There are many ways to achieve this:

- Moving towards more compact designs
- Increasing the efficiency of the energy conversion
- Integrating more cost-effective solutions

Vincotech's power-integrated module (PIM) with an interleaved power factor correction (PFC) circuit is a unique and innovative topology for power modules featuring a high level of integration as well as improved energy conversion efficiency.

The interleaved configuration offers several benefits:

- Simplified PCB design
- Higher energy conversion efficiency
- Better heating distribution
- Smaller components on the PCB
- Easier EMI filtering design
- Reduced output RMS current

Designed for power ranges up to 8 kW, Vincotech's 600V flowPIM + PFC family comprises three different sub-families featuring a two-leg interleaved PFC circuit, both with and without an integrated input rectifier, and a three-leg interleaved PFC without an input rectifier (see Figure 1).

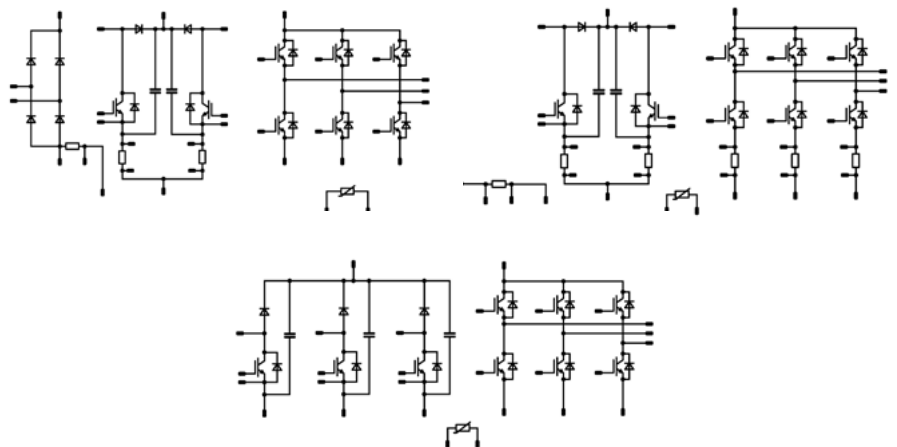


Figure 1: The three sub-families of the Vincotech 600V flowPIM + PFC family featuring a two-leg interleaved PFC circuit with and without an integrated input rectifier and a three-leg interleaved PFC without an input rectifier.

MAY 09- 11



Vincotech

JOIN US AT PCIM

PCIM Europe is coming up on May 9 through 11 in Nürnberg, Germany. Vincotech is all about teamwork. Your project is our priority; your success is our first concern. Take advantage of Vincotech's experience and innovative powers. Let us go from strength to strength, together.

To make the most of your designs, you have to strike the right balance between performance and cost. That can be tricky if you don't have a way of assessing every alternative. Our PCIM booth lets you explore every option. Putting the latest technologies and innovations at your fingertips, our simulation tool enables you to find the perfect match for your solar, EV charger, UPS or motion control product.

Our presentations at PCIM

Tuesday 09.05. | 15 - 17 | PCIM Conference – Poster presentations
Analysis of Tandem Diodes Solutions for Power Modules in Motor Drives Applications

Tuesday 09.05. | at 13:20 | Exhibitor Forum
Enhanced functional integration and power density for heat pumps: single-phase and three-phase PFC modules for power ranges up to 15 kW

Thursday 11.05. | at 10:00 | Exhibitor Forum
Flying capacitor inverters and 1500 V utility-scale PV systems – the perfect match

vincotech.com/PCIM

VINCOTECH @
PCIM
EUROPE 2023
BOOTH 7-411

STRONGER TOGETHER WITH VINCOTECH

All variants are equipped with a three-phase motor inverter and a temperature sensor.

Products with two-leg interleaved PFC also feature shunt resistors in the motor inverter and in the PFC circuit. The PFC's common and leg shunts make it possible to perfectly balance the current in the PFC circuit, increasing the chipset's lifetime. Shunt resistors integrated in each leg of the inverter vastly improve motor control.

Furthermore, on-board capacitors dramatically reduce the DC-link voltage overshoot (see Figure 2).

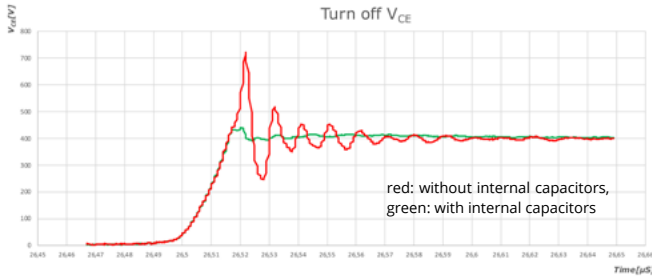


Figure 2: The Vincotech 600V flowPIM + PFC family's on-board capacitors dramatically reduce the DC-link voltage overshoot

The products' carefully designed layout offers the best compromise between cost and performance. For one, positioning the power pins at the edge of the power modules simplifies their PCB design and lowers their cost. Moreover, separating the inverter and PFC parts optimizes their thermal design.

A new era starts now with the PIM + 3-ph PFC product family

Higher power ranges in heat pumps are accelerating the adoption of three-phase PFC topologies, driven by the requirements for high power density and more efficient and effective power distribution and power conversion.

Enabling power ranges up to 15 kW, Vincotech's new 1200V flowPIM® S3 + 3xPFC featuring current-synthesizing PFC (CS-PFC) addresses these challenges, optimally balancing performance and system cost.

The current synthesizing PFC requires more switching components than the state-of-the-art NPFC topology, but only the half-bridge switches at a high switching frequency (HF) and only at the 3rd harmonic current.

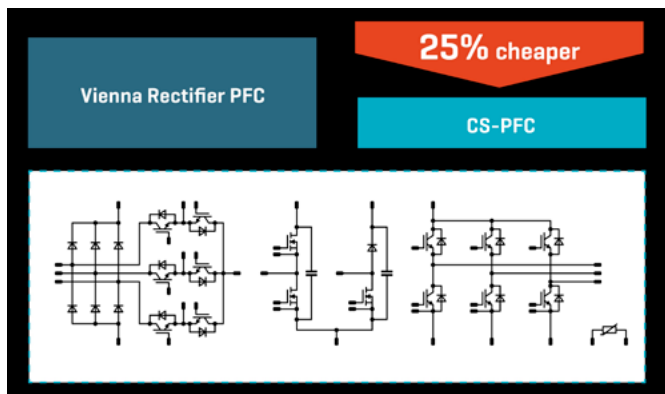


Figure 3: The Vincotech flowPIM S3 + 3xPFC with inverter stage for up to 15 kW applications based on CS-PFC topology

It's a tradeoff that pays off. Current-synthesizing PFC slashes module costs by 25% (up to 40% without a booster stage) while achieving a conversion efficiency up to over 99% (Figure 3).

Meanwhile, our new 1200V flowPIM® 1 + 3xPFC targets high-end applications in heat pumps. It is an all-in-one solution that uses 3-phase PFC, the AN-PFC topology, and an inverter stage to achieve a superior level of efficiency while reducing the system costs (Figure 4).

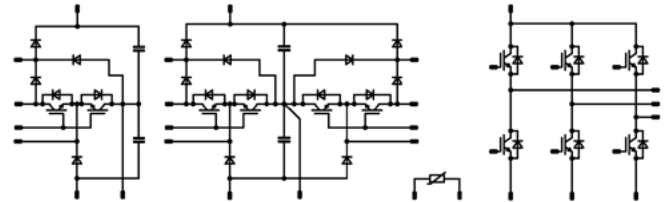


Figure 4: Vincotech's new 1200V flowPIM® 1 + 3xPFC for high-end heat pump applications.

The AN-PFC topology with SiC diodes assures high efficiencies for switching frequencies up to 150kHz. This lets drive designers dramatically reduce the size and cost of the passive components on the PCB, leading to huge cost savings at the system level (Figure 5).

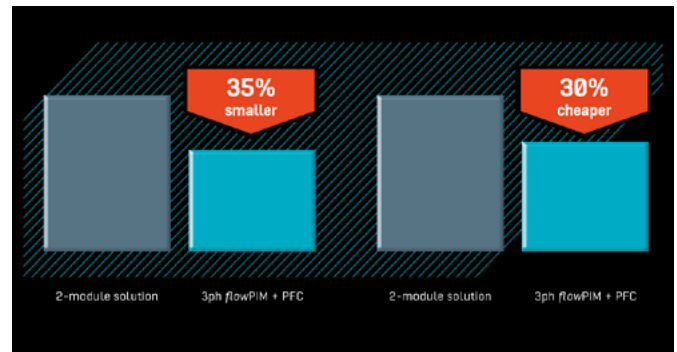


Figure 5: The AN-PFC topology with SiC diodes dramatically reduces the size and cost of the 3ph flowPIM + PFC solution.

Finally, the inverter stage's high-speed IGBTs and diodes enable high switching frequency operation and enhance efficiency.

A one-stop solution provider

Vincotech's motion control solutions for heat pump applications build on the deep experience developing power electronics solutions for public grid-connected motion control applications. Combining speed and flexibility, we can help you design and develop applications that meet your power range and design specifications, optimally balancing the cost and performance of the end solution.

Vincotech's one-stop power solution offering for complex motion control applications includes application-specific power modules, such as the 600V flowPIM + PFC and 1200V flowPIM® 1 + 3xPFC families presented in this article, full PCB design services, and a feature-rich evaluation board. And as a chip-independent power module manufacturer, we can build solutions around all chips on the market, offering you the best compromise between cost and performance.

www.vincotech.com/EmbeddedDrives

IF IT'S NOT THE HEAT,



IT'S THE HUMIDITY

Meet the 1,500-hour THB-rated ALH/BLH capacitors

At 85°C and 85% relative humidity, with rated voltage applied, our new inverter-grade film capacitors are tested 50% longer than the industry standard requirements for Temperature-Humidity-Bias. Improve the reliability of your power electronics design with outstanding capacitor performance at high humidity.

cde.com/harsh-environments



85°C 85%RH
AEC-Q200

DC/DC Converters For Industrial Applications

Electronic components are designed and manufactured with specific performance characteristics tailored to their target application environments. These environments are segregated based on how harsh they are and what sort of reliability they require.

By Mitch Van Ochten, Application Engineer, Rohm Semiconductor

The Industrial Environment

The “commercial” space is the least demanding, with temperature ranging from 0° C to 70° C and relatively lax reliability expectations. At the other end of the spectrum are “military” grade components, with temperatures ranging from -55 °C to 125 °C and extremely strict requirements for radiation tolerance, shock, moisture, and the like. In between these two extremes one can find a handful of niche application spaces, among which the “industrial” grade components find their home.

In addition to a -40 °C to 85° C operating temperature range, one of the most important characteristics of industrial components is their voltage tolerance. This is especially important for DC/DC converters, which are required to handle a wide input voltage range and switch it down to the more common 5 V and 3.3 V rails. Typical industrial voltage inputs include 60 V, 48 V, and 24 V. Industrial components also carry specifications for ingress and physical handling. Many are IP67 rated, which specifies a high level of ingress protection against dust and water. Vibration ratings may also specify that a product can be in an environment that moves or shakes and will survive temporary or constant oscillation.

Lastly, an often overlooked feature of many industrial components is a 10-year supply guarantee. Since these components are likely to be deployed into environments that are difficult to service, the overall product lifecycle is generally quite long. Ensuring a plentiful supply of replacement devices provides a competitive advantage by guaranteeing a long serviceable life.

ROHM offers a wide range of DC/DC converters specifically tailored to the requirements of industrial applications. The table below provides an overview of these ICs across their range of input and output voltages.

Input*	3.3	5.0	12	24	48	60
Output*						
6.0						
5.0		BD9Cxxx Series				
4.0	BD9Axxx Series BD9Bxxx Series					
3.0		BD9Dxxx Series		BD9Gxxx Series		
2.0			BD9Exxx Series			
1.0				BD9Vxxx Series		
0.5			BD9Gxxx Series			

*Input Power Rail Voltage (V) / *Output Current (A)

Figure 1: ROHM voltage converters for industrial input/output ranges

ROHM Technology

ROHM’s DC/DC converters employ two proprietary technologies to achieve best-in-class performance -- Nano Pulse Control™ and QuiCur™. Nano Pulse Control is a DC/DC switching technology that offers the industry’s smallest pulse width of only 9 nanoseconds. This is 3-4X faster than the nearest competitor, as shown in the following figure.

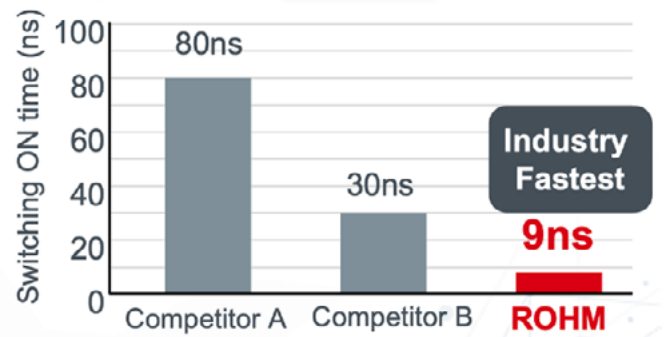


Figure 2: Reduced switching time enables large voltage conversion ratios

This miniscule pulse width allows ROHM’s DC/DC converters to handle large input to output voltage ratios, which is often required for industrial environments. With Nano Pulse Control, these converters can directly buck a 48 V input rail down to a 1 V output in a single stage. Competitive products, on the other hand, require an intermediate step and two separate conversion ICs.

QuiCur is another ROHM technology upon which their industrial DC/DC converters are built. It is a circuit level technique that solves several of the main problems plaguing feedback networks for maximum response performance. As shown in the figure below, this technology relies on introducing two dedicated error amplifiers. In particular, the second stage is critical as it uses a technique whereby its gain is scaled by the overall drive current. The result is

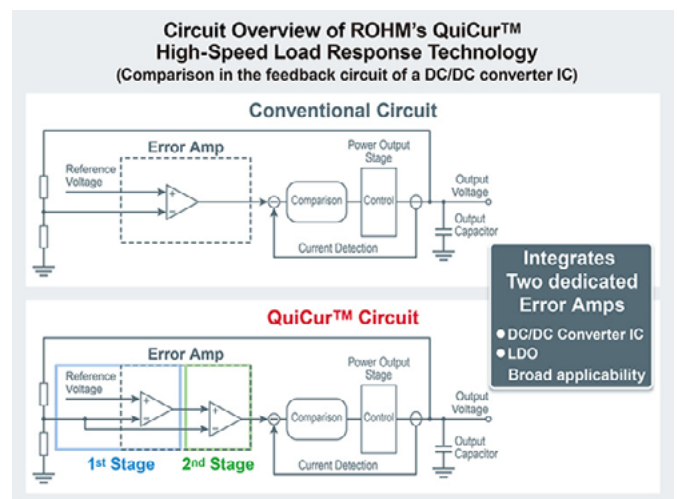
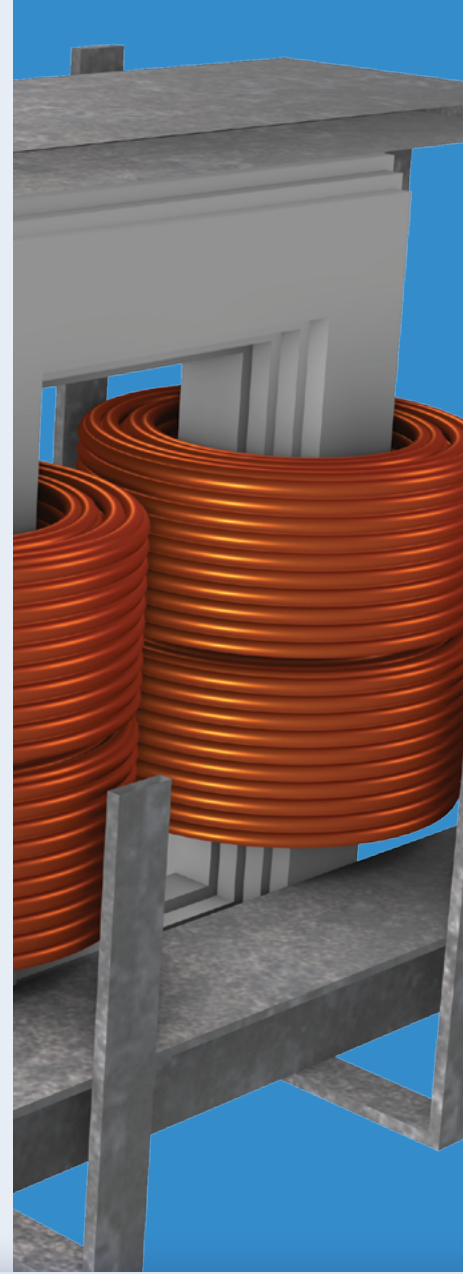
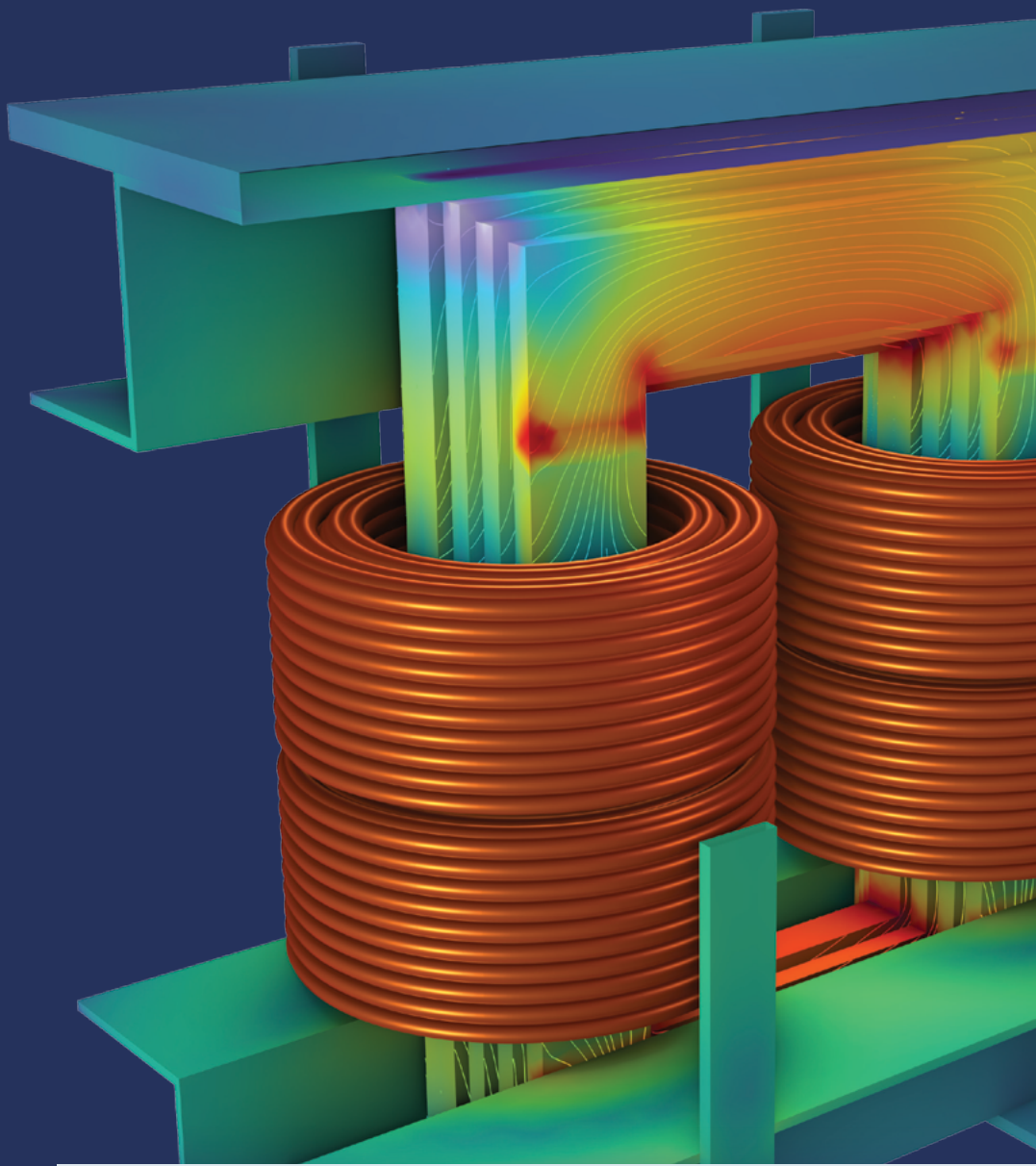


Figure 3: ROHM's QuiCur circuit topology



Power Innovation in Electrical Design

with COMSOL Multiphysics®

Electrification success calls for smart design innovation and fast-paced product development. To achieve this, industry leaders are turning to multiphysics simulation to accurately test, optimize, and predict the performance of high-voltage equipment and power systems.

» comsol.com/feature/electrical-innovation

a much more flexible frequency response, allowing the designer to choose between optimal stability, minimal undershoot, and reduced physical size.

By using ROHM's Nano Pulse Control and QuiCur technologies, designers can choose from a broad portfolio of DC/DC converters and LDO's for industrial applications ranging from high voltage/high current to space constrained, and everything in between.

High Voltage, High Current Solutions

Several common industrial applications start with high voltage AC mains or battery inputs in the range of 48 V to 60 V. As shown in the example below, EV charging stations often include an AC/DC module to provide a 60 V supply from 380 VAC mains. This 60 V rail must be bucked down to 12 V for both the interface circuitry and the high-voltage control circuitry. ROHM's BD9Gxxx series of regulators is able to reliably deliver this 5:1 conversion ratio in a single stage.

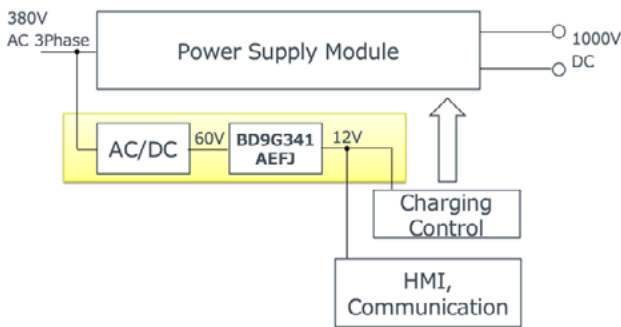


Figure 4: EV Charging Station

Similarly, electric bicycle (eBike) batteries based on Lithium chemistries provide DC outputs in the realm of 60 V. The eBike's supporting circuits, as shown in the figure below, include communication interfaces, high power gate drivers, and battery management modules, which can draw in excess of 3A of current at 5V. Once again, the ROHM BD9Gxxx series of DC/DC converters is the perfect choice for efficiently delivering this type of load current at such a high step down ratio.

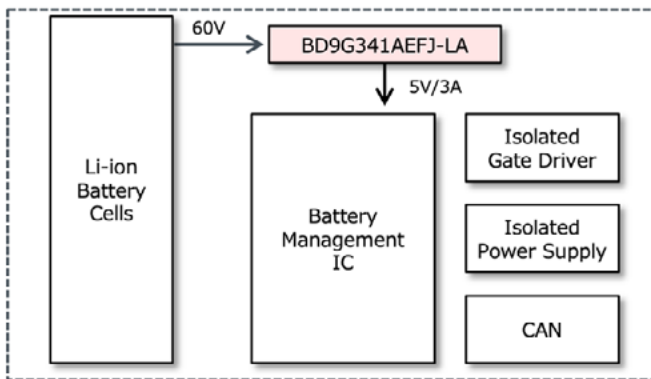


Figure 5: eBike Battery Interface

Space Constrained Solutions

For industrial applications where the input voltage is 24 V or less, but physical space is a premium commodity, ROHM's Nano Pulse Control and QuiCur technologies offer a significant leg up on the competition. This is due to the relative reduction in the size of supporting passives required for these DC/DC converters. The BD9Fxxx series is an excellent example and is compared to the traditional BD9Exxx series in the figure below. The required inductor size and package size yield an area benefit of over 70% while simultaneously offering an increased load current of 67%.

BD9F500QUZ / BD9E303EFJ comparison

	BD9F500QUZ	BD9E303EFJ
Package	VMM16L3030 3.0 x 3.0 mm	HTSOP-J8 4.9 x 6.0 mm
I _{out}	5 A	3 A
Frequency	600 kHz / 1 MHz / 2.2 MHz	300 kHz
L value	1.5 µH - 4.7 µH	10 µH - 22 µH
L size	8.0 x 8.0 mm	10.0 x 10.0 mm

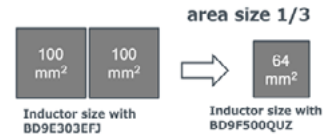


Figure 6: Area reduction due to smaller inductors and smaller IC package

In a similar vein, the improved efficiency of these devices results in less waste heat, in turn reducing the heat sink requirements for reliable operation. As shown in the figure below, the ROHM part operates nearly 35 degrees Celsius cooler than the competitor when pushing 4 A of current. The required heatsink, PCB stackup, and thermal planes will be much less expensive and require significantly less volume.

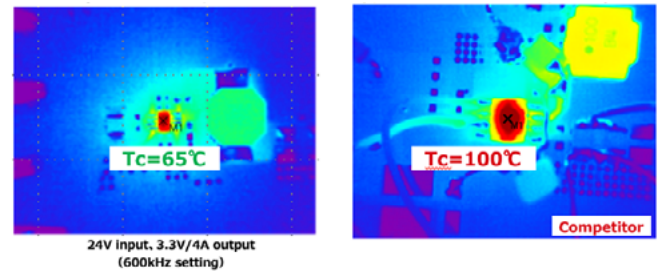


Figure 7: Improved thermal performance eliminates heat sink requirement

When considering QuiCur for improved frequency response, one potential design implication is the reduction of output capacitor size. As shown in the figure below, when stepping from 0.1 A to 3A, the ROHM part exhibits one third of the ripple compared to a competitor switching from a much smaller step. As a result, the designer may choose to reduce the output capacitor size by 70% for the same performance, and save in both space and cost.

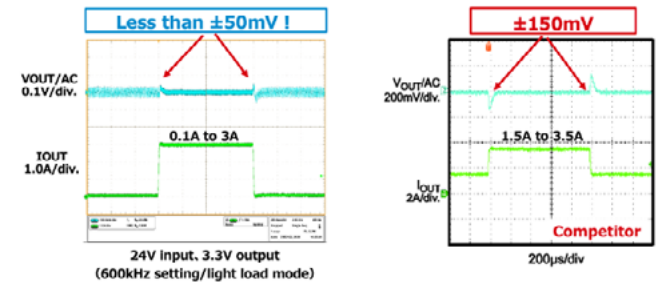


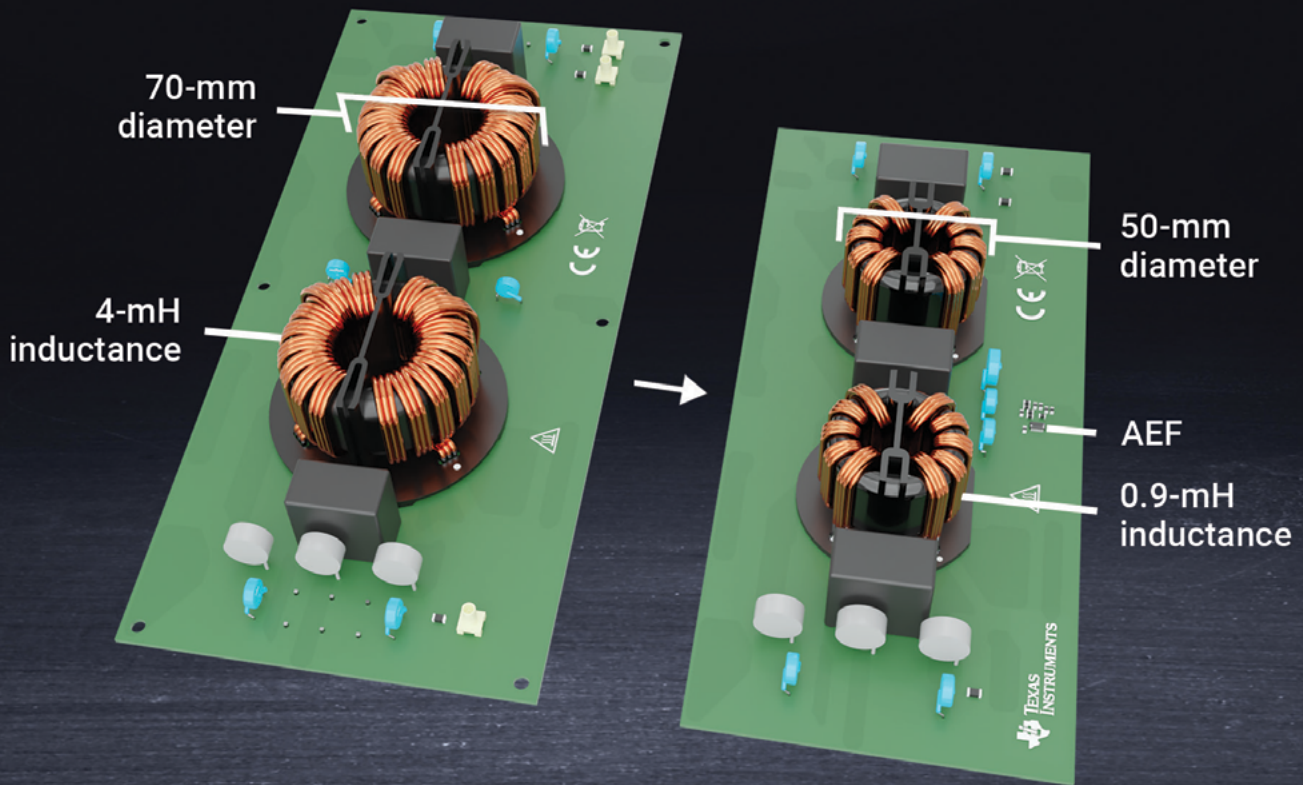
Figure 8: Fast transient response reduces output capacitor requirements

Conclusion

Industrial applications present a unique set of environmental constraints that commercial grade electronics components cannot survive in. Foremost among these are high input voltage and high temperature. ROHM's proprietary Nano Pulse Control and QuiCur technologies are at the heart of a suite of DC/DC converter products that thrive in these environments. They provide large input to output ratios, high performance frequency response, and an overall reduction in physical volume and supporting componentry. As such, these devices find themselves at the front end of many industrial systems and should be on the top of the designer's toolbox when tackling these challenging problems.

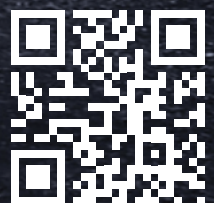
To learn more, visit: <https://www.rohm.com/support/nano> and https://www.rohm.com/documents/11303/9976301/Introduction_NewRelease_QUICur-e.pdf

Meet stringent EMI requirements and cut choke size in half.



Our new portfolio of stand-alone active EMI filter (AEF) ICs help designers meet stringent EMI requirements while reducing system size, weight and cost for single- and three-phase AC/DC systems. The TPSF12C1/-Q1 and TPSF12C3/-Q1 allow engineers to shrink the value of common-mode chokes by up to 80% inductance, resulting in over 50% smaller size compared to purely passive filter solutions. Meet your EMI performance standards and increase power density with AEF ICs today.

▶ [Learn more > www.TI.com/AEF](http://www.TI.com/AEF)



Advanced Inductor Circuit Models

In this article, Dr. Ridley describes new advanced circuit models that can be used to accurately predict the performance of off-the-shelf inductors. This allows the designer to rapidly assess power supply inductor losses by using standard circuit simulation packages.

By Dr. Ray Ridley and Art Nace, Ridley Engineering

Off-The-Shelf Inductors

Over the past 10 years, magnetics manufacturers have made great progress in providing power designers with standard magnetics at reasonable prices. After the product development, the main focus of the technical teams has been to develop comprehensive application test results. These results are provided in custom programs which show the losses with different operating conditions of voltage and frequency.

Figure 1 shows the example inductor that we will be discussing in this article. It is a helical foil inductor from Coilcraft, rated for use up to about 20 A. A lot of time and effort has been spent to provide detailed loss characteristics for the component which can be found interactively by using their DC-DC optimizer program [1].

This data is tremendously useful to a power designer. It's an important step in providing detailed circuit models that are verifiable with test data.

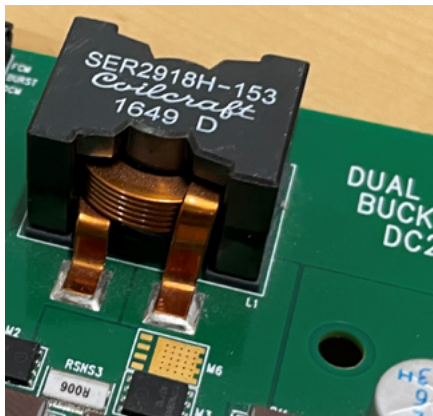


Figure 1: Coilcraft Inductor with Helical Foil Windings

Buck Converter Circuit with Basic Inductor Model

Figure 2 shows a buck converter application with the inductor in place. Notice that the basic circuit model for the inductor includes just the dc resistance and

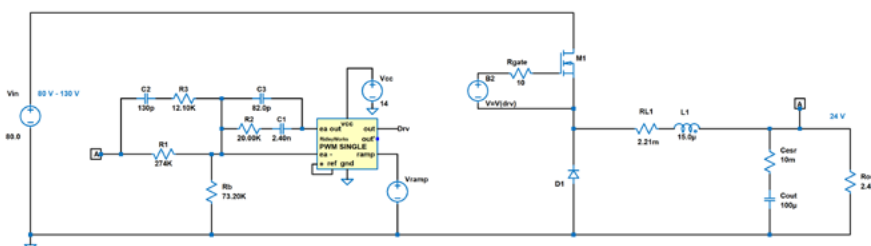
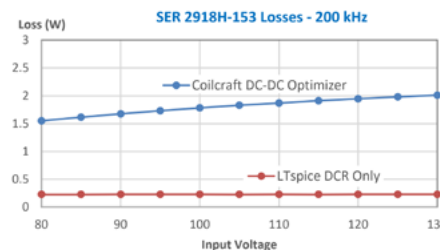


Figure 2: Buck Converter Circuit with Coilcraft Inductor DC Parameters

the fixed inductor value. As we will see, the dc resistance value will provide a very low estimate of the inductor dissipation. There are two ways to assess the performance of the inductor. From the designer's point of view, the most convenient way would be to run an LTspice simulation and just click on the inductor component to see the loss during the simulation. This is what we can do with every other component in the schematic, and it has become a standard for every component EXCEPT the magnetics.

The other way to assess the inductor performance is to use the customized tools developed by the manufacturer of a component for the operating point of the converter. For the inductor being used here, extensive data has been collected and this can be seen by running the Coilcraft DC-DC Optimizer program [1]. Figure 3 shows the graph of this data for different operating points of the buck converter. The graph on the left is for 200 kHz operation with the input voltage varied from 80 V to 130 V. (Output is 24 V at 10 A).



On the right hand graph, the input voltage is fixed at 130 V (highest dissipation voltage) and the frequency varies from 100 kHz to 300 kHz. At low frequencies, the losses increase substantially. Ripple currents are higher and flux excursions in the core are higher. This is not intuitively obvious since you will often read papers claiming that magnetics losses will increase with frequency, not decrease.

While the data is available for the inductor losses through the software from Coilcraft, this is not exactly convenient for the designer. Imagine what a chore it would be if every component of the circuit required a custom program from the vendor to assess its losses. In the semiconductor world, you cannot sell a part unless it has a reasonably accurate simulation model. This expectation has not been applied to the magnetics. There are many reasons for this, but it does not need to be that way.

Advanced Inductor Model in Buck Converter Circuit

Figure 4 shows a much more advanced simulation model for the inductor. In addition

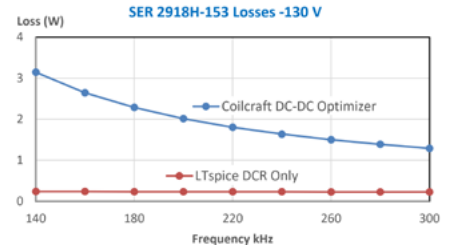


Figure 3: LTspice Simulation Results for DC Inductor Loss Plotted versus Coilcraft DC-DC Optimizer

You can see from the left hand graph how the losses increase with input voltage on the data provided by the Coilcraft DC-DC optimizer. The red curve shows the losses predicted straight from the simulation of the circuit in LTspice. With the dc model, the predicted losses are very low, and there is minimal variation with input voltage.

In addition to the series DC resistance, you can see a block labelled Rac. The resistance of the windings increases with frequency due to proximity losses. There is also a block representing the core loss of the inductor. This is very specific to the core material, number of turns used, and the core dimensions.

All of the parameters of the ac resistance and the core loss model were derived with the help of RidleyWorks design software [2]. These are described later in this article.

Figure 5 compares the data produced by an LTspice simulation of the advanced model with the measured manufacturer's data. The deviation between measured and simulated is very small. This is exactly what the circuit designer wants – a straightforward model that predicts the losses from the

RIDLEYBOX[®]

Light. Portable. Precise. And it talks.

A complete **Design and Test Center**
at your fingertips:

- 4-Channel Frequency Response Analyzer
- 4-Channel 200 MHz Oscilloscope
- **RIDLEYWORKS[®]** Lifetime License
- Ridley Universal Injector
- Intel[®] Computer
- 40 Years of Design Experience
- Only \$6500



simulation, just like every other component in the circuit. Once the designer has a trusted circuit model, it's no longer necessary to use customized software to get the needed results. You can also put the circuit model in ANY topology you like, with arbitrary circuit waveforms, and expect to get reliable results.

network. This type of circuit was first proposed for magnetics winding modeling in [4] and has been used for many years by a few select researchers. It is the basis of the circuit models generated by RidleyWorks. We don't see any usage of this by magnetics manufacturers yet.

This circuit will provide the needed characteristics - the resistor value decreases with frequency showing highest core loss at the lowest frequency. Further explanation of this model will be included in the next installment of this article.

Summary

It is quite reasonable to expect that you can have an accurate simulation model for inductors which will give the power designer exactly what is needed - losses found directly from the simulation that correspond closely with actual measured results. We have shown that for a specific inductor this can be done reliably and with relatively little effort. We hope that the inductor manufacturers will start providing users with these kinds of accurate and advanced models to speed up the design process for working engineers.

References

You can read more information on this topic in each of these references.

1. Coilcraft DC-DC Optimizer software <https://www.coilcraft.com/en-us/tools/dc-dc-optimizer>
2. RidleyWorks design software <https://www.ridleyengineering.com/software-ridley/ridleyworks/ridleyworks-software.html>
3. Measurement of Rac using the Ridley-Box <https://www.ridleyengineering.com/hardware/ridleybox>
4. Francisco de Leon, Adam Semlyen, "TIME DOMAIN MODELING OF EDDY CURRENT EFFECTS FOR TRANSFORMER TRANSIENTS" IEEE Transactions on Power Delivery, Vol. 8, No. 1, January 1993. https://tspace.library.utoronto.ca/bitstream/1807/9972/1/Semlyen_9842_2827.pdf
5. Join 6000+ engineers in our Power Supply Design Center Group on Facebook. <https://www.facebook.com/groups/ridleyengineering/>

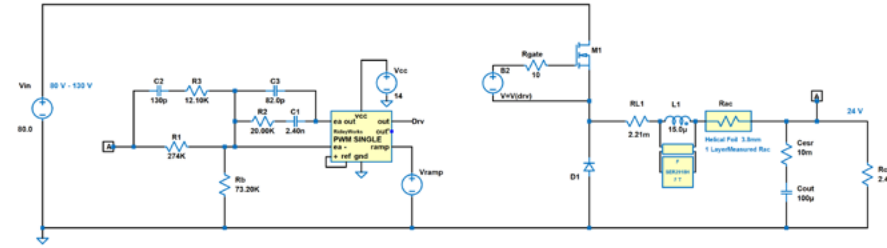


Figure 4: Advanced Inductor Model in Buck Converter Schematic

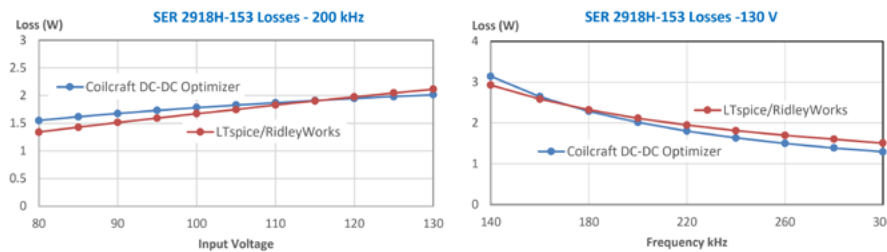


Figure 5: LTspice Simulation Results for Advanced Inductor Model Loss Plotted versus Coilcraft DC-DC Optimizer

Winding Proximity Loss Model

There are two elements needed to match the total losses in the inductor. The first is the winding loss which should be frequency dependent. This is achieved with the circuit diagram shown in Figure 6 which is comprised of 5 inductors and 5 resistors. The circuit values are chosen automatically by RidleyWorks to match the desired ac resistance characteristics. (In the next installment of this article, we will explain how the ac resistance values were derived to give accurate simulation models.)

Advanced Core Loss Model

The second element needed to provide accurate simulation data is a good core loss model. You will find many attempts in the literature to solve the problem of core loss simulation, but none of them have become mainstream.

Figure 7 shows the circuit model derived by RidleyWorks for the sample Coilcraft inductor. This is a set of six parallel R-L branches driven by the voltage across the inductor. A dependent voltage source is used to model the nonlinear exponent of core loss with amplitude, while the R-L branches model the proper frequency dependence.

At dc, all the inductors of the network are short circuits, and the only resistance left is Rdc. The inductors become higher impedances with increased frequency, sequentially increasing the resistance of the

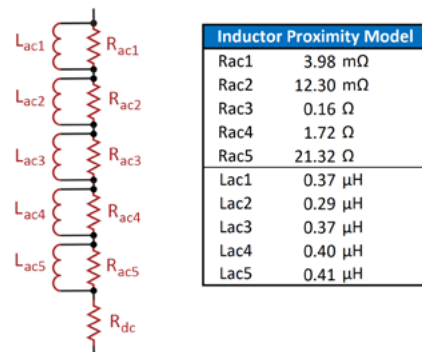


Figure 6: Winding Loss Circuit Model for the Coilcraft Inductor

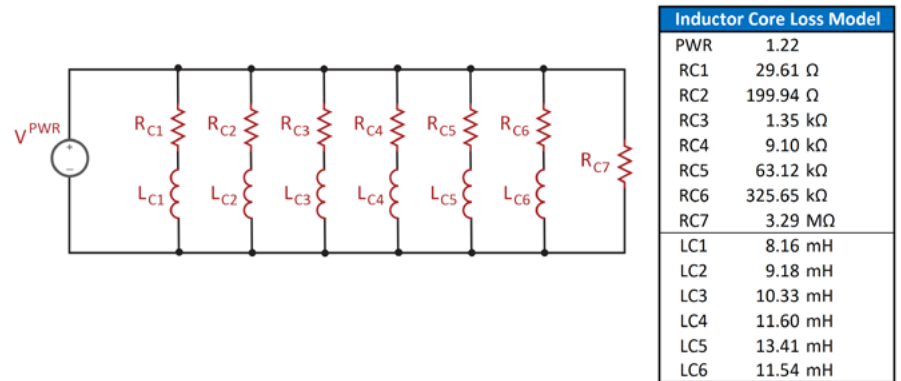


Figure 7: Core Loss Circuit Model for the Coilcraft Inductor

mesago

pcim

EUROPE

9 – 11.5.2023
NUREMBERG, GERMANY

**EXPERIENCE
A WORLD
OF POWER
ELECTRONICS!**

**Get your
ticket now.**

Messe Frankfurt Group

pcim

ASIA

29 – 31 August 2023
Shanghai New International
Expo Centre, Shanghai, China

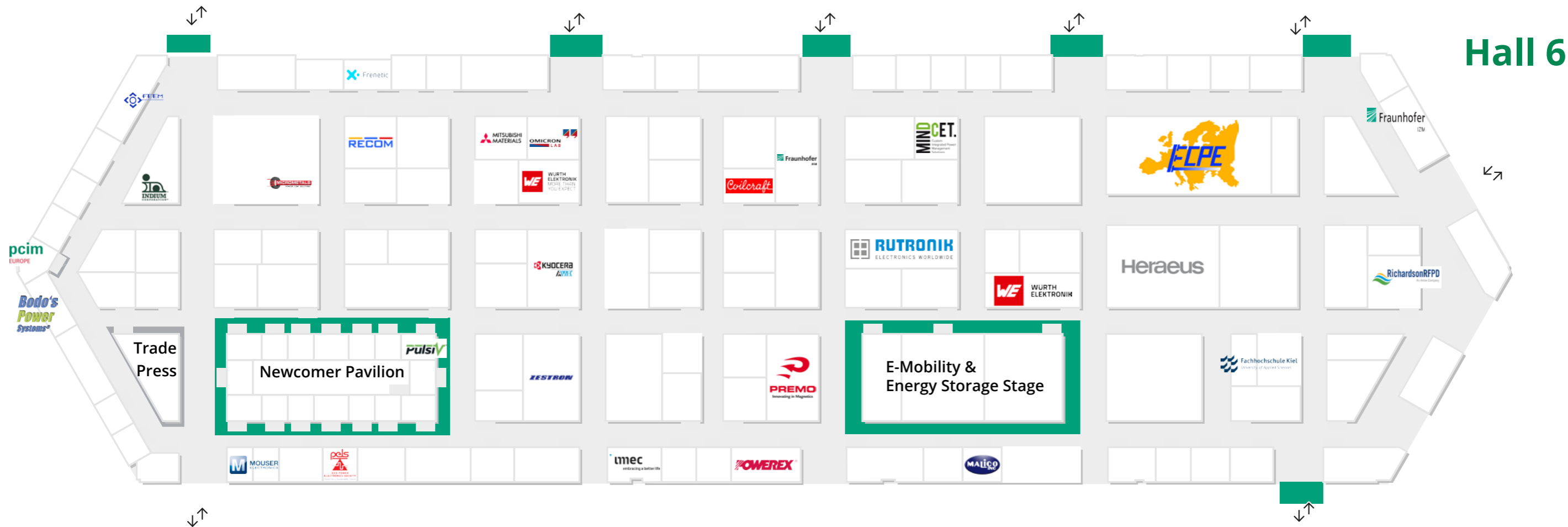
International Exhibition and Conference for
Power Electronics, Intelligent Motion, Renewable
Energy and Energy Management

**Power electronics
towards a sustainable
new era**

www.pcimasia-expo.com

mesago

messe frankfurt



pcim

EUROPE

International Exhibition and Conference
for Power Electronics, Intelligent Motion,
Renewable Energy and Energy Management
Nuremberg, 9 – 11 May 2023

Industry Stage | Hall 7, 480 | Industry Stage

1:05 - 2:05 PM
(GMT+2)
10. May '23

Wide Bandgap Design with GaN HEMT and Vertical GaN

Panel discussion

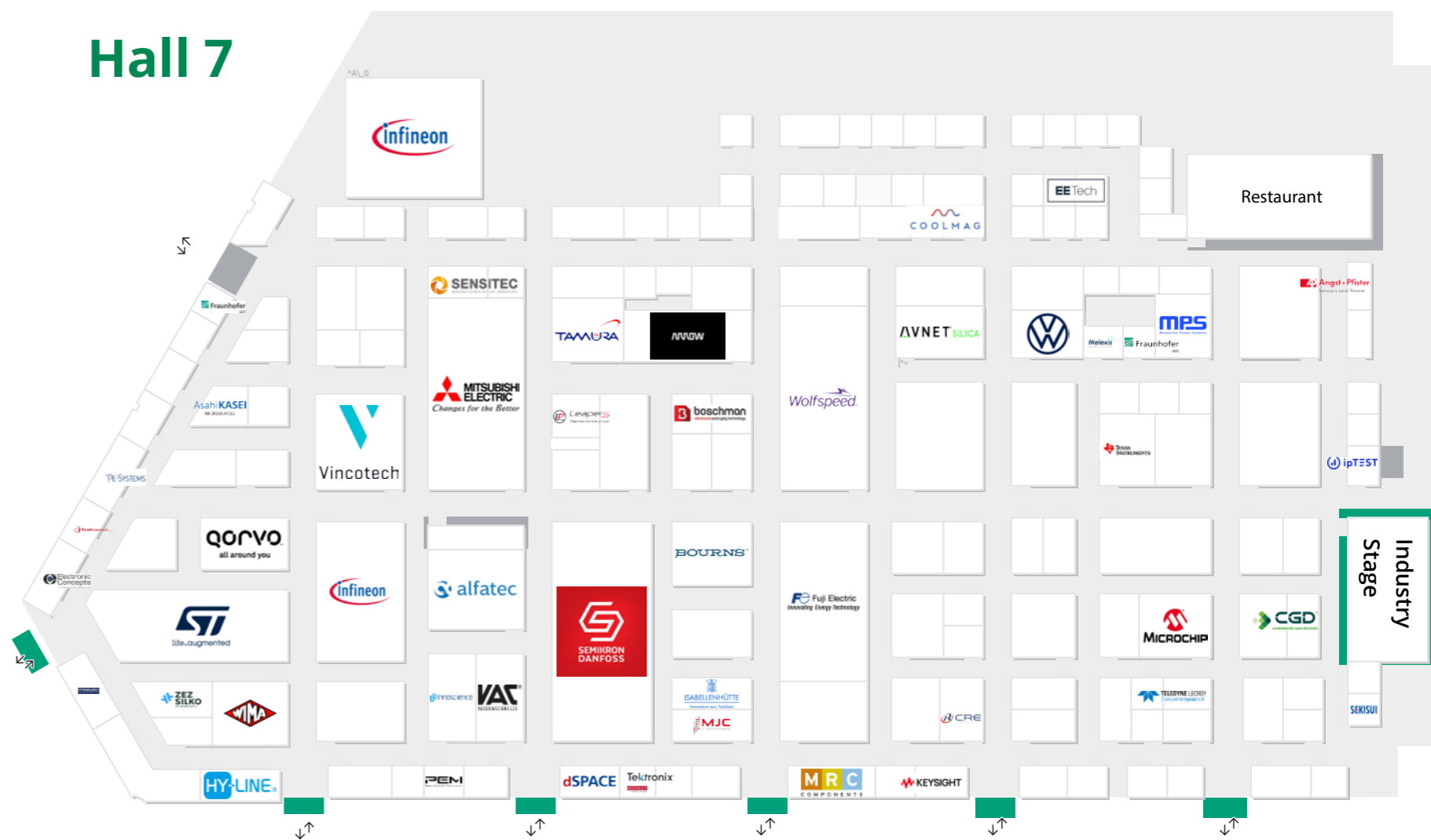
Industry Stage | Hall 7, 480 | Industry Stage

2:10 - 3:10 PM
(GMT+2)
10. May '23

Wide Bandgap Design with SiC for High-Voltage Applications

Panel discussion

Hall 7



Hall 9



Designed for the Future

30 years of SKiiP® IPM

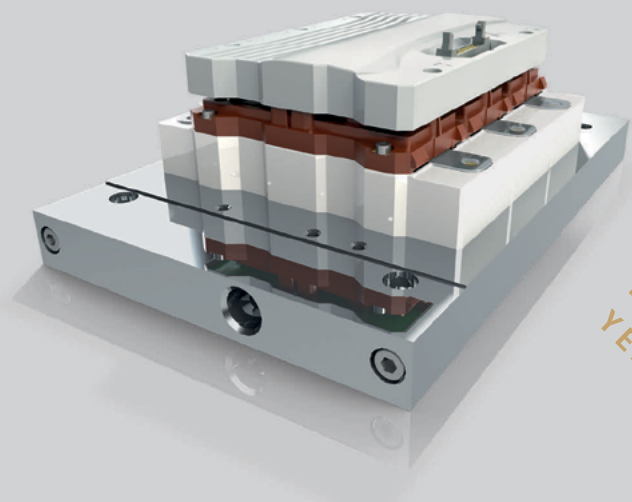


Visit us at
PCIM Europe
Nuremberg, 9 - 11 May
Hall 7, Booth 422

SKiiP® IPM

Two million modules in the field

- 1993** Start of SKiiP technology development
- 1995** First module with pressure-contact technology
- 1997** First IPM on the market with overcurrent protection
- 2022** More than 500 GW installed worldwide
- 2023** Launch of SKiiP7



30
YEARS
SKiiP IPM

Learn more about the
SKiiP success story



Extending Output Power of Unified, AC-Input Light Industrial Applications Through Low $R_{DS(ON)}$ SiC MOSFETs

For light industrial applications, a unified platform for single and 3-phase AC input can be designed using a 1200 V SiC MOSFET and a diode in the Power factor correction (PFC) stage to maintain a constant DC link voltage of 540 V.

By Simon Kim and Kwok Wai Ma, Infineon Technologies

Commercial fridge applications of 5.25 kW can be realized using a 30 m Ω SiC MOSFET in the PFC stage. Using a low $R_{DS(ON)}$ 14 m Ω , 7 m Ω , or two 30 m Ω SiC MOSFETs in parallel, can mitigate the thermal bottleneck at PFC, and extend the output power to 7 kW for commercial air conditioner applications. Paralleling SiC MOSFETs gives a better thermal performance by effectively reducing the case-to-heat sink thermal resistance by half.

Commercial refrigerators and air conditioners (CAC) are two major types of light industrial applications, with maximum power levels of 5.25 kW and 7 kW respectively with single-phase AC input. The power electronics circuit of these applications is composed of a single-phase input rectifier, a PFC boost circuit, and a 3-phase inverter circuit (often with forced air cooling) [1][2]. The requirement for different topology and voltage classes, in the input stage and inverter stage, can be substantially simplified by a unified platform that uses 1200 V class power devices for rectifier, inverter, and PFC stages. An example of such a unified platform with a power integrated module (PIM), a SiC MOSFET, and a diode is shown in figure 1.

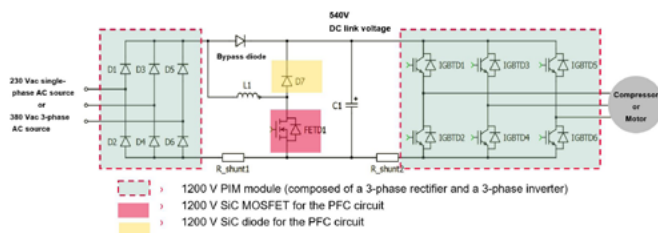


Figure 1: Concept of the unified platform with a 1200 V PIM IGBT module, a SiC MOSFET, and a diode

SiC MOSFETs and diodes are essential for the PFC stage due to their low losses and high switching frequencies. In this platform, a 6-channel gate driver IC, 6ED2230ST, and an IGBT module, FP25R12W1T7, have been used in the inverter stage. When a 230 V_{ac} single-phase AC is used, the DC link voltage is boosted to 540 V by the PFC stage. On the other hand, when a 380 V_{ac} 3-phase AC is used, the PFC circuit is bypassed by the diode or relay but the DC link voltage can still reach 540 V. As shown in previous works, for a 5.25 kW commercial fridge inverter application a 30 m Ω SiC MOSFET in the PFC stage will help meet all thermal requirements [1]. When the same design is used for 7 kW CACs, the junction temperature, T_{Vj} , of all power devices remains within the thermal limit, except of the PFC SiC MOSFET and this becomes a thermal bottleneck [3]. This article discusses how using a SiC MOSFET with lower $R_{DS(ON)}$ to reduce power loss can extend the system power level from 5.25 kW to 7 kW for both commercial refrigerator and air conditioner applications.

To resolve the thermal bottleneck created at the PFC stage of a 7 kW CAC, while using a 30 m Ω SiC MOSFET (IMW120R030M1H), a SiC MOSFET with an $R_{DS(ON)}$ of 14 m Ω and a junction-to-case thermal resistance, R_{thjC} , of 0.25 K/W (IMZA120R014M1H) was investigated; assuming an R_{thCH} of 1 K/W [4], and a junction-to-heat sink thermal resistance R_{thjH} of 1.25 K/W. A demo board was used to measure the loss at operating conditions to get a more accurate simulation model than the one prepared using datasheet conditions. Power loss simulation using PLECS showed a total loss of 41.8 W with 29.4 W of switching loss and 12.4 W of conduction loss, which was significantly lower than that with IMW120R030M1H. Mersen R-TOOLS thermal simulation [5] gave the heat sink temperature, T_{Hs} , and the junction temperature, T_{Vj} , of the PFC SiC MOSFET as 82.1°C and 134.4°C respectively, as listed in Table 1. The thermal design requirement for 7 kW systems was thus met.

A SiC MOSFET, IMZA120R007M1H, with an even lower $R_{DS(ON)}$ of 7 m Ω and an R_{thjC} of 0.15 K/W was also evaluated for the 7 kW CAC; assuming an R_{thCH} of 1 K/W and R_{thjH} of 1.15 K/W. The power loss by simulation of this SiC MOSFET was 41.7 W, with an estimated T_{Vj} of 130.1°C as listed in Table 2. The thermal performance improved only marginally because the reduction in conduction loss was offset by an increase in the switching loss. R_{thjH} , however, also reduced only marginally.

Item	PFC SiC M	PFC SiC D	Rec.	Inv. IGBT	Inv. FWD
P_{loss} [W]	41.8	21.3	18.1	16.4	3
T_H [°C]	82.1	79.1	95.8	95.8	95.8
R_{thjH} [K/W]	1.25	1.7	1.54	1.55	2.04
T_{Vj} [°C]	134.4	115.3	123.7	121.2	101.9

Table 1: Device temperature for 7 kW output power when using a 14 m Ω SiC MOSFET, IMZA120R014M1H, with $V_{DC} = 540$ V

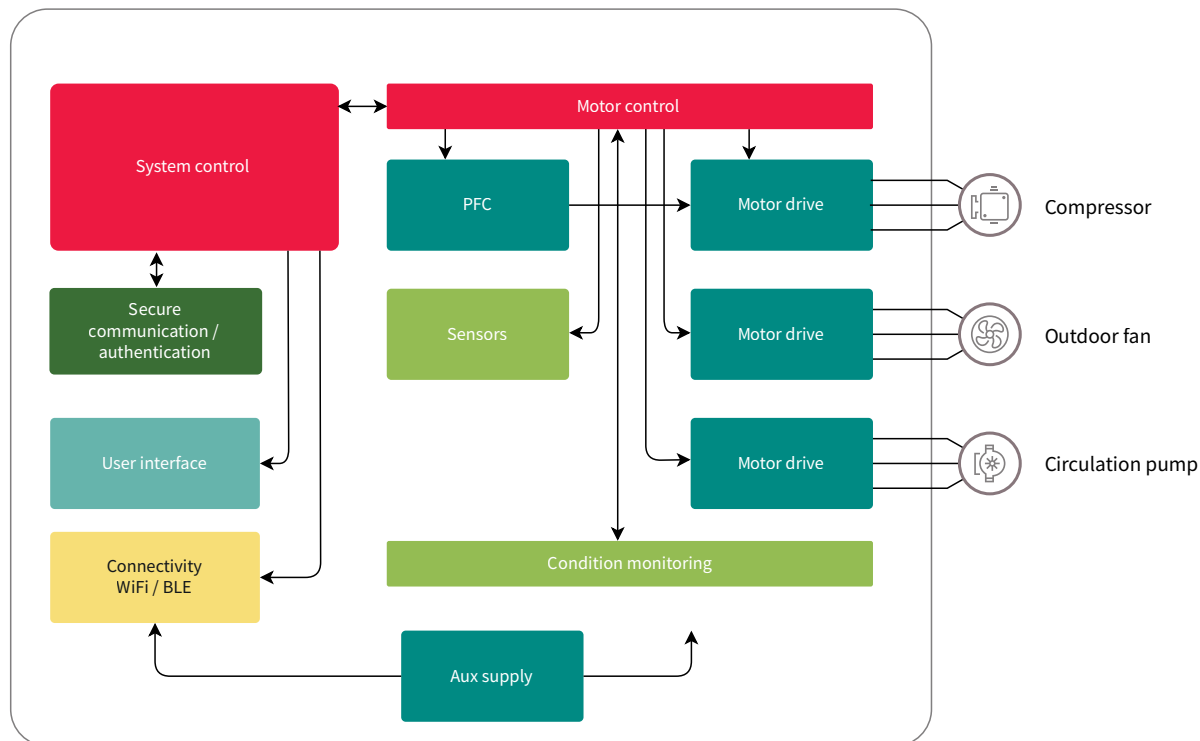
Item	PFC SiC M	PFC SiC D	Rec.	Inv. IGBT	Inv. FWD
P_{loss} [W]	41.7	21.3	18.1	16.4	3
T_H [°C]	82.1	79.1	95.8	95.8	95.8
R_{thjH} [K/W]	1.15	1.7	1.54	1.55	2.04
T_{Vj} [°C]	130.1	115.3	123.7	121.2	101.9

Table 2: Device temperature for 7 kW output power when using a 7 m Ω SiC MOSFET, IMZA120R007M1H, with $V_{DC} = 540$ V



Smart, energy-efficient solutions for heat pumps

To meet CO₂ reduction commitments, traditional heating systems like gas and oil boilers will be replaced with more sustainable alternatives like heat pumps. Discover our broad portfolio – from power control, predictive analytics, and connectivity to HMI and sensing – for the design of tailored system solutions with less conversion loss, smaller form factor, and reduced development time.



See you at PCIM Europe 2023, Hall 7, Booth #412



Check it out:
www.infineon.com/heat-pump



Another approach to 7 kW light industrial applications is to use two pieces of the SiC MOSFET, IMW120R030M1H, with an $R_{DS(ON)}$ of 30 m Ω , in parallel. For devices in parallel, the current sharing imbalance should be considered. Assuming a current imbalance of 10 percent, the power handled by one SiC MOSFET in a 7 kW PFC, for example, would be 3.85 kW. To simplify the evaluation, the output power was set to 7.7 kW with equal current sharing in both the SiC MOSFETs. The power loss of one SiC MOSFET in PLECS simulation was 21.3 W as shown in figure 2. Thermal simulation by R-TOOLS gave the T_H of the PFC SiC MOSFET and inverter IGBT as 79.9°C and 96.6°C respectively, as shown in figure 3. T_{VJ} of all power devices were within their thermal limit as listed in Table 3. The thermal design requirement for 7 kW systems was thus met.

It is notable that the T_{VJ} of the PFC SiC MOSFET is lower with two pieces of 30 m Ω devices in parallel than a single 14 m Ω device (112.1°C versus 134.4°C) despite the 10 percent margin added to compensate for the current sharing imbalance. This is due to the effective reduction in R_{thCH} by half when two packages are in parallel. R_{thCH} is a dominant portion of the total R_{thJH} , with a nearly 80 percent share in low $R_{DS(ON)}$ devices such as the 14 m Ω IMZA120R014M1H.

Item	PFC SiC M	PFC SiC D	Rec.	Inv. IGBT	Inv. FWD
P_{Sloss} [W]	21.3	24.6	18.1	16.4	3
T_H [°C]	79.9	78.3	95.8	95.8	95.8
R_{thJH} [K/W]	1.51	1.7	1.54	1.55	2.04
T_{VJ} [°C]	112.1	120.1	124.5	122	103.2

Table 3: Device temperature for 7 kW output power when using two 30 m Ω SiC MOSFETs in parallel with $V_{DC} = 540V$

The power loss and estimated maximum junction temperature of different SiC MOSFETs used in the PFC stage for 7 kW system output power are shown in figure 4. Power loss and T_{VJ} of a PFC SiC MOSFET can be reduced using a single device with low $R_{DS(ON)}$ or two devices in parallel. Paralleling SiC MOSFETs gives a better thermal performance despite current sharing imbalance due to the effective reduction in the case-to-heat sink thermal resistance, R_{thCH} , by half.

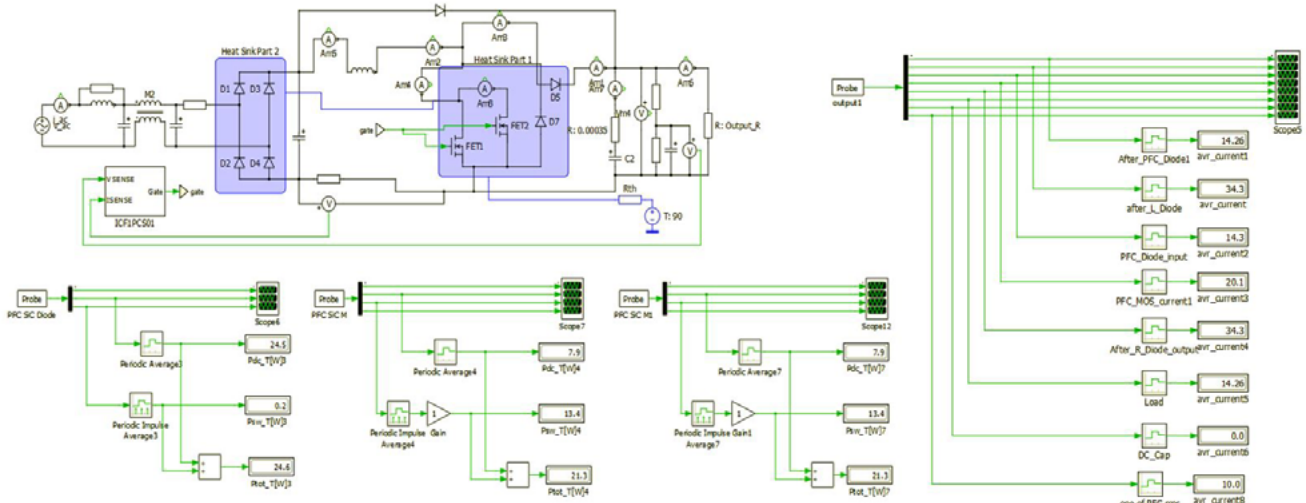


Figure 2: PFC and rectifier power loss simulation, using PLECS, with two pieces of SiC MOSFET, IMW120R030M1H, in parallel. The SiC MOSFET's power loss at rated output power of 7.7 kW with 10 percent current imbalance, is 21.3 W with 7.9 W conduction loss and 13.4 W switching loss

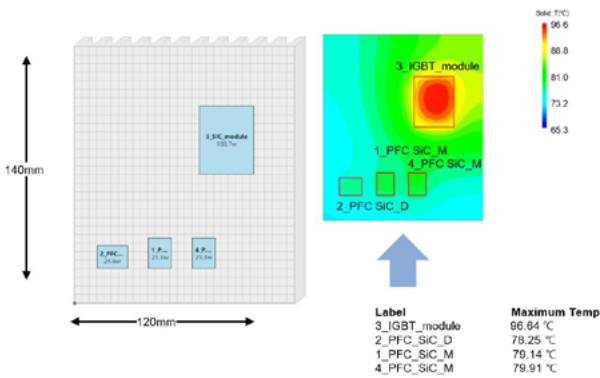


Figure 3: R-TOOLS thermal simulation with a heat sink of dimensions 140 mm (L) x 120 mm (W) x 60 mm (H), and an air flow velocity of 3.7 m/s with paralleled MOSFETs for 7.7 kW

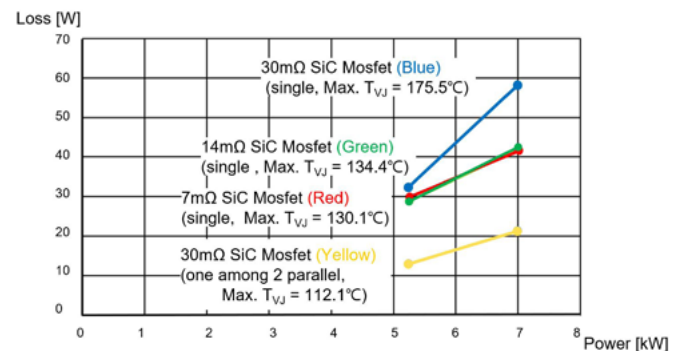


Figure 4: Power loss and estimated junction temperature of different SiC MOSFETs used in the PFC stage for 7 kW output power

References

[1] S. Kim, and K. W. Ma, "Unified platform with single- and 3-phase input for light industrial application using SiC power device," ICMRA 2021. Zhanjiang, China, DOI 10.1109/ICMRA 53481.2021.9675728

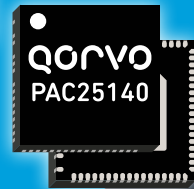
[2] S. Kim, B. S. Swaminathan, K. W. Ma and D. W. Chung: "Unified design approach for single- and 3-phse input air conditioning system using SiC device", KIPE Conference, Busan, Korea, 2020, pp. 205-208

[3] S. Kim, and K. W. Ma, "Extending output power of unified AC input light industrial applications by SiC MOSFET", PCIM Europe 2022, DOI:10.30420/565822182

[4] Infineon Technologies, "AN2015-13 Explanation of discrete IGBT's datasheet"

[5] Mersen R-TOOLS MAXX: <https://www.r-tools.com>

Industry's First Single-Chip Intelligent Battery Management Solutions for 10s-20s Cell Systems



PAC22140/PAC25140:

- Save 50%+ space of PCB and 30% of total BOM cost
- Integrated 32-bit Arm® Cortex® M0 or M4F
- Includes cell balancing, monitoring and protection for 10s-20s battery packs
- Single-supply 145V-buck DC/DC controller generates a 5V system rail
- 5V/225mA regulator
- CHG/DSG FET driver
- 9x9mm, 60-pin QFN with power pad
- Applications: industrial, e-mobility and battery backup



[LEARN MORE >](#)

Minimize Current Consumption While achieving high accuracy with Current Sensors

Engineers designing high-efficiency power electronics systems need small current sensors that consume less power and measure high currents with high measurement accuracy.

By WangSam Jang; President, J&D Electronics

Selecting a current sensor for current measurement

Current measurement is one of the most common parameters used to evaluate, control, and diagnose the operating efficiency of electronic systems. Although current is a very common measurement, problems can arise when designers underestimate the nuances of several variables when measuring current. Top engineers use SiC MOSFET modules to design highly efficient inverters that meet the following design criteria. Current sensors also need to be designed with low operating power consumption and compact size, as these are the most important design criteria.

There are two main current measurement techniques: current measurement using shunt resistors and current measurement using the Hall effect.

Shunt resistors consume power as a result of the load current passing through the resistor, so the resistance value must be very low. Other important parameters of a current shunt resistor for measurement stability are TCR and thermal EMF. These two parameters can have a significant impact on current measurement accuracy. Current shunt resistors must operate over a wide current range. At low currents (such as in sleep or standby mode in battery applications), the thermal EMF of the shunt adds a measurable error voltage to the voltage produced by the current through the resistor. To minimize measurement error, this error voltage must be much lower than the minimum expected voltage produced by the associated current through the shunt resistor. The first step in measuring current flow is to convert the current into a more easily measured

voltage parameter. A current shunt resistor is an inexpensive component that accomplishes this task. However, the value of the shunt resistor must be low to optimize the insulation technique and minimize its impact on the circuit and the power dissipation of the resistor itself. Solutions that use shunt resistors have different thermal aspects. The working principle of shunt current measurement is that the load current flows through the resistor and the resulting voltage drop is measured. This results in power dissipation in the shunt resistor. Inverter designers must take care that the maximum shunt temperature does not exceed 200°C.

When using Hall-effect sensors, you must consider the maximum temperature of the busbar. Typical sensors are specified to operate below 85°C or below 105°C housing temperature, depending on the device used (Figure 1).

Power consumption test with new current sensor-based module (Figure 1).

Low-power Hall-effect sensors for current measurement

Typically, at certain power levels above 50 kW, shunting is not a viable option due to excessive power losses. Therefore, for high power inverters, Hall effect sensors should be used around the output AC busbar. A schematic of this type of system is shown in Figure 1. This configuration provides a good solution for inverters with a simple interface to the controller and high electrical isolation properties. Because it uses the Hall effect to measure current, there is no power loss in the load current. There are two main types of Hall effect sensors: Open-loop and closed-loop current sensors. Open-loop

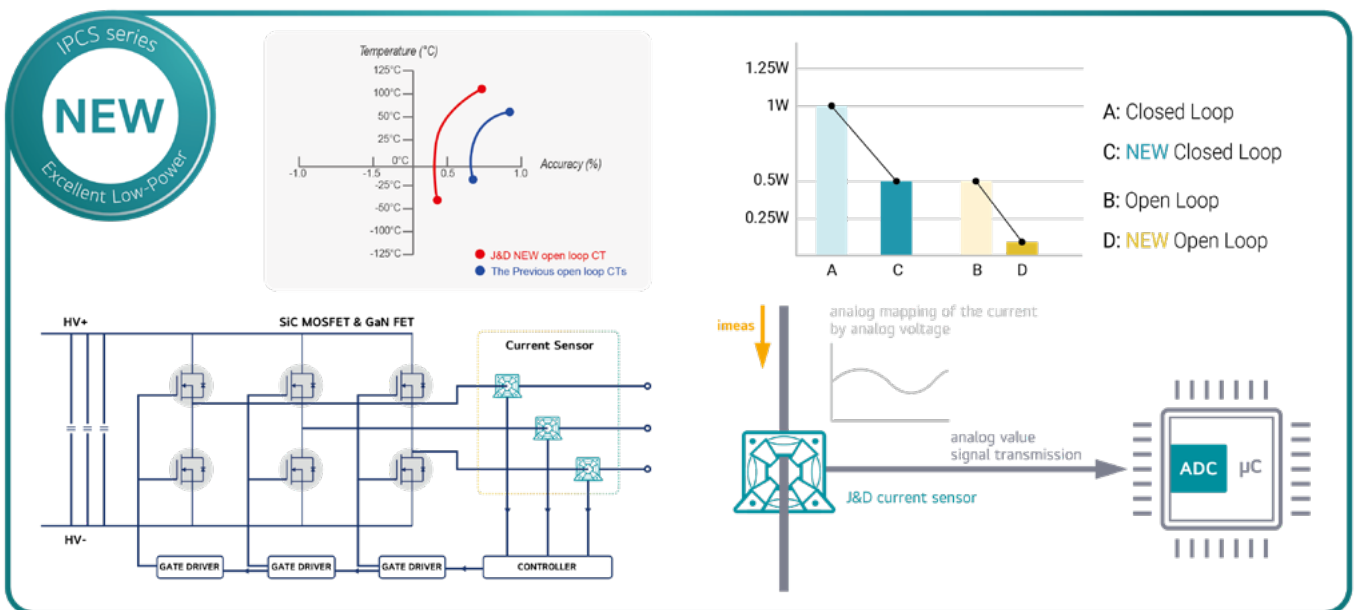
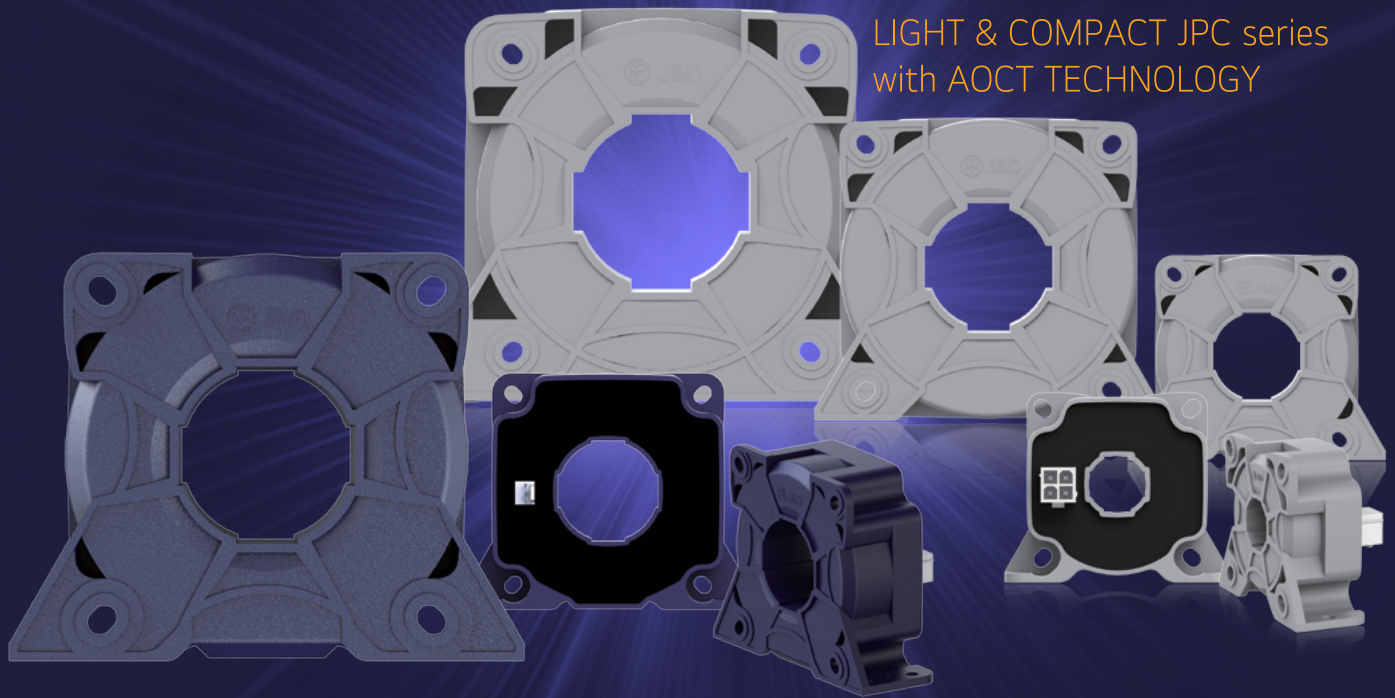


Figure 1: Temperature characteristics of a current sensor and power consumption measurement data

Meet the newly upgraded

JPC SERIES in 2023 at PCIM2023

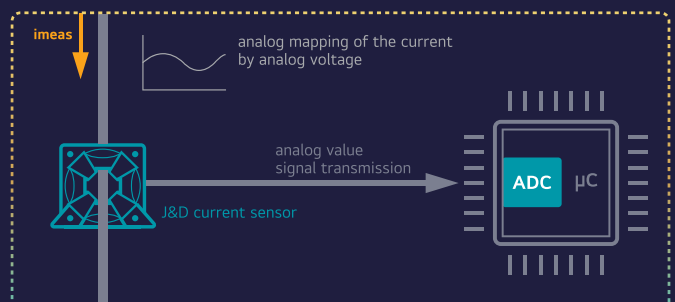
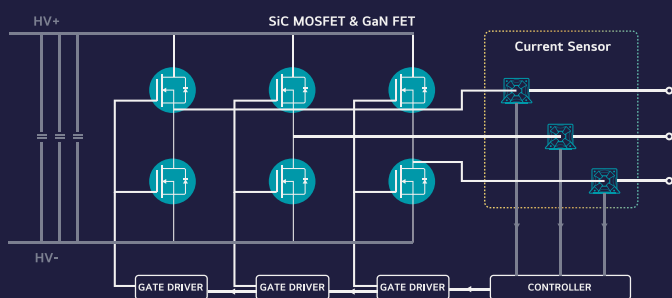
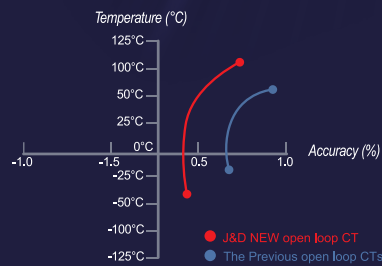
HALL 9 NO. 608



LIGHT & COMPACT JPC series with AOCT TECHNOLOGY



AOCT A new technology based on high precision closed-loop technology
AOCT TECHNOLOGY



Temperature characteristics of a current sensor and power consumption measurement data

sensors are less expensive, require less power supply, and have lower requirements, but they typically have error characteristics in terms of dynamic bandwidth, offset voltage, and drift over temperature. Closed-loop sensors overcome these error characteristics but are more expensive and have very high current consumption.

	Hall Effect Sensor Closed Loop (A)	Hall Effect Sensor Open Loop (B)	NEW Hall Effect Sensor Closed Loop (C)	NEW Hall Effect Sensor Open Loop (D)
Accuracy	high	medium	high	high
Cost	high	medium	high	medium
Physical Space required	very small	very small	very small	very small
Assembly/ Mounting effort	easy mounting, cable & plug connection	easy mounting, cable & plug connection	very easy mounting, cable & plug connection	very easy mounting, cable & plug connection
Withstand voltage	AC2000V, 1min	AC2000V, 1min	AC2000V, 1min	AC2000V, 1min
Step response time	typ. <1µs	typ. <3µs	typ. <1µs	typ. <3µs
Power supply	±15V (20mA)	±15V (25mA)	+5V (18mA)	+5V (15mA)

Table 2: Summary of key differences Four Approaches to Current measurement

In typical applications, open-loop Hall-effect sensors provide sufficient error characteristics. However, closed-loop Hall-effect sensors are used in very demanding applications where the highest control accuracy is required. The power supply requirements of closed-loop Hall-effect sensors are very high compared to other sensor types. A conventional cross-loop current sensor with a rated current of 100A and a secondary output of 50mA requires a power consumption of 1W when using an operating power supply of ±15V. However, a cross-loop current sensor with a rated current of 100A and a secondary output of 500mV requires 0.5W of power consumption when the operating power is +5V. And an open-loop current sensor with 100A and a secondary output of 500mV requires only 0.1W when the operating power is 5V. Therefore, for a three-phase converter, the power supply must provide 3 W of power for a conventional closed-loop current sensor. However, the new open-loop type current sensor can improve power efficiency by 2.7W compared to the existing ones when supplying total power of 0.3W.

See Figure 1 and Table 2 for the technical differences between Hall-effect current sensor solutions.

J&D applies the latest AOCT technology inspired by DC metering design. We recently launched the IPCS series, which boasts the highest precision available. This innovative technology has been incorporated into J&D's latest IPCS current sensor series, designed for non-intrusive and isolated measurement of DC, AC and pulsed currents in the nominal range of 100A to 800A.

The IPCS sensors are one of the best options for top engineers: they meet high precision with low power consumption.

The IPCS sensors feature closed-loop and open-loop current sensors that enable high-precision, error-free measurements with a 5 V operating power supply. The technology is based on a zero-draft OPAMP IC that utilizes Hall effect technology in either closed-loop or open-loop mode. The technology offers excellent temperature characteristics from -40°C to +85°C and low offset drift, making it ideal for applications requiring high accuracy.

The sensors feature a solid-core type PCB mount design and a split-core type panel mount or DIN rail mount type, and customers have the flexibility to select AC or DC currents from 5 A to 800 A. The IPCS current sensors are available in a variety of sizes.

IPCS current sensors are suitable for use in a wide range of applications, including modern string inverters that generate power on the AC side of 70-250 kW solar inverters, which by standard require very low DC components for output current. They are also ideal for DC billing meters, ESS, and EV charging modules (Figure 2).

Overall, J&D's IPCS family of current sensors provides engineers with solutions to design efficient, lightweight, and compactly sized power modules while ensuring that they can deliver the highest levels of accuracy and precision in non-intrusive, isolated measurement of DC, AC, and pulsed currents.

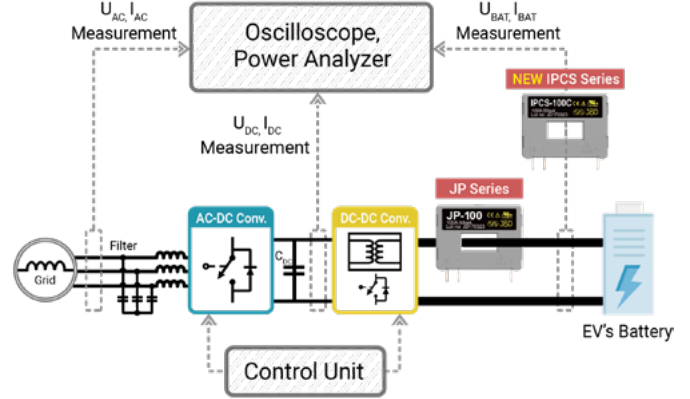


Figure 2: Conceptual diagram of EV charging module efficiency measurement

New DC current sensors for DC side metering (Figure 3)

Cost-effective DC current sensors are used to measure DC current in industrial environments. Designed for accuracy and durability, the IDCS series products are ideal for providing precise current measurements in DC applications such as renewable energy or transportation.

The IDCS-I DC current sensor measures the DC load current of an electrical installation and transmits the information to a DC energy meter module on a cable connected to the sensor via RJ12. The family consists of solid-core and split-core sensors in various sizes ranging from 50 to 5000 A for use in new or existing electrical installations.

Benefits

- Plug and play
- Quick RJ12 connections allow for easy and reliable wiring.
- Sensor classes can be configured quickly.
- Flexible
- Solid-core and split-core DC current sensors from 50 to 5000 A, designed for new or existing electrical installations, are available in a variety of installation options.

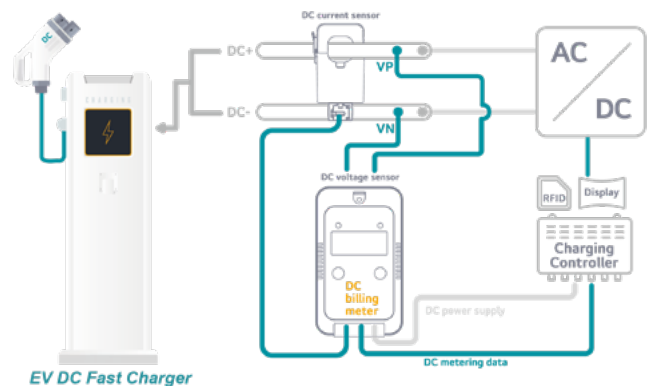
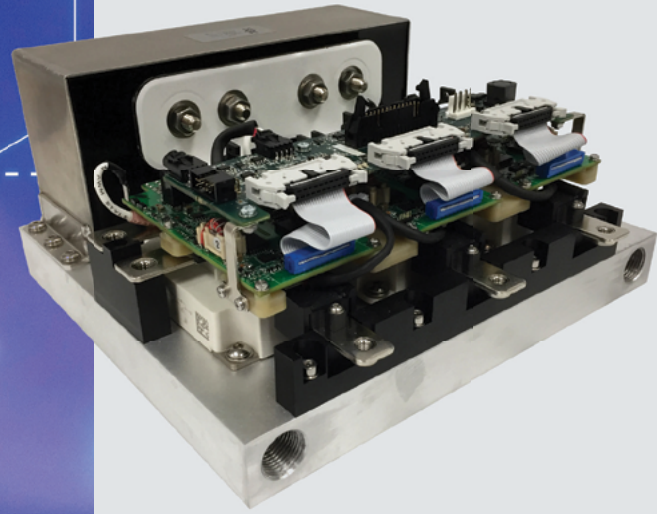


Figure 3: Power measurement diagram of a DC current sensor and DC meter for DC-side EV fast charging.

SiC POWER STACK

DESIGN OPTIMIZATION & EVALUATION KITS



- Cooled, connected, protected, filtered, and assembled by **MERSEN** powered and controlled by **MICROCHIP**
- Standard power stack evaluation kits and custom designs
- Co-design, optimize, assemble and test any Si, GaN, or SiC-based power stack
- Global footprint to address any region

**LIVE PRODUCT
DEMO AT PCIM**

**MAY 9-11,
NUREMBERG
HALLE 9-433**



More about our SiC Power Stack

Package for the Highest Voltage Classes Si IGBTs and SiC MOSFETs

HV LinPak is a new package that adds to several options that converter designers have for using Si IGBTs and SiC MOSFETs with nominal blocking voltages above 3.3kV. It brings to the high voltage range the advantages demonstrated by its LV variant, such as low stray inductance, very good paralleling performance, high power density and the ideal distribution of power and auxiliary terminals.

By Virgiliu Botan, Roman Ehrbar, Antoni Ruiz, Andreas Baschnagel, and Lluís Santolaria, Hitachi Energy Semiconductors, Lenzburg, Switzerland

Introduction

As electricity increasingly becomes the lifeblood of modern society, so is the importance of power electronics and its efficiency. In order to minimize the loss of energy in power electronics, we need to more closely examine all aspects of the components involved.

For the topologies used in these power electronics systems, from the classic two-level converters to more advanced 3L NPC with passive or active control or T type - to even more complex converters like Modular Multi-level or Cascaded H-Bridge Multi-level - there are numerous optimizations for efficiency, component count, harmonic distortion, reliability and cost. Of all the components used in a power electronics system, the switches used to turn-on and turn-off the current are some of the most important.

In the very high voltage switches range (>3kV), we have observed an aggregation of available options in recent years. On one hand we have the current-controlled devices like Phase Control Thyristors (PCTs) [1] or Integrated Gate-Commutated Thyristors (IGCTs) [2], and on the other hand the voltage-controlled switches like the Insulated Gate Bipolar Transistor (IGBT) or the SiC Metal Oxide Semiconductor Field Effect Transistor (SiC MOSFET).

There are two main classes of packages available for these switches: press-pack solutions (i.e. Hockey Pack for BiPolar and StakPak for IGBT [3]) and isolated modules. For isolated, high voltage modules,

HiPak has been the workhorse of the industry [4]. It is intensively used in traction converters, medium voltage drives and grid applications (i.e. SVC, interties, STATCOMs, HVDC valves, etc.). More recently, a new package has been proposed [5], and at Hitachi Energy this package is called LinPak. We launched the first LV LinPak version ($V_{iso}=6kV$) for commercial operation in early 2016 [6]. The HV LinPak ($V_{iso}=10.2kV$) has now come to market (see figure 1). Acceptance for these packages has been immediate and demand for

them has been widespread due to their improved performance characteristics.

HV LinPak Features

HV LinPak is designed on the same principles of the LV version. It is a dual (or phase leg) module, with the main power terminals on each side of a long axis. This allows the convenient placement of the gate unit in the middle of the module without any constraints on the busbar design. Moreover, the DC+ and DC- terminals are fed into the module in a co-planar geometry to achieve the lowest commutation inductance. Special care in the design of the module was taken so that the paralleling of these modules can be done with minimal, or no, current de-rating [7]. In addition to all these improved characteristics, the HV LinPak is available with an optional NTC thermistor, the first module in its class with this option. The following variants for Si IGBT HV LinPak are in development: 3.3kV 600A, 4.5kV 450A and 6.5kV 300A. Equivalent ratings with SiC MOSFET are in development as well.

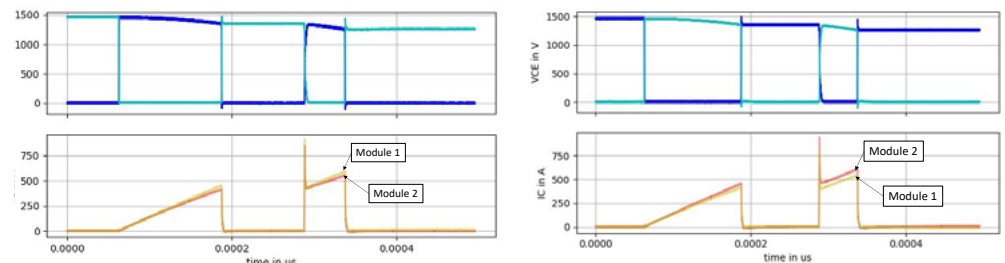


Figure 2: High side (left) and low side (right) double pulse switching curves of two 3.3kV 600A HV LinPak modules in parallel

Parallel Operation

We have created a setup for testing the HV LinPak in parallel, in accordance with existing literature recommendations [8]. We started the paralleling tests with the 3.3kV 600A HV LinPak modules and observed very good current sharing between modules taken randomly from our production (see figure 2). The position of the modules in the test setup was the most important factor in determining current asymmetries. We obtained the same variance even when we swapped the modules used in the test. The variation of the module parameters (V_{CESat} , V_F , V_{th} , $t_{d(on/off)}$, ...) was representative of the typical distribution of these parameters.

Additionally, we also noted a difference in the parallel switching behavior of the high-side versus the low-side. We saw a big impact on this imbalance when we altered the test setup, i.e. connecting or disconnecting a circuit breaker. Moreover, this difference is, as previously stated, position dependent and does not change when exchanging or swapping modules.

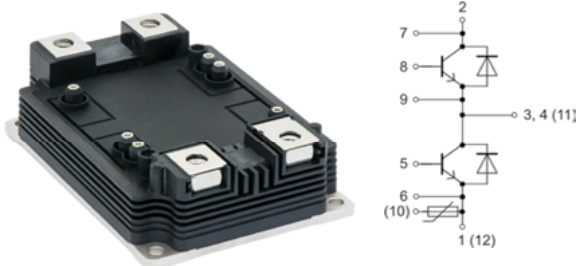


Figure 1: The HV LinPak module



SiC LinPak boosting the efficiency of high- power applications

Hitachi Energy extends the well-established LinPak family with devices based on SiC technology to deliver the highest current rating. Available at 1700 V and 3300 V, the SiC LinPak offers several benefits, including a massive reduction of switching losses, increased current density in the lowest inductance package of its class. [Visit us at PCIM Europe, Stand 302/9, May 9-11, Nuremberg, Germany.](#)



NTC Option

To enhance the features of this module for the high voltage range, an NTC thermistor is now available as an optional feature. The NTC sensor is mounted on the same substrate as the semiconductor chips, which ensures that the temperature readings are as close as possible to the chip temperature. This enables customers to further optimize the use of the module by reducing the design margins. For instance, when a high temperature is detected, the switching frequency can be temporarily changed to reduce switching losses. Furthermore, if only one module is experiencing increased temperature, condition monitoring management can be applied to avoid a catastrophic failure. Such information would not be available if only the temperature of the cooling water, or a sensor on the heat sink, was used as the trigger.

In figure 3 below, we see the voltage signal that was measured over the NTC. We applied a voltage divider technique that is common for such measurement, where we have a resistor (820 Ohm) in series with the NTC thermistor. We see that the NTC sensor is following the temperature of the main substrate on which it is mounted, and the signal has some coupling with the emitter dv/dt. It is important to understand this behavior in order to avoid a false reading. As we can see, a higher temperature implies a lower resistance, which in turn means a lower voltage drop over the NTC.

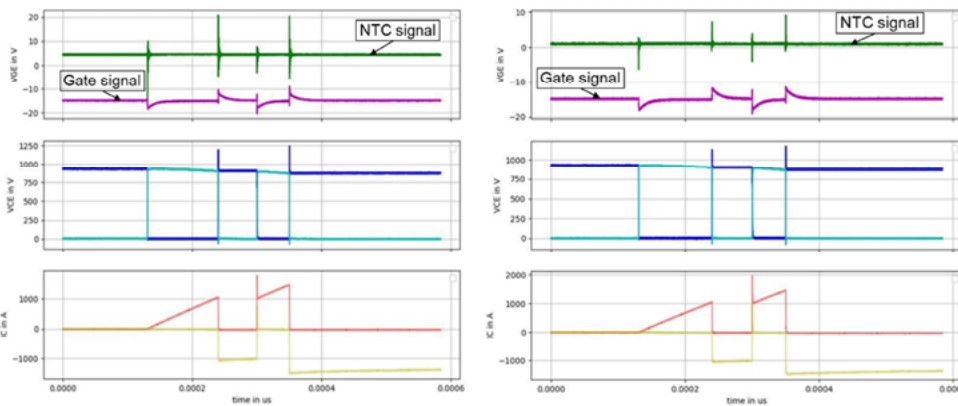


Figure 3: NTC signal curves measured at RT (left) and 150°C (right) of the HV LinPak, assessed with high current switching during a double pulse test

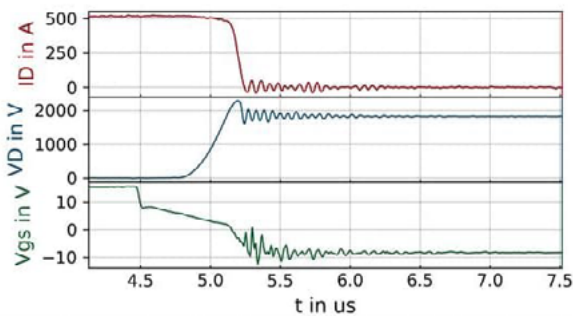


Figure 4: Turn-off of a SiC 500A 3.3kV HV LinPak module, 25°C, $R_g=3.30\Omega$

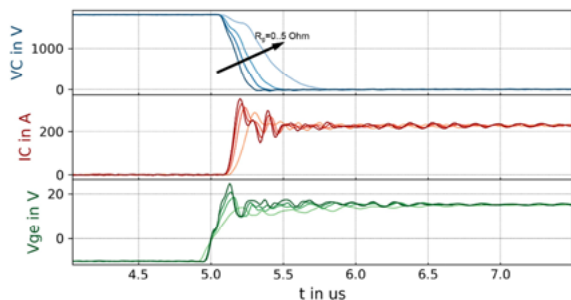


Figure 5: Scanning of R_g for the turn-on of a 3.3kV SiC on substrate level ($I_{nom}=225A$), 25°C

HV LinPak with SiC MOSFETs

Due to its low stray inductance, the HV LinPak can also be equipped with fast switching SiC MOSFETs. In our improved version of this package, we decreased the internal inductance to ca. 23nH, which enables the device to switch much faster. In this way the very low switching losses of the SiC devices can be fully utilized. Not only is the internal inductance lower, but the substrate design is optimized to ensure that each SiC device experiences the same commutation inductance, the same gate inductance and that the coupling is very homogenous. To ensure a good balance between the two substrates inside the module, we equip each of them with an own gate resistor.

In Figure 4 we show the switching waveforms of a 500A 3.3kV SiC LinPak. Our target was to have very good controllability, i.e., to be able to vary the switching speed by applying different values for the R_g . It can be seen from the wave-curves that good switching is achieved even with external $R_g=0\Omega$ (see figure 5). When going from a value of R_g of 0 Ohm to 5 Ohm/ substrate the di/dt is slowed down from 3.5 kA/us to 1.2kA/us. The same was observed in the turn-off curves, where the dv/dt was reduced by ca. factor 3 when increasing the R_g from 0 Ohm to 5 Ohm/ substrate. This gives a converter designer the flexibility to choose the gate resistor value that offers the optimal compromise between losses and di/dt or dv/dt constraints.

Conclusions

In this article we have shown the newest available module for designers of medium voltage converters in applications like traction, industrial drives, frequency converters for grid applications and many others. With state-of-the-art characteristics like low stray inductance, high current density, optional NTC thermistor, optimal electric design for paralleling and optimal mechanical design for compact inverter design, the HV LinPak has established itself as the new industry standard.

References

- [1] V. Botan, J. Waldmeyer, M. Kunow, K. Akuratti, "Six Inch Thyristors for UHVDC Transmission", Proc. PCIM 2009
- [2] T. Wikstroem, U. Vemulapati, B. Oedegard, "A 4.5kV RC-IGCT with Diode Segmentation for MMC Inverters", Proc. PCIM 2022
- [3] B. Boksteen, D. Prindle, F. Dugal, W.A. Vitale, E. Tsyplakov, V. Botan, G. Pâques, "Second generation BIGT chip advancing the StakPak platform", Proc. PCIM 2020
- [4] V. Botan, D. Schneider, "A journey from one to a million HiPaks", Bodo's Power Systems, May, 2020
- [5] T. Wiik, et al., Roll2Rail, D1.2 "New generation power semiconductor - Common specification for traction and market analysis, technology roadmap, and value cost prediction", 2016
- [6] R. Schnell, et al., "LinPak, a new low inductive phase leg IGBT module with easy paralleling for high power density converter designs", Proc. PCIM 2015
- [7] R. Ehrbar, G. Salvatore, A. Rosch, A. Baschnagel, A. Ruiz1, W. Vitale, V. Sundaramoorthy, F. Fischer, V. Botan, G. Pâques, "HV LinPak - A high voltage half bridge IGBT power module with balanced switching behavior for easy paralleling", Proc. PCIM 2022
- [8] J. Weigel, J. Boehmer, E. Wahl, A. Nagel, E. Krafft, "Paralleling of high power dual modules: Standard building block design for evaluation of module related current mismatch" 2018 (EPE'18 ECCE Europe), P.1-P.10, 2018.



High Power

GaN

A silver electric car is shown from a front-three-quarter view, with a charging cable plugged into its front. The car is partially obscured by the large "GaN" text, which is rendered in a blue and green gradient.

VisiC Technologies's unique semiconductor technology, D³GaN, is designed for the highest reliability and lower losses to support the automotive power industry.

D³GaN

DIRECT DRIVE D-MODE

- ✓ Half Inverter Losses
- ✓ Lower Car Cost
- ✓ Longer Driving Range
- ✓ Smaller, Lighter and Cheaper OBC



Helping Power Solutions Keep Up with Moore's Law

The article discusses the usual attention given to Moore's Law and MEMS in creating roadmaps for electronics and electrical equipment. It also highlights the importance of power solutions that allow systems to leverage Moore's Law and notes that the disparity between the source-side and load-side of the analysis is not as substantial as it appears.

By Steve Roberts, Innovation Manager, RECOM Power

Separating the Source & Load

When evaluating any system (or collection of systems) in terms of the power solution(s) and/or other analyses related to power consumption, energy efficiency, or overall energy/carbon footprint, it helps to separate the sources from the loads. In the simplest form, that is separating the power supplies/solutions from the end loads consuming the power these sources provide. Think of the SOURCES and LOADS as independent black boxes that "talk" to each other. The figure below shows an arbitrary breakdown of a system in block diagram form, in this case, a computing or server-like architecture highlighted to show the difference between the typical sources and typical loads in the system.

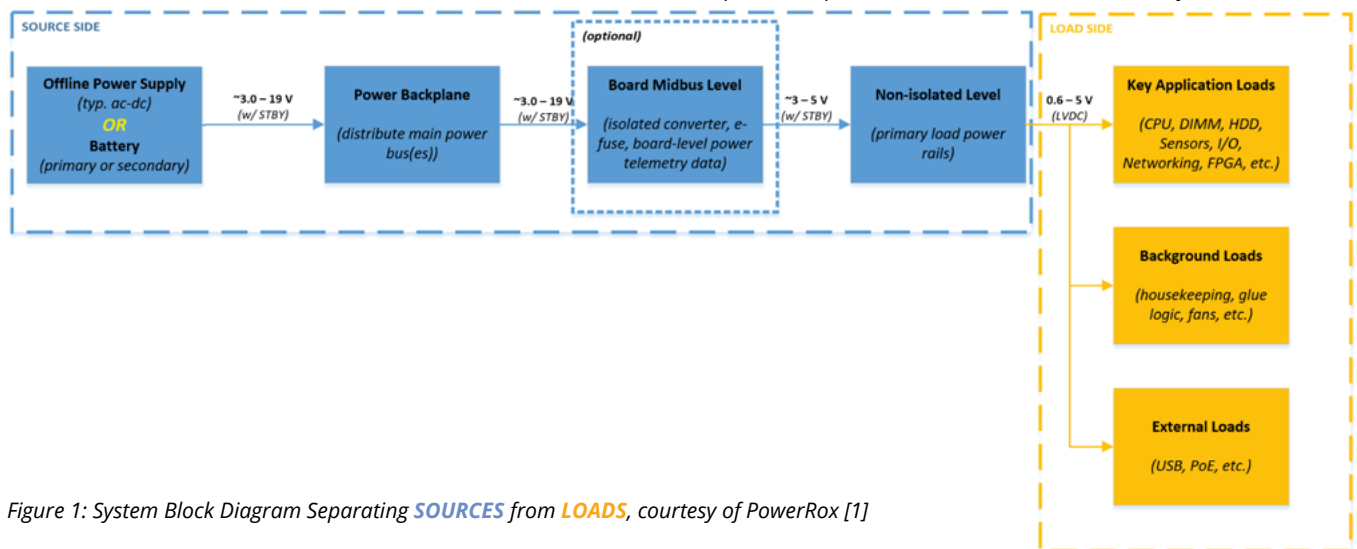


Figure 1: System Block Diagram Separating SOURCES from LOADS, courtesy of PowerRox [1]

This distinction of separating the sources from loads is particularly important when trying to understand the pace of technology in a complicated system that contains numerous components (perhaps each complicated system in its own right) impacted by an endless number of engineering, manufacturing, supply chain, and global economic variables. It is no coincidence the trends of exponential improvement (whether it be a metric characterizing transistor count, feature size, power density, energy efficiency, etc.) tend to be far more associated with the load side than the source-side source side of things. The source-side components tend to be dominated by magnetics, power transistors, and energy storage. These kinds of components tend to double their key figures of merit (FOM) closer to each decade than each year like low-voltage semiconductors.

What does Moore's Law have to do with power solutions?

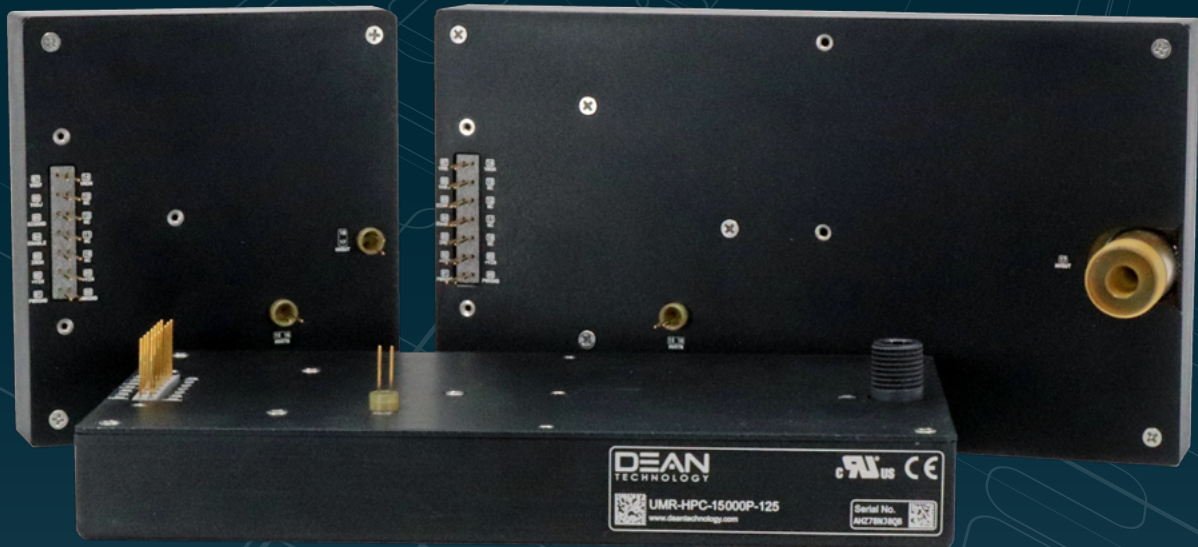
The consideration of the pace of development of roadmaps for electronics and electrical equipment will commonly converge around Moore's Law [2], which is more of an economic trend of transistor scaling as opposed to any kind of technical scaling rule

(see Dennard Scaling [3]) or physical law in the traditional sense. So even if not technically tracking any of this stuff, there seems to be a general perception in the electronics industry that everything (e.g. – all components, supply chains, and engineering efforts) somehow adhere to this pace of doubling performance every 18-24 months. Of course, even the semantical definition of "performance" can be the target of much debate so that will be left to the wayside for purposes of this discussion.

Aside from Moore's Law's impact on transistor size/count in an integrated circuit (IC), there is another trend driving major system power budget reductions. Moore's Law keeps logic shrinking at an exponential pace and microelectromechanical systems (MEMS [4])

shrink and integrate sensors to the point of being nearly invisible to the naked eye. It should be clearly distinguished though that Moore's Law tends to drive a major INCREASE in load power (i.e. – per transistor power goes down, but packing in more of them makes the power density or dissipated power in a given footprint to constantly go up), where MEMS tend to drive a major DECREASE in load power because applications will not tend to necessitate an exponential increase in the number of sensors even with an exponential decrease in individual sensor power. On the other hand, MEMS is driving the integration of multiple sensors (and sometimes co-packaging of processing and/or communications as well) though this will be discussed in more detail in the next section.

With a reduction in transistor feature size comes a reduction in threshold voltage, which effectively means ICs can operate with ever-decreasing bias voltage rails. This is why microprocessors went from requiring ~2.5/3.3V rails to ~1.2/1.5V rails, and now even <<1.0V power rails. As mentioned, power density still tends to increase by packing in more of these lower-voltage transistors, which



High Voltage Power Supplies

Outputs 125V to 30kV @ 60W & 125W

**Fast Charge Time
Low Overshoot
High Stability
High Efficiency
Competitive Pricing**

**Lead times stock to 3 weeks
Samples are available now**

Dean Technology's **UMR-HPC Series** of capacitor charging high voltage power supplies is a **form-fit-function replacement** for industry standard modules at a competitive cost. UMR-HPC modules feature regulated output voltage, a wide input voltage range, indefinite output short circuit protection, and are UL/cUL recognized.

All models come standard with voltage and current monitoring and can be upgraded to include buffered monitors and current regulation.

Contact DTI today to discuss your high voltage design.

pcim
EUROPE Hall 9-250

DEAN
TECHNOLOGY

+1.972.248.7691 | www.deantechnology.com

translates into a constant trend of driving up the input currents demanded by these dense loads. The densely packed loads also put a bigger strain on power supplies by increasing the transients demand in terms of faster voltage (~100V/ns) and current (~1,000A/μs) transitions.

How do power solutions keep up with the pace of Moore's Law?

As highlighted in many resources regarding the design and optimization of power solutions, the most common FOMs for a system are its size, weight, and power (a.k.a. – SWaP factors) characteristics. When combined with a cost metric, this can also be referred to as SWaP-C factors [5]. It is obvious how shrinking loads drive regular SWaP improvement, but less so on the source side.

In the more pragmatic sense, it seems the conversation should be around how system components, particularly power solutions in the context of this blog, are enabling systems to take advantage of the advances brought on by Moore's-Law-like, generational improvement in compute transistor density and integration of MEMS devices. The power solutions are not required to shrink with the low-voltage transistors or even meet their power densities at a 1:1 ratio to enable systems to utilize the evolutionary enhancements of the loads.

The increased transients described above will organically drive the need to bring the power supply closer to the high-transient load. This is not only for efficiency optimization by mitigating thermal dissipation ($P=I^2R$) and voltage drop ($V=IR$), made more challenging by higher currents, but also for preventing catastrophic voltage overshoot resulting from even little bits of parasitic equivalent series inductance (ESL, 1s – 10s of nH) previously considered negligible in older generations of systems. This highlights a major design challenge for power solutions that work to keep up the pace with Moore's Law and MEMS by utilizing faster power switches, particularly using wide-bandgap (WBG) chemistries, such as gallium nitride (GaN), silicon carbide (SiC), gallium arsenide (GaAs), or aluminum nitride (AlN) [6]. The figure below highlights how such little ESL, from the component package alone, can have catastrophic effects on your design. This is even before one has put extreme time and effort into a very clean, tight layout that contains these current flows as best as possible. It should be noted that a lack of R&D in the advancement of high-frequency magnetics materials is currently the ultimate bottleneck in unlocking the full potential of ultra-fast switching speeds WBG power switches are capable of.

$$\Delta V_{\text{overshoot}} = L_{\text{parasitic}} \times di/dt$$

	IGBT Module	TO247	SMD
Achievable Power Circuit Loop Inductance (typical)	100 nH	20 nH	1 nH
Typical Current Rating	500 A	100 A	50 A
Overshoot (ΔV) @ 100 A / μs	10 V	2 V	0.1 V
Overshoot (ΔV) @ 10 A / ns	1000 V	200 V	10 V

Figure 2: Calculation of Parasitic-inductance-induced Voltage Overshoot by Common Device Packages and Characteristics, courtesy of PowerRox [7]

Integration and advanced packaging techniques are the driving force keeping power solutions on pace with their shrinking, load counterparts. Moore's Law directly facilitates power conversion by allowing the integration of power management and control functionality into more consolidated power management ICs (PMIC), which can integrate power conversion (even integrating power switches), control logic, power conditioning, digital control and/or telemetry reporting, and management of external energy storage and feedback. This integration of power subsystems brings discrete solutions into the IC domain to dramatically reduce board footprint

space along with enhancing control and optimizing the overall efficiency of energy commutation.

Heterogeneous integration of MEMS sensors along with other miniaturized components such as microcontrollers, wireless radios, and antennae have led to reduced power consumption of these loads directly as well as the savings that comes with mitigating the distinct system overheads of supporting each load independently. There mere act of supporting so many system components with such little power inherently increases the value proposition of a given power solution since the same amount of power can now support more load, but SWaP is even further improved by enabling physically smaller power supplies to concurrently provide more power output (even while supporting wider input voltage ranges).

Three-dimensional power packaging (3DPP®) is at the convergence of everything discussed in this blog [8]. Even with a slower pace of improving magnetic material properties, the overall performance and size of major magnetic constituents of power solutions have seen a dramatic improvement with the migration from wire-wound (often involving manual, hand-winding techniques) to planar magnetics that use finely controlled features to layout windings and integrate into the printed circuit assembly (PCA) with embedded magnetic core material. This enables even highly-complex magnetics structures to be integrated in a way that allows for tight process control (e.g. – increased reliability), while concurrently taking advantage of manufacturing economies of scale to check just about every box in the SWaP-C checklist of goals. The figure below is an example of a cutaway in a point-of-load (PoL) converter that integrates a control/switch IC die, power magnetics, and module packaging into a compact solution that is optimized for space and thermally-enhanced for ease of heat spreading as well.

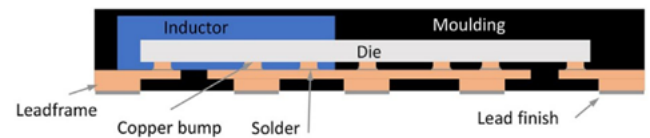


Figure 3: The 3DPP® Concept in RECOM's RPX Series of Point-of-Load (PoL) Converters

Getting Creative, While Keeping the Pace

Given the aforementioned point about the load (system) power budget on a much faster reduction trend than the increase of source (power solution) availability, the ability to keep on pace with Moore's Law is far more attainable by putting the maniacal focus on reducing the system power budget than putting most of the engineering cycles into implementing a bigger power supply. This is where intelligent power management (IPM) techniques shine. IPM is a "combination of hardware and software that optimizes the distribution and use of electrical power in computer systems and data centers" [9]. This is more a frame of mind in design approach than anything else so for instance, changing the approach to power subsystem architecture from an "always on" to an "always available" mentality can bring paradigm shifts in the results of the end solution.

There is always a demand and use for increased energy density and cycle life FOMs for energy storage components. Like magnetics roadmaps, evolutionary improvement in (safe, practical) energy storage is closer to an order of magnitude off the pace of Moore's Law. Even with that being the case, it does not imply a showstopper in helping the power keep the pace of system improvement (e.g. – mostly SWaP-C) targets. The area where this is most apparent is when sizing the power solution to the worse case (in terms of demand, transient, temperature, manufacturing tolerance, safety margin, etc.) can provide a very wide spectrum of subjectivity in terms of finding the balance between meeting the needs of the system/application and not getting too out of hand in terms of overdesign. This point also really accentuates the importance

and justification of careful characterization of loads before designing/implementing their respective power solutions. For instance, a system may have infrequent peaks of high-power draw, where most of the time is spent at a significantly lower, steady-state power level. It is highly wasteful (in terms of capital and operational expenditures, a.k.a. – CAPEX/OPEX) to engineer all the system's power supplies, upstream distribution/holdup, etc. to those infrequent peaks when that demand can be met with some localized energy storage, therefore leaving the rest of the system to be optimized for that lower steady-state. This is the concept of peak shaving, which can be applied to any system from micro-power to macro-power footprints.

Another variation of IPM is the utilization of load shedding/consolidation/allocation techniques. Nothing utilizes less power than something that is off and nothing utilizes active power more efficiently than a load operating at the peak point of the load vs. efficiency curve of the upstream power solution. So, whether it means turning off power to subsystems when not in use (i.e. – radio in a sleep state, dark silicon blocks of IC) or consolidating smaller loads that might otherwise require independent power supplies, this enables the implementation of effectively denser, more efficient power solutions. An example of intelligent power allocation can be in understanding a realistic scenario of external power needs, such as with universal serial bus (USB) or Power-over-Ethernet (PoE) ports that may be capable of sourcing more power as an aggregated peak (i.e. – all ports operating at max power concurrently), but will not all be operating concurrently and therefore should not have an upstream power supply designed to source that aggregated peak.

Furthermore, it is uncommon for all system loads to be operating at their maximums all simultaneously so creating a system power budget by simply summing the maxima (e.g. – data sheet worst-case maximums) of all loads is highly impractical in just about any use case. If possible, then disaggregating loads in a complex system to group them enables the optimization of their specific power subsystem(s) and therefore will lend itself to optimizing SWaP-C. This allows a design engineer to take advantage of the best of both worlds (Moore's Law/MEMS and non-Moore's Law/MEMS direct impacts).

Conclusion

No one is kidding themselves by making the bold statement that all aspects of power solutions will keep a direct pace with Moore's Law and the advancement of MEMS (soon to be referred more often too as nanoelectromechanical systems or NEMS) devices. As commonly depicted in industry news of the past several years, it hardly even seems clear Moore's Law, itself, will continue (either

in its existing form or something like it) into the foreseeable future. Even though this can create a gap between the source available power and the load power demand, it is not a gap that continues to grow exponentially and create an ever-widening chasm that makes power subsystems a reason to have to scale back system functionality.

As discussed, there are many creative techniques that power solution designers and system engineers use to keep pace to continue taking advantage of the technology enhancements Moore's Law and MEMS provide regularly. IPM techniques are at the heart of this because we are being a lot smarter with every watt instead of a more rudimentary matching of source to load in the traditional (e.g. – worst-case peak) sense. Energy storage is also a highly underappreciated and underutilized tool in the toolbox of helping to meet full system performance expectations, both reliably and while maintaining a roadmap of reduced system size and increased power density.

At the end of the day, 3DPP® and other advanced packaging techniques are really at the forefront of managing the gap between source and load because they are enabling more dramatic improvement to key FOMs than are seen purely in magnetics or energy storage devices.

References

- [1] B. Zahnstecher, "Best Practices for Low-Power (IoT/IloT) Designs: SEPARATING THE SOURCE-SIDE & LOAD-SIDE ANALYSES," ECCE 2022 Tutorial, Detroit, MI, October 9, 2022.
- [2] Wikipedia contributors, "Moore's law," Wikipedia, The Free Encyclopedia, https://en.wikipedia.org/w/index.php?title=Moore%27s_law&oldid=1139518707 (accessed February 24, 2023).
- [3] Wikipedia contributors, "Dennard scaling," Wikipedia, The Free Encyclopedia, https://en.wikipedia.org/w/index.php?title=Dennard_scaling&oldid=1134445777 (accessed February 24, 2023).
- [4] Wikipedia contributors, "Microelectromechanical systems," Wikipedia, The Free Encyclopedia, https://en.wikipedia.org/w/index.php?title=Microelectromechanical_systems&oldid=1139870714 (accessed February 24, 2023).
- [5] "Power Supply Design for maximum Performance," RECOM Blog, Oct 21, 2022, <https://recom-power.com/rec-n-power-supply-design-for-maximum-performance-229.html> (accessed February 15, 2023).
- [6] "DC/DC for GaN," RECOM Blog, Sep 16, 2022, <https://recom-power.com/rec-n-dc!sdc-for-gan-225.html> (accessed January 23, 2023).
- [7] E. Shelton, P. Palmer, A. Mantooth, B. Zahnstecher, G. Haynes, "WBG Devices, Circuits and Applications," APEC 2018 Short Course, San Antonio, TX, March 4, 2018.
- [8] "Introducing RECOM 3D Power Packaging® (3DPP®)," RECOM Blog, Feb 26, 2021, <https://recom-power.com/rec-n-introducing-recom-3d-power-packaging-%283dpp%29-145.html> (accessed January 23, 2023).
- [9] Data Center Facilities Definitions, "Intelligent Power Management (IPM)," TechTarget, <https://www.techtarget.com/searchdatacenter/definitions/Data-center-design-and-facilities> (accessed February 24, 2023).

www.recom-power.com



WIMA DC-Link Capacitors

WIMA DC-LINK capacitors are designed for the high power converter technology. At high frequencies they show a higher current carrying capability compared to electrolytic capacitors. Further outstanding features are e.g.:

- Very high capacitance/volume ratio
- High voltage rating per component
- Very low dissipation factor (ESR)
- Very high insulation resistance
- Excellent self-healing properties
- Long life expectancy
- Dry construction without electrolyte or oil
- Particularly reliable contact configurations
- Customer-specific contacts, capacitances or voltages

WIMA DC-LINK capacitors are available with capacitances from 1 µF through 8250 µF and with rated voltages from 400VDC through 1500VDC. The components are environmentally compatible with the RoHS 2011/65/EU regulations.

pcim
EUROPE
Nuremberg, May 09.-11. 2023
Hall 7 / Booth 208

www.wima.com

Power ICs Enable High-Efficiency and High-Power-Density 140 W, PD3.1 Adapter Designs

This article presents an ultra-high-efficiency and high-power-density design of a power factor correction (PFC) and asymmetrical half-bridge (AHB) flyback converter for 140 W PD3.1 adapter applications. GaNSense power ICs are used in the boost PFC design for higher frequency, smaller inductor, and higher efficiency.

By Tom Ribarich, Sr. Director Strategic Marketing, and Xiucheng Huang, Sr. Applications Engineering Director, Navitas Semiconductor

GaNSense half-bridge ICs are used to enable the ZVS AHB flyback topology to operate at higher frequencies with a smaller transformer and higher efficiency. A 140 W PD 3.1 evaluation board is presented that demonstrates the functionality and performance of the complete system design. The evaluation board achieves 94.5% efficiency at 90 VAC and 95.8% at 230 VAC which is at least 1% higher efficiency and with up to 20% energy savings vs. prior state-of-the-art designs. The estimated cased size is 100 cc, for power density of 1.4 W/cc.

Higher Speed + Higher Efficiency = Smaller Size

The growing demand for size reduction of power supplies has continuously challenged the industry to produce higher and higher efficiencies and power densities. The ability to improve the performance of silicon-based power supplies has slowed due to silicon devices reaching their maximum frequency limit (<100 kHz), which has prevented further optimization of circuit topologies and magnetic design. Emerging GaN wide-bandgap devices have enabled significant incremental efficiency and size improvements due to their 15x lower QG gate charge, 16x lower Qoss output charge, and higher switching speeds. GaNSense power ICs have enabled these devices to finally exit the lab and enter actual real-world fast chargers and adapters by integrating all of the missing ingredients needed for reliable and robust designs. These include integrated gate drive, regulated gate voltage, loss-less current sensing, and protection features and are included in GaNSense power ICs and GaNSense half-bridge ICs (Figure 1). These latest products are enabling new circuit topologies, and the industry is using them to progress ahead with smaller and more efficient designs.

GaNSense Boosts PFC Frequency and Efficiency

Power factor correction (PFC) is required for output powers greater than 75 W. The traditional boost PFC converter has dominated due to its simplicity, low harmonic current, and low cost. Many off-the-shelf PFC controllers are available that provide multi-mode CRM or DCM operation to improve system efficiency and line-current harmonics. GaNSense power ICs improve this topology by increasing the switching frequency to reduce the inductor size and increasing efficiency to reduce losses and thermals (Figure 2). The integrated GaN FET allows the frequency to be increased easily due to the lower output-charge and lower gate-charge compared to silicon FETs. To increase the efficiency, GaNSense power ICs integrate a loss-less current sensing method that completely eliminates the external RCS current-sensing resistor and its associated hotspot and footprint.

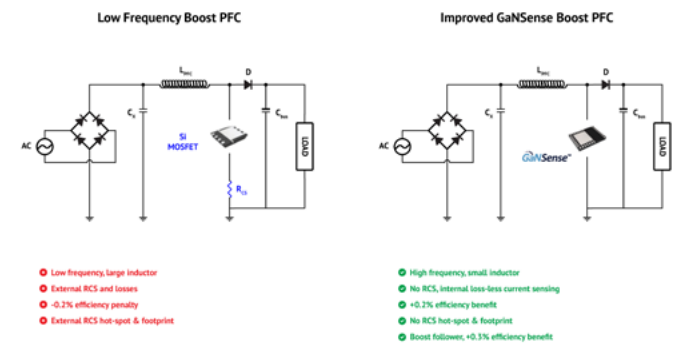


Figure 2: Si-based boost PFC (left) vs Loss-less GaNSense boost PFC (right)

To further improve efficiency, a boost-follower function can be added so that the DC bus operates at a lower voltage during low-line AC input. This gives lower peak-current levels, lower negative current and circulating energy, and lower core losses (Figure 3). All of these improvements combined give an additional +0.3% efficiency benefit.

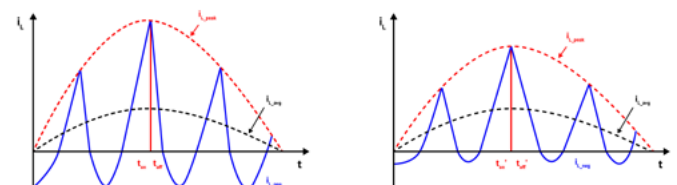


Figure 3: Boost peak-inductor currents over AC half-cycle at full-load and different DC-bus voltage levels, 90 VAC/400 V (left) and 90 VAC/260 V (right)

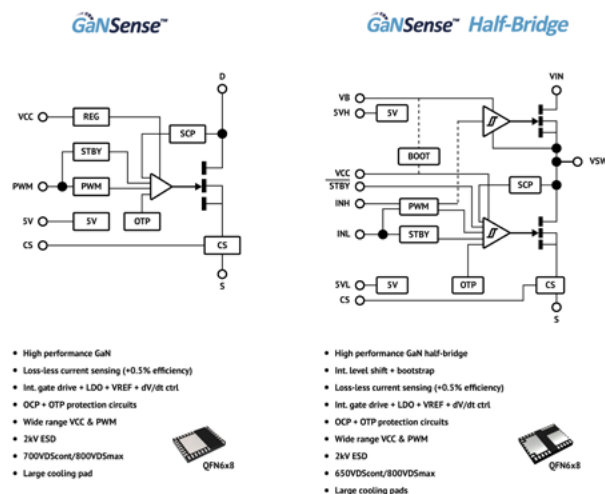
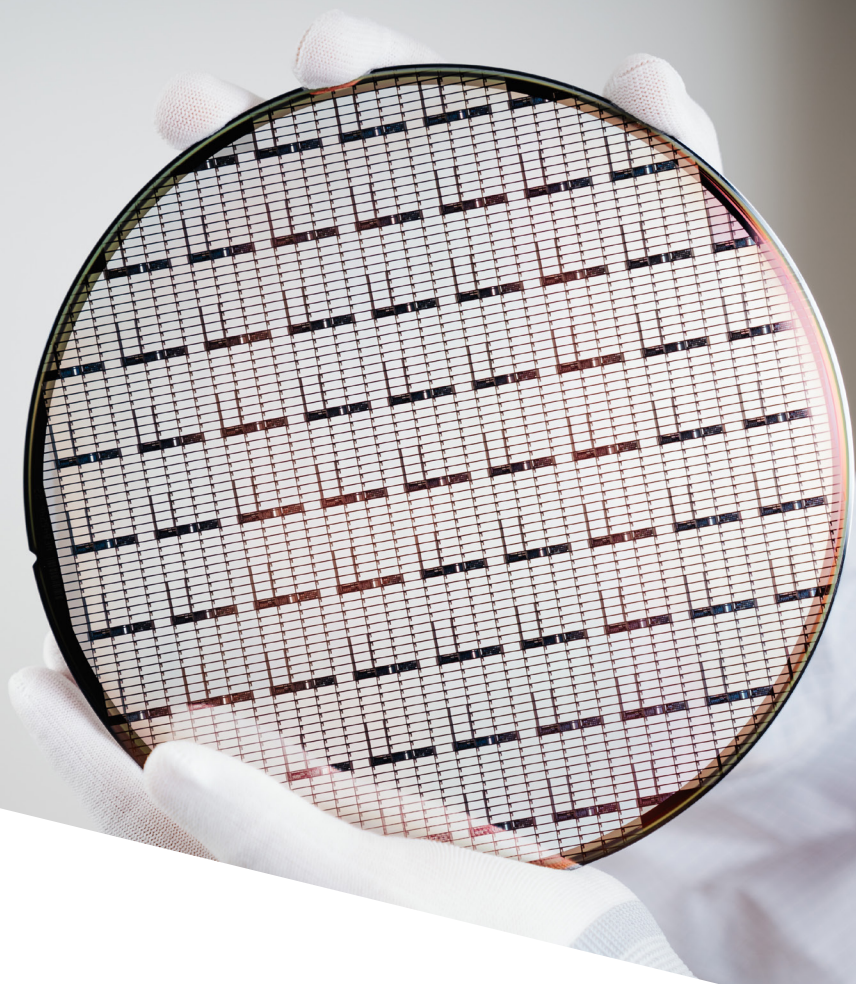


Figure 1: GaNSense power IC and GaNSense half-bridge IC simplified block diagrams and key features.



CoolGaN™ HEMTs

The new power paradigm. Ultimate efficiency and reliability.

Why to choose Infineon

- Full system solution provider including GaN HEMTs, gate driver and control ICs as discrete and integrated solution
- Most reliable GaN technology based on the Gate Injection Transistor (GIT) concept
- Extensive application testing assures highest product reliability over lifetime
- Global design-in support and stable supply security

Reach the next level of energy efficiency

A passionate team of global experts with more than a decade of in-depth GaN system-understanding helps you unleash the full potential of GaN. The outstanding reliability, performance and robustness of CoolGaN™ adds a significant value to a broad variety of systems such as server, telecom, SMPS, adapter and charger, TV/monitor, motor drives, LED lighting and solar.

For more details visit our [web](#).



GaNSense enables AHB, and AHB enables PD 3.1

The quasi-resonant flyback is a popular topology for the downstream converter due to its wide voltage gain capability. However, as power levels increase above 100 W, the transformer leakage energy increases significantly. As the leakage energy increases, the voltage stress on the primary switch and secondary SR switch also increases, including higher voltage spikes and EMI noise. In addition, the USB Power Delivery Specification Revision 3.1 enables higher output-voltage levels, e.g., 28 V to 48 V, which makes the flyback transformer turns-ratio more difficult to design. The voltage stress on both primary and secondary is much higher than the traditional 20 V output condition. The asymmetrical half-bridge flyback converter operates with zero-voltage switching (ZVS) of the primary-side switches and zero-current switching (ZCS) of the secondary-side rectifier. Moreover, the primary switches are clamped at the PFC output voltage, typically around 400 V, so the stress and voltage ringing issues are significantly relieved. For these reasons, the AHB topology is the preferred choice for PD 3.1 applications, and GaNSense half-bridge ICs enable high-frequency operation for small transformer size and loss-less current sensing for higher efficiency (Figure 4).

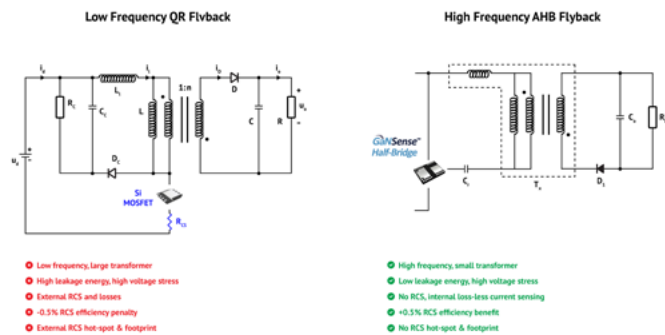


Figure 4: Si-based QR flyback (left) vs Loss-less GaNSense AHB flyback (right)

140 W, PD 3.1 Evaluation Board

A complete PFC+AHB 140 W, PD 3.1 evaluation board (EVB, Figure 5) has been built and tested for functionality and performance. The design achieves an impressive 100 cc estimated cased size, with 1.4 W/cc power density. The EVB includes optimized PFC, AHB, and SR power stages and magnetics and uses off-the-shelf controllers. The PFC and AHB power trains are designed around the NV6138A GaNSense power IC and the NV6245C GaNSense half-bridge IC. The EVB also includes EMI filtering and passes both conducted and radiated emissions.

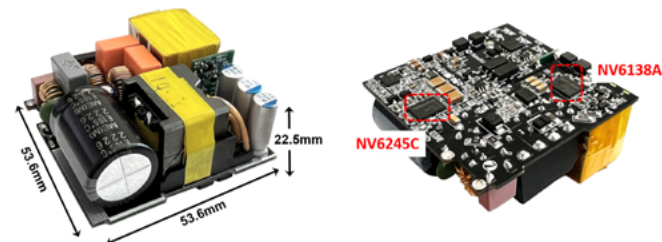


Figure 5: 140 W, PD 3.1 evaluation board, efficiency = 94.5%, estimated cased size = 100 cc

The full-load boost PFC waveforms are shown in Figure 6. During 115 VAC line input, the boost circuit operates in zero-voltage switching (ZVS) conditions, where the boost-switched node-voltage (VSW) slews down to zero before the GaN power FET turns on, in each switching cycle. During 230 VAC line input, the boost circuit operates in partial-ZVS conditions, where VSW slews down to approximately 100 V and then hard-switches from there to zero. The controller automatically detects the valley of the VSW node during the off-time for turning on again each switching-cycle to

optimize the turn-on point at the lowest voltage level possible to minimize hard-switching losses. Since GaN power ICs have very-low output capacitance, the drain voltage will slew quickly down to the valley each cycle. It is critical that the controller has fast valley-detection to ensure that turn-on occurs at the lowest point before the VSW voltage can ring back up. The boost-follower function can also be seen working with the DC bus voltage down at 300 VDC during low-line conditions and up at 400 VDC during high-line conditions.

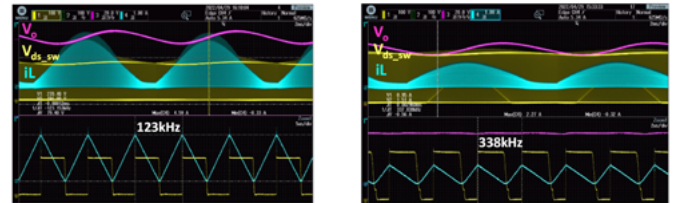


Figure 6: Boost PFC switching waveforms during full load conditions, 115 VAC input (left), 230 VAC input (right), IL=blue (1 A/div), VDS=yellow (100 V/div)

The AHB half-bridge switch node (VSW) and tank current (IL) waveforms during 115 VAC input and full load conditions are shown in Figure 7. The resonant tank current ramps up linearly during each half-bridge low-side on-time and then resonates during each half-bridge high-side on-time. This results in clean and smooth ZVS operation at the GaNSense half-bridge IC VSW output node during each switching cycle. The AHB operating frequency ranges from 125 to 300 kHz, depending on input line and output load conditions.

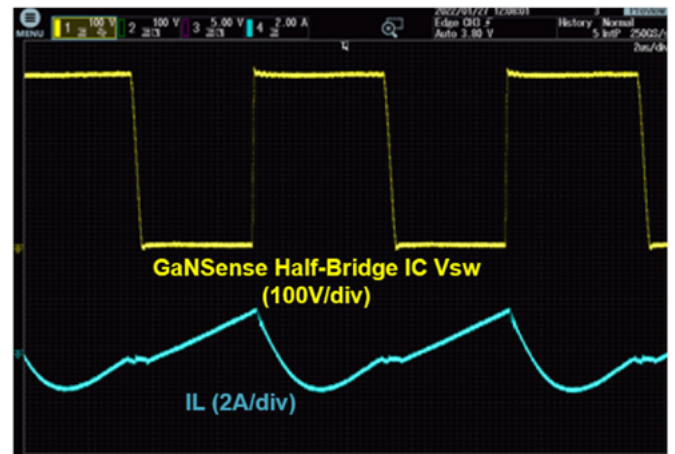


Figure 7: AHB switching waveforms during 115 VAC input and full load conditions, IL=blue (2 A/div), VSW=yellow (100 V/div)

The efficiency curves (Figure 8) show both 4-point efficiency and maximum load efficiency. This design achieves amazing 94.5% full-load efficiency at 90 VAC input which is at least 1% higher than the state of art product, representing up to 20% energy savings. The efficiency at 90 VAC and full-load is the efficiency that determines the cased size and resulting case touch-temperature of the final adapter product.

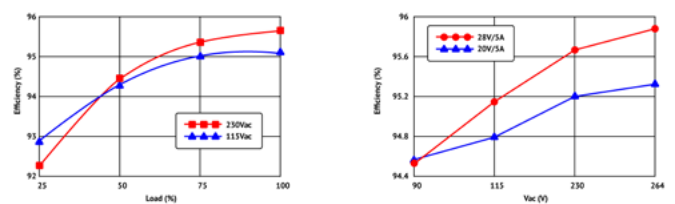


Figure 8: 4-point efficiency (left) and maximum load efficiency (right) curves

Finally, the conducted and radiated EMI are always a major concern with power supply designs. New designs with GaN continuously come into question concerning challenges with EMI due to the faster switching speeds and frequencies. Designers typically do not tackle the EMI portion of their design until it is nearing the completion phase, only to be surprised and learn that the emissions are far above the allowable limits. From the EMI scans for this design (Figure 9) it can be seen that both conducted and radiated EMI both are well below the limits with sufficient margin for manufacturing tolerances. These results are achievable by implementing proper EMI guidelines as early in the design phase as possible, and include such good practices as PCB ground planes, inductor shielding, properly designed EMI filter components, correct PCB floor planning and component locations and proximity.

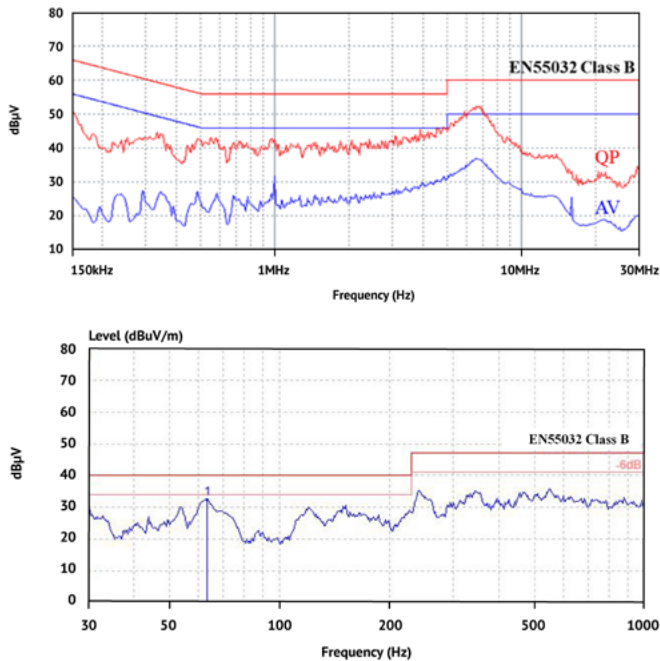


Figure 9: Conducted emissions at 115 VAC/140 W (left) and radiated emissions at 230 VAC/140 W (right)

Conclusion

With the industry in pursuit of higher-density designs, GaNSense power ICs and GaNSense half-bridge ICs lead the way to higher frequencies, improving existing topologies, unlocking future topologies, and ultimately achieving higher efficiencies. Next-generation, high-frequency controllers are also required, as well as new magnetic materials to enable a complete high-speed eco-system, which enables lower temperatures and smaller sizes. Improving existing PFC circuits or using new circuits such as AHB are only small examples of what is possible. More innovation is waiting around the corner as GaN continues to improve and unlock existing and new topologies.

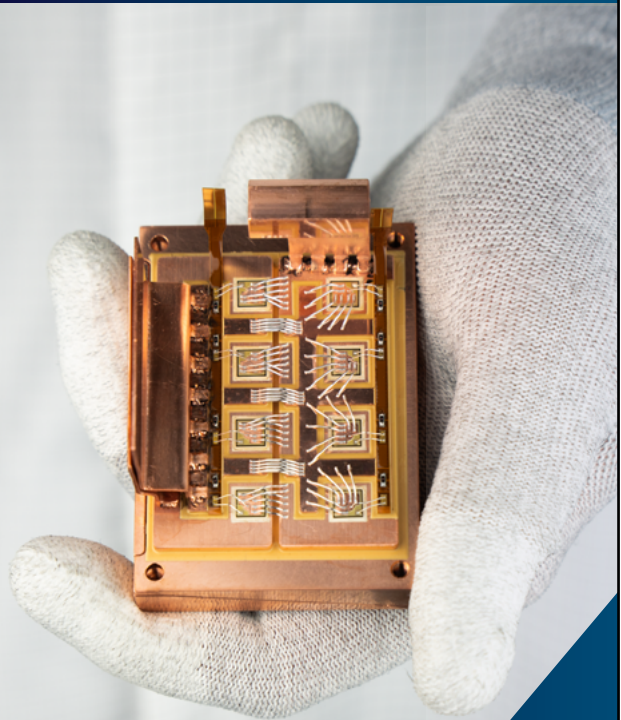
References (www.navitassemi.com)

- 1) GaNFast NV6123, NV6125, NV6127 datasheets, Navitas Semiconductor, 2019
- 2) GaNFast NV613x power ICs with GaNSense technology datasheets, Navitas Semiconductor, 2022
- 3) GaNSense NV624x half-bridge ICs datasheets, Navitas Semiconductor, 2022
- 4) Xiucheng Huang, An Ultra-High Efficiency High Power Density 140W PD3.1 AC-DC Adapter Using GaN Power ICs, APEC Technical Paper, 2023

www.navitassemi.com



RESEARCH PROTOTYPES TALENTS



**SEE US
AT pcim
09.-11.05.23
Hall 6, 210**

SERVICE PORTFOLIO:

- design & simulation
- process development
- sample-production
- testing & validation
- technology workshops

CONTACT:

Prof. Dr. Ronald Eisele | ronald.eisele@fh-kiel.de
 Prof. Dr.-Ing. Aylin Bicakci | aylin.bicakci@fh-kiel.de

Contribution to the Turn-On Losses W_{on} of a 600V MOSFET Caused by the FWD's Storage Charge Q_{rr}

By theory, turn-on and -off losses W_{on} and W_{off} of MOSFETs can become calculated from the data for t_{rise} and t_{fall} given in the datasheets. In fact there is a freewheeling diode FWD which has a turn-off behaviour that determines the turn-on losses of the MOSFET due to its storage charge Q_{rr} . In this article a brief description why there is an impact of the diode turn-off to the MOSFET turn-on is given, also measurement results of a double-pulse test stand are shown. Finally, a formula for a first estimation of the MOSFET turn-on losses from diodes Q_{rr} and the operating conditions is given.

By J. Ranneberg, Professor, HTW Berlin

Introduction

In principle, there are two kinds of losses in a power semiconductor: on-state losses and switching losses. The latter are consisting of turn-on and turn-off losses. The on-state losses are determined by the current, the on-state voltage (for a MOSFET by its R_{Dson}) and the duty-cycle. Within the several parameters describing a power semiconductor, the so-called characteristic switching frequency gives a hint of the useful switching frequencies. To estimate the efficiency and to design the cooling the total losses are decisive. Therefore, the switching losses are important in different ways. Former test in the same set up showed that the gate resistor has only limited impact on the switching losses and the turn-on losses transgress the turn-off losses. Therefore, here the impact of the reverse recovery charge Q_{rr} on the turn-on losses W_{on} is analysed.

Diode turn-off at MOSFET turn-on

One typical application of a MOSFET is its use as a low-side single switch together with an inductive load, see figure 1. When turned-on the load current I_L flows through the load and the MOSFET, when turned-off the load current commutates into the free-

wheeling diode (FWD). This current returns to the MOSFET at its next turn-on. The turn-off of the MOSFET is the turn-on of the FWD and vice versa. Therefore, the turn-off of the diode affects the turn-on of the MOSFET.

Also in figure 1, the stray inductance L_σ is mentioned. This is important for the voltage overshoot at the MOSFET when it turns-off.

Turn-off behaviour of bipolar diodes

At diode turn-off, the current is decreasing with a determined slope di/dt . In bipolar diodes, after the current has become zero it reduces further to negative values until the mobile carriers in the diode have recombined. This causes a negative current I_{rr} together with a reverse recovery charge Q_{rr} . While the diode current decreases towards its peak reverse value I_{rr} , the storage time t_s elapses. After the mobile carriers have recombined, the diode gains its capability to block voltages [1] [2]. As a consequence the MOSFET has to withstand (nearly) the DC-voltage U_D for t_s , see fig. 2.

This causes a high turn-on loss energy in the MOSFET. After the reverse recovery peak the reverse recovery current fall time t_f starts, both times together are the reverse recovery time t_{rr} :

$$t_{rr} = t_s + t_f \tag{1}$$

Because the load current I_L remains nearly constant during these short switching transitions the reverse recovery current of the diode causes a current overshoot in the MOSFET, see figure 2. This additional current also causes additional losses in the MOSFET.

The turn-off behaviour of the diode depends on several parameters, as the di/dt at turn-off, the load current and the tem-

perature as well as the diode type [2]. In reality the peak reverse current I_{rr} can be higher than the load current I_L , see figure 4!

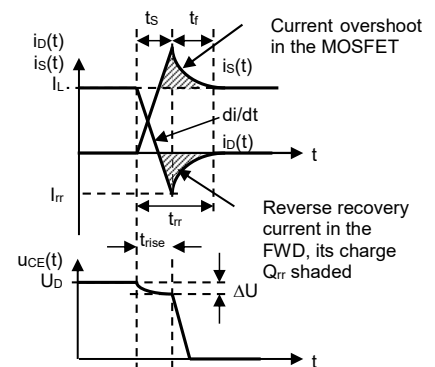


Figure 2: Principle coherence of diodes behaviour at turn-off to the turn-on of the MOSFET

The high di/dt at current turn-off in the diode can induce voltages in the stray inductances L_σ and therefore cause emc problems. So for bipolar diodes attempts were made to give them a "softer" turn-off behaviour by reducing the di/dt during t_f which increase t_f . The turn-off behaviour can be distinguished in "soft" and "snappy" by the ratio of t_f and t_s giving the factor S , called "snappiness factor" [3] resp. soft factor [4] [2]:

$$S = \frac{t_f}{t_s} = \frac{t_{rr} - t_s}{t_s} = \frac{t_{rr}}{t_s} - 1$$

$$S + 1 = \frac{t_{rr}}{t_s} \quad \frac{t_s}{t_{rr}} = \frac{1}{S + 1} \tag{2}$$

Because the diode turn-off behaviour is crucial for the switch (MOSFET or other technology), several attempts were made to improve it [5]. Unfortunately, a reduction of Q_{rr} enlarges the on-state voltage [2].

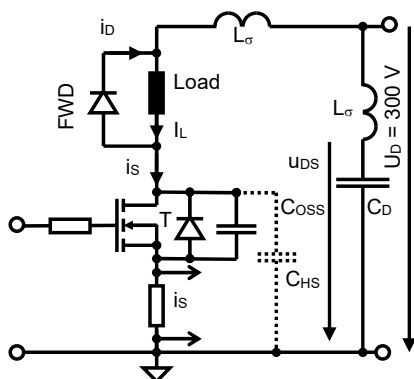


Figure 1: Schematic diagram of the test stand

Turn-off behaviour of Schottky diodes

A diode with nearly ideal switching waveforms is the so-called Schottky diode, see figure 5. This is a unipolar diode without a p-n junction but with a metal-semiconductor contact building a depletion zone. The threshold voltage is lower than for bipolar diodes, for silicon about 300 – 400 mV. The very small recovery charge is of capacitive origin and caused by the growth of the depletion zone due to the reverse voltage. Unfortunately, Schottky diodes made from silicon are limited in their blocking voltage to about 200 V [2] [3].

Loss calculation in theory

The theoretical method to calculate the switching loss energies W_{on} and W_{off} of a MOSFET switching a current I_L at a voltage U_D is

$$W_a = \frac{t_{rise} * U_D * I_L}{2}$$

$$W_{off} = \frac{t_{fall} * U_D * I_L}{2}$$

$$W_{COSS} = \frac{C_{OSS} * U_D^2}{2} \tag{3}$$

where W_{COSS} is the energy stored in the output capacitance C_{OSS} . This stray capacity is charged to U_D at turn-off of the MOSFET. At turn-on the MOSFET shortens this capacity. Therefore, the discharge current of C_{OSS} cannot be measured by the shunt shown in figure 1. For the used MOSFET C_{OSS} is given to be 48 pF resulting in 2,2 µJ at 300 V. Usually this energy is small compared to W_{on} , compare table 1. However, it should be checked for higher voltages because it depends on the square of U_D and the capacity from Drain to ground can be increased by the capacity C_{HS} of a heat sink (dashed in figure 1). The discharge of C_{HS} would be visible in the current i_S , see figure 1.

It should be kept in mind that in the formulas for W_{on} and W_{off} the factor ½ is because the area of a triangle is calculated whereas for W_{COSS} this factor is due to the integral of the capacitor formula.

The switching loss power P_{VS} is the product of the energies W_{on} and W_{off} with the switching frequency.

By the curves given in figure 2 it can be seen that for turn-on the voltage is slightly reduced by D_U which is the product of the stray inductance L_σ and the current slope di/dt . In practice, these stray inductances must be kept small to provide a safe turn-off with a low voltage overshoot.

Also it can be seen from figure 2 that there is a part of the reverse recovery charge Q_{rr} that is flowing through the MOSFET while this MOSFET is exposed to the full voltage U_D . This lasts for t_S . Therefore, in theory this additional part of losses at turn on is

$$W_{Qrr} \approx \frac{t_S * Q_{rr} * U_D}{t_{rr}} = \frac{Q_{rr} * U_D}{S + 1} \tag{4}$$

The other part of Q_{rr} causes turn-off losses in the diode. However, in practice this is hard to handle, especially because the definition given in (2) has drawbacks [2].

Double Pulse Test Stand

The test stand was realized on a PCB. The DC supply and the double pulse generator are externally and therefore not shown in figure 3. To estimate the stray inductance a turn-on transient with a standard 600 V 1 A diode was measured. As shown in figure 4 the source current increases within 100 ns from 0 to 13 A (!) while the voltage across the MOSFET decreases by approximately 15 V corresponding to a stray inductance of about

$$L_\delta \approx \frac{15V * 100ns}{13A} = 115nH \tag{5}$$

Proven Reliability in Military / Aviation / Traction & Industrial Demanding Applications

POWEREX Power Semiconductor Solutions

High Voltage IGBTs

Rugged, High Reliability, Field Proven Packaging
 Extended temperature range -40°C to 150°C
3.3 KV, 4.5 KV, & 6.5 KV Modules

Powerex HVIGBTs outperform competition with lower losses. Higher isolation voltage and greater creepage and strike clearance than the competition is now available. Customizable for volume opportunities.

- 100% partial discharge tested
- 100% serialized test data retention
- 100% dynamic testing offered on all HVIGBTs
- Advanced Mitsubishi R-Series chip technology
- Aluminum nitride (AlN) ceramic substrate for low thermal impedance
- Rugged SWSOA and RRSOA
- Isolation voltage available up to 10.2 KV
- Full reliability/qualification capability provided by Powerex
- High voltage diodes in same mechanical footprints available
- Si/SiC hybrid available upon request

Flexible, Convenient Online Ordering Options
 For more information contact: OrderManager@powerex.com

www.powerex.com 001-724-925-7272


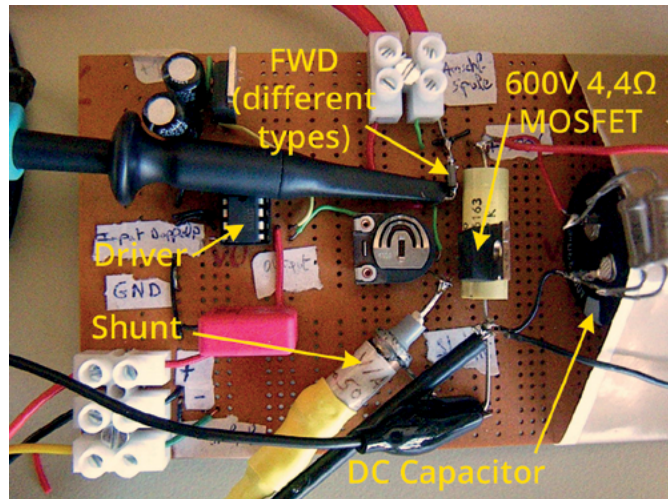



Figure 3: Test stand used for the measurement

By this stray inductance the current increase at turn-on is limited to $U_D / L_\sigma = 2,6 \text{ kA} / \mu\text{s}$. However, this is beyond the MOSFET capabilities. It can be seen in figure 4 by the high reverse current i_{rr} and the long t_{rr} that the used 600 V 1 A bipolar standard diode is not the best choice for this application. The bandwidth limitation in this measurement is for explanation only, all measurements for W_{on} , W_{off} and Q_{rr} were made with full bandwidth of 100 MHz.

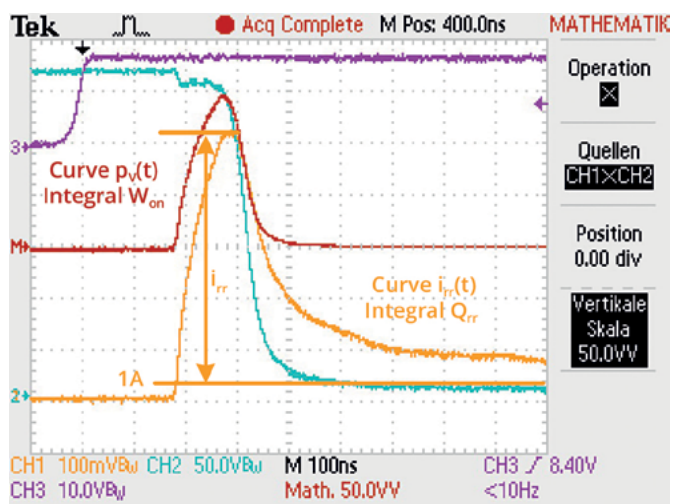


Fig 4: Turn-on behaviour of a MOSFET with a 600V 1A bipolar standard diode used as FWD, bandwidth limitation for better survey only, time 100ns / Div
 CH1: i_S 2,5 A / Div, CH2: u_{DS} 50 V / Div, CH3: trigger signal for second pulse
 MATH = CH1 X CH2: $p_V(t)$ 1250 W / Div

Measurements of Loss Energies and Q_{rr}

As shown in figure 1 a shunt providing 40 mV / A into 50 Ω was placed in the Source connection of the MOSFET. The Drain-Source voltage was measured with a 10:1 probe and both were multiplied by the oscilloscopes MATH function. In contrast to fig. 3 the full 100 MHz bandwidth of the scope was used. These data were exported as “comma separated values” (“CSV”) and further analysed with a chart calculation program on a PC. The instantaneous power pV(t) of each measured point was multiplied with the time interval Dt and summed up during the switching transitions to get W_{on} resp. W_{off} .

For the measurement of Q_{rr} the load current of $I_L = 1$ A was subtracted from the measured source current i_S during t_{rr} . All source current above the load current is driven by Q_{rr} , see figure 2.

This part of the current was multiplied with the time interval Δt to get the charge and these were summed up from $i_S > 1$ A to $i_S = 1$ A. In this way, Q_{rr} was calculated.

Diodes used in Test Stand

For different types of diodes used as FWD the diode reverse recovery charges Q_{rr} , as well as the MOSFET turn-on loss energies W_{on} where measured at 300 V, 1 A and room temperature. The MOSFET remained the same for all freewheeling diodes. The results are given in table 1 in order of increasing reverse recovery charge Q_{rr} .

For the used MOSFET a t_{rise} of 23 ns is given in the datasheet resulting in 3,5 μJ for W_{on} at 300 V for 1 A according to equation (3). The measured values for W_{on} shown below are higher (for bipolar diodes far higher) and depend strongly on the Q_{rr} of the FWD.

The first attempt would by a 600 V 1 A bipolar standard diode because its maximum ratings would fit the requirements. Unfortunately, it provides very large I_{rr} and Q_{rr} (see figure 4) resulting in high turn-on losses of the MOSFET. The same occurs with a 1000 V 1 A bipolar standard diode.

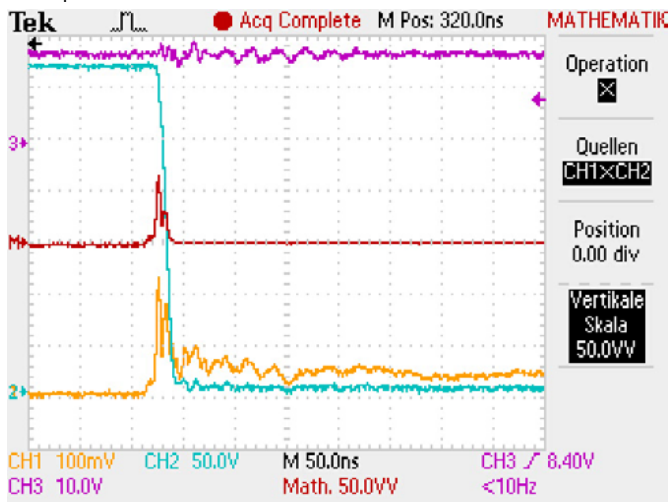


Figure 5: Turn-on behaviour of a MOSFET with a 600 V 2 A SiC-Schottky diode used as FWD, full bandwidth, time 50ns / Div

CH1: i_S 2,5 A / Div, CH2: u_{DS} 50 V / Div, MATH = CH1 X CH2: pV(t) 1250 W / Div

Better choices where the fast bipolar diodes. The tested 600 V 1 A type is still in production whereas the 1500 V 1 A type is of an obsolete type (but still performing good).

Because MOSFETs were often used in bridge topologies, the bodydiode in a second MOSFET of the same type was tested. It gave lower I_{rr} and Q_{rr} resulting in lower W_{on} than for the standard bipolar diodes but performed not as good as the two fast bipolar diodes.

Also two types of Schottky-Diodes were tested. First a series connection of three 150 V 1 A Si-Schottky diodes. This series connection was used because no 600 V Si-Schottky diodes are available. The blocking capability of 3 * 150 V = 450 V was sufficient for experi-

FWD type	Q_{rr} [μC]	W_{on} [μJ]	eq. (6) [μJ]
600V 2A SiC-Schottky	0,03	5,5	10
600V 1A bipolar fast (in production)	0,08	24,1	18
Three 150V 1A Si-Schottky in series	0,085	20	18
1500V 1A bipolar fast (obsolete)	0,33	95	55
MOSFETs body diode (MOSFET of same type)	1	233	156
600V 1A bipolar standard in parallel to 600V 1A bipolar fast (in production)	2,35	365	358
600V 1A bipolar standard in parallel 3 x Si-Schottky in series	2,58	407	393
1000V 1A bipolar standard	2,63	362	400
600V 1A bipolar standard	2,65	386	403

Table 1: Measured Q_{rr} , measured W_{on} and approximation of W_{on} by equation (6)

mental purposes. This gave about 6% more Q_{rr} but 17% less W_{on} compared with the fast bipolar diode in production. The best diode used in this test was a 600 V 2 A SiC-Schottky diode. It gives among the tested diodes by far the lowest values for Q_{rr} and W_{on} .

Also a parallel connection of the 600 V 1 A standard diode with the series connection of the three 150 V 1 A Si-Schottky diodes was tested. The idea is that at least a part of the current is flowing through the Schottky diodes so that the turn-off behaviour will be somewhere between that of the standard diodes and that of the Schottky diodes. However, this gave about only 3% less Q_{rr} but about 5% more W_{on} compared with the standard diode alone. This will be within the tolerances of the measurements. This small difference compared to the 600 V 1 A standard diode alone is not surprising because in the series connection of the three Schottky diodes their threshold voltages are added too so that only very few current will flow through them.

Better performed the parallel connection of the same 600 V 1 A bipolar standard diode with the fast bipolar diode type that is still in production. Here the threshold voltages are similar so that a certain amount of the current should flow through the fast diode. That gave about 11% less Q_{rr} but only about 5% less W_{on} compared to the slow standard diode.

Approximation of W_{on} by Q_{rr} and U_D

The calculation of the MOSFET loss energy W_{Qrr} at turn-on by eq. (4) is difficult to calculate. So an approximation to estimate the complete turn-on losses by t_{rise} , I_L , U_D , C_{OSS} and Q_{rr} according to eq. (6) was made.

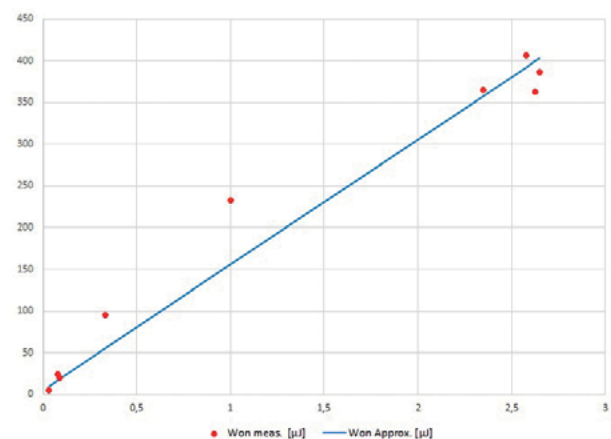


Figure 6: Measured W_{on} (red dots) and their approximation according to equation (6) (blue line) as function of the measured Q_{rr}

$$W_{on} \approx \frac{t_{rise} * U_D * I_L}{2} + \frac{C_{OSS} * U_D^2}{2} + \frac{Q_{rr} * U_D}{2} \tag{6}$$

It was assumed that the half of Q_{rr} is flowing through the MOSFET at full voltage producing loss energy in it. For linear slopes this corresponds to a factor $S = 1$, see equation (2) and figure 2. Therefore the factor $\frac{1}{2}$ in the last term of equation (6) represents t_s / t_{rr} and should be compared to the remark about the factor $\frac{1}{2}$ given for equation (3). For t_{rise} the value from the datasheet (145 ns) was used. If there is a capacity C_{HS} (see figure 1), it should be added to C_{OSS} in equation (6).

The resulting values of equation (6) are given also in table 1 (right column). Sometimes the individual measured values differ from the values calculated according to equation (6). However, if measured and calculated values are shown in the same diagram it can be seen that equation (6) gives at least a useful approximation. It must be kept in mind that the Q_{rr} exploited in (6) is the measured value and not a datasheet value.

The approximation equation (6) gives a linear dependency of W_{on} from Q_{rr} but an interpolation of the measured values in figure 6 would have a bended curvature. A possible explanation could be that manufacturing measures to reduce Q_{rr} by shortening the carrier lifetime gives the diode a more snappy reverse recovery behaviour and therefore a changed ratio of t_s / t_{rr} .

Conclusion

Especially together with bipolar freewheeling diodes, the turn-on energy of a MOSFET is higher than calculated in theory. The freewheeling diodes storage charge has a strong impact on the turn-on losses of the MOSFET. This is important especially in applications with high switching frequencies. Therefore the use of fast bipolar or Schottky diodes can reduce the total losses of the MOSFET.

The discrete parallel connection of a standard bipolar with a fast bipolar diode had only little advantage whereas the discrete parallel connection of the bipolar standard diode with a series connection of three Si-Schottky diodes gave a slightly smaller Q_{rr} but also a slightly increased W_{on} .

Together with Schottky diodes the losses caused by the stray capacitance C_{OSS} can be considerable, especially if there is an additional capacity C_{HS} of a heat sink.

References

- [1] K. Heumann, Grundlagen der Leistungselektronik, 6. Auflage, B.G. Teubner, Stuttgart 1996
- [2] J. Lutz, Halbleiter-Leistungsbaulemente, Springer Verlag Berlin 2006
- [3] N. Mohan et al., Power Electronics, 2nd Edition, Wiley and Sons, New York 1995
- [4] H. Gebhardt, Untersuchung von schnellen Halbleiterdioden (Recovery) in Verbindung mit abschaltbaren Ventilen in PWM- und Resonanz-schaltungen, Dissertation TU Berlin 1993
- [5] U. Nicolai et al., Applikationshandbuch IGBT- und MOSFET-Leistungsmodule, Verlag ISLE Ilmenau, 1998

www.htw-berlin.de

We've Got Power!

Now an RFMW Company

PCIM Europe
Hall 7, #136

Strategically Aligned Distribution
With World-leading Manufacturers
in Power, RF and Microwave

mrccomponents.com
info@mrccomponents.com

Ask the
Experts

Bodo's Power Systems® · bodospower.com

How to Design an Intelligent Battery Junction Box for Advanced EV Battery Management Systems

As electric vehicles (EVs) become more popular, the challenge for automakers is to reflect true range while making the vehicle more affordable.

This translates into making the battery packs lower cost with higher energy densities. Every single watt-hour stored and retrieved from the cells is critical to extend the driving range.

By Issac Hsu, Product Marketing Engineer, Brushless DC Motor Drivers, Texas Instruments

The main function of a battery management system (BMS) is to monitor cell voltages, pack voltages and pack current. In addition, due to the high-voltage design of the BMS, insulation resistance measurement between the high-voltage domain and low-voltage domain is needed in order to catch defects in the battery structure and protect against hazardous conditions.

Traditional BMS → Intelligent Battery Junction Box (BJB)

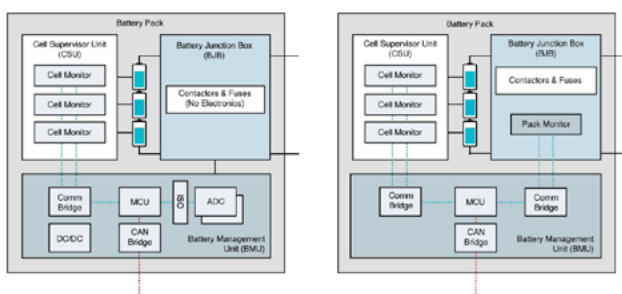


Figure 1: A traditional BMS architecture (a); a BMS architecture with an intelligent battery junction box (BJB) (b)

Figure 1 presents a typical BMS architecture containing a battery management unit (BMU), cell supervisor unit (CMU) and a battery junction box (BJB). A BMU typically has a microcontroller (MCU), which manages all of the functions within the battery pack. The traditional BJB is a relay box or a switch box with power contactors that connects the entire battery pack to the load inverter, motor or the battery charger.

Figure 1a shows the traditional BMS. There are no active electronics inside of the junction box. All of the measurements in the BJB are measured at the BMU. There are wires connecting the BJB into the analog-to-digital converter (ADC) terminals.

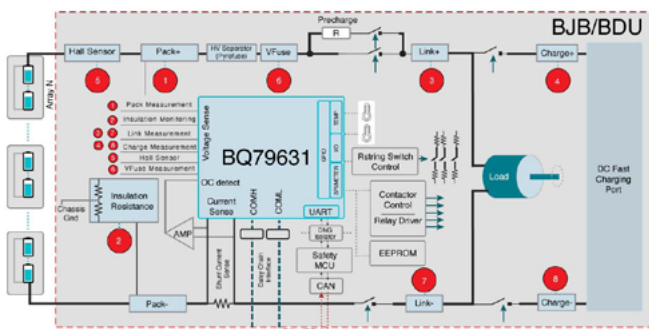


Figure 2: High-voltage measurements inside the BJB

Figure 1b shows the intelligent BJB. There is a dedicated pack monitor inside the box that measures all voltages and currents and passes the information to the MCU using simple twisted-pair communication. It helps eliminating wires and cabling harnesses; and improves voltage and current measurements with lower noise.

Voltage, temperature and current measurement

Figure 2 shows the different high voltages, current and temperatures that the pack monitor measures inside a BJB enabled by the BQ79731-Q1 battery pack monitor.

- **Voltage:** The high-voltage is measured using divided-down resistor strings. These voltage measurements monitor the state of high-voltage components in the system.
- **Temperature:** The temperature measurements monitor the temperature of the shunt resistor so that the MCU can apply compensation, as well as the temperature of the contactors to make sure that they are not stressed beyond the normal operating conditions.
- **Current:** The current measurements are based on either:
 - A shunt resistor - Because the currents in an EV can go up to thousands of amperes, the shunt resistance values are extremely small - in the range of 25 μOhms to 50 μOhms ; or
 - A Hall-effect sensor - Used to measure the EV current on the high-voltage rail, while still being isolated. Its dynamic range is typically limited, thus there can be multiple sensors in the system to measure the entire range.

Over current fault detection and protection

Detection and prevention of an over-current even is required in a BMS in order to prevent catastrophic damage that can occur to the battery pack in the event of a short circuit, exposed high-voltage terminal or defective equipment. An over current circuit integrated in the BJB unit will use the current sense information measured through either the shunt resistor or hall-effect sensor and the battery pack monitor. This measurement is then processed and compared to a threshold inside the battery pack monitor while the same has the capability of signaling an over-current event through dedicated outputs which will be used to enable a fuse-driver in order to blow the high-voltage separator (pyro-fuse). Since the reaction time for this needs to be as fast as possible, a dedicated signal processing path is implemented in the battery pack monitor device.

Voltage and current synchronization

Voltage and current synchronization is the time delay that exists to sample the voltage and current between the pack monitor and cell monitor. These measurements are mainly used for calculat-

ing state of charge and state of health through electro-impedance spectroscopy (EIS). Calculating the impedance of the cell by measuring the voltage, current and power across the cell enables the BMS to monitor the instantaneous power of the car.

The cell voltage, pack voltage and pack current have to be time-synchronized to provide the most accurate power and impedance estimations. Taking samples within a certain time interval is called the synchronization interval. The smaller the synchronization interval, the more accurate the power estimate or the impedance estimate. The more accurate the state-of-charge estimation, the more accurate remaining mileage drivers get.

Synchronization requirements

Next-generation BMS will require synchronized voltage and current measurements in less than 1 ms, but there are the challenges in meeting this requirement:

TI's battery monitors can maintain a time relationship by issuing an ADC start command to the cell monitor and the pack monitor. These battery monitors also support delayed ADC sampling to compensate for the propagation delay when transmitting the ADC start command down the daisy-chain interface.

Remote device communication support

Another benefit of the intelligent BJB is the streamlined data communication by using the versatile daisy-chain interface not just for battery pack and battery cell monitor devices, but also remote devices like EEPROM memory or any type of sensors that are placed in the modules with different physical placement in the vehicle. In this case the pack and monitor device also act as an interface translator offering I2C or SPI data to be transferred through the daisy-chain interface which eliminates wires and cabling harnesses and in turn reduces the overall EV weight.

The massive electrification efforts happening in the automotive industry are driving the need to reduce the complexity of BMS by adding electronics in the junction box, while enhancing system safety. A pack monitor can locally measure the voltages before and after the relays, the current through the battery pack. The accuracy improvements in voltage and current measurements will directly result in optimal utilization of a battery. The BQ79631-Q1 and BQ79731-Q1 from TI can optimize the performance and reduce the future cost of intelligent BJBs by integrating all necessary functions of the system in a single device. Effective voltage and current synchronization enable precise state-of-health, state-of-charge and EIS calculations that will result in optimal utilization of the battery.

In addition, TI's BQ79616-Q1 and BQ79718-Q1 battery cell monitor families offer accurate cell voltage and temperature measurements as a part of the CSU implementation which enables a complete BMS eco-system.

Additional resources

- Watch these TI training videos:
 - "Intelligent Battery Junction Box for Voltage and Current Synchronization." <https://training.ti.com/intelligent-battery-junction-box-voltage-and-current-synchronization>
 - "xEV Battery Pack Autonomous Management in Park Mode." <https://training.ti.com/xev-battery-pack-autonomous-management-park-mode>
- Check out the white paper, "Functional Safety Considerations in Battery Management for Vehicle Electrification." <https://www.ti.com/lit/wp/sliy006/sliy006.pdf>

www.ti.com

Modular SiC Inverter Reference Design

Powered by CISSOID SiC Intelligent Power Module & Silicon Mobility OLEA® T222 FPCU & OLEA® APP INVERTER Software.

This Inverter offers a modular electrical and mechanical integration of a 3-phase 1200V/340A-550A SiC MOSFET Intelligent Power Module from CISSOID with OLEA® T222 FPCU control board and application software from Silicon Mobility. This unique hardware and software supports the rapid development of e-motor drives up to 350kW/850V, setting new levels in terms of power density and efficiency.



- Up to 350kW/850V
- Modular SiC power module
- Low-ESL DC-Link capacitor
- 900V/400A EMI filter
- Liquid cooling

- Robust SiC gate driver
- OLEA® T222 FPCU controller
- DC & phase current sensors
- Advanced control algorithms
- SVPWM or DPWM up to 50kHz

www.cissoid.com



Ionic Mineral Technologies: Unearthing the Nano-Silicon Solution

As the demand for higher capacity, more scalable and greener next-generation battery materials accelerates, Ionic MT presents a nano-silicon solution.

By Andre Zeitoun, CEO and Founder, and Dr Jake Entwistle, Director of Battery Materials, at Ionic MT

The interest in silicon anodes is intensifying. The silicon anode battery market is predicted to grow from \$1.2 bn USD in 2021 to \$208 bn USD by 2031, according to Transparency Market Research. Silicon anodes, the negatively charged parts of lithium-ion batteries that store lithium ions flowing from the positively charged cathodes during charging, store more lithium ions than graphite, the incumbent technology. This is why silicon's credentials as an anode is overtaking that of graphite, which is currently the most commonly used anode material, as silicon has a significantly higher energy density. When you add into consideration graphite shortages, global legislative pushes to curb an over reliance on imported battery materials, as well as the demand for more efficient electrification driven by the highest carbon emissions on record, it is clear that silicon offers a promising solution. Ionic MT's mission is to electrify the future and power the next generation with our nano-silicon battery material.



Ionic MT has in house battery testing

Ionic MT is addressing the unmet need for next-generation silicon anode battery materials with our drop-in nano-silicon anode product, Ionisil™, in a unique way. Based in Utah, U.S.A., Ionic MT is vertically integrated through control of our Utah-based halloysite clay deposit, the source of our nano-silicon feedstock which is refined at our nearby battery materials production facility.

The vertically integrated approach, which has been attributed to the success of the likes of Tesla, allows full control of our process and the ability to apply, adapt and innovate technologies domestically. It also exemplifies the domestic approach to green technologies, a movement legislated by the U.S. Government's Inflation Reduction Act. Other countries such as the U.K. are exploring similar legislative equivalents to regulate and strengthen the battery materials supply chain.

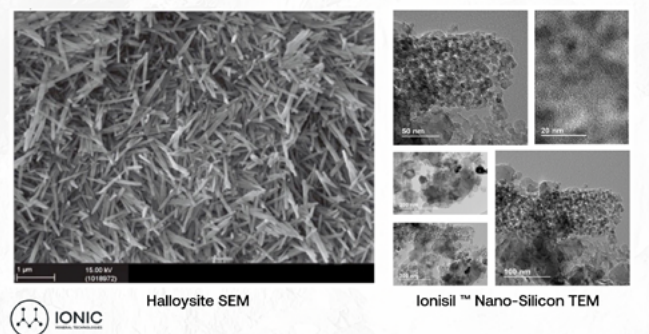
The company's halloysite deposit, Halloysite Hills, is the largest high-purity deposit in the world. It is an open pit mine that can be easily mined without the need for water, chemicals or explosives.

The mine appears very different to the typical image that a 'mineral mine' may conjure as it blends with the surrounding mountain range and is reseeded with natural flora after exploration. Sustainability is central to our company ethos and starts at the source with our halloysite feedstock; we are proud to have developed the greenest, most scalable process to produce nano-silicon material on the market for higher capacity lithium-ion batteries. Based on initial reserves, we are capable of producing over 600,000 metric tonnes of finished nano-silicon over the life of the mine, equivalent to 6 million metric tonnes of synthetic graphite based on silicon having approximately 10x higher energy density. We are also discovering significant new halloysite reserves via extensive drilling programmes.



Nano-silicon material in the Ionic MT lab

Our innovative nano-silicon technology utilizes the natural nanotubular structure of halloysite, a naturally occurring aluminosilicate mineral. Halloysite has a nano structure that was synthesized in the ground over the last 35 million years, which we apply using a top-down synthesis process that requires significantly less energy input using a continuous process. The unique nano-silicon structure allows us to address the challenges conventional silicon commonly faces, namely the swelling and degradation of the battery which can occur over repeated charge-discharge cycles, causing capacity



Halloysite and nano-silicon electron microscopy images

loss. Conventional silicon swells to 3x its size when in contact with lithium during charging, which causes capacity loss per charge and rupturing, reducing battery lifespan.

However, Ionisil™, with its nanotubular porous structure inherited from the halloysite, means that the silicon can swell into its own pore volume, reducing battery degradation. The nano sized particles can also improve the cycling stability.

Our nano-silicon production process also creates important critical mineral byproducts. Every metric tonne of nano-silicon produced results in two metric tonnes of alumina, which is listed as a US critical mineral. The acid used during the manufacturing process can also be reclaimed as well as producing additional by-products from reductants.

It is not just our approach to battery materials that is different; our results are, too. Ionisil™ Gen-1 has achieved the highest stable capacity nano-silicon on the nano-silicon market, which is key to a longer range battery. As product development continues, we are breaking new ground with the capacity of our nano-silicon material and exciting further developments are to come.

Ionic MT is gearing up; we will move to our new 36,000 sq ft facility in August to commence commercial scale nano-silicon production where we will be working towards our 2,000 metric tonnes per year target to continue our mission to electrify the future.

Ionic MT will be exhibiting at the Battery Show Europe in Stuttgart from 23-25 May 2023; you can find them at booth 8-G56 where they will be happy to discuss their developments.

Learn more about Ionic Mineral Technologies at Ionicmt.com.

www.ionicmt.com

PAYTON PLANAR MAGNETICS
 The global leader of Planar Magnetics Technology

UK USA JPN CHN KOR

- All SMPS Planar Magnetics
- 10Watts to 150kWatts
- Fast Custom Designs & Samples

PAYTON PLANAR MAGNETICS
 1805 S. Powerline Road, Suite 109
 Deerfield Beach, FL 33442 USA
 Tel: (954) 428-3326 x203 | Fax: (954) 428-3308
 jim@paytongroup.com
 www.PaytonGroup.com



NEW!

XFlux® Ultra

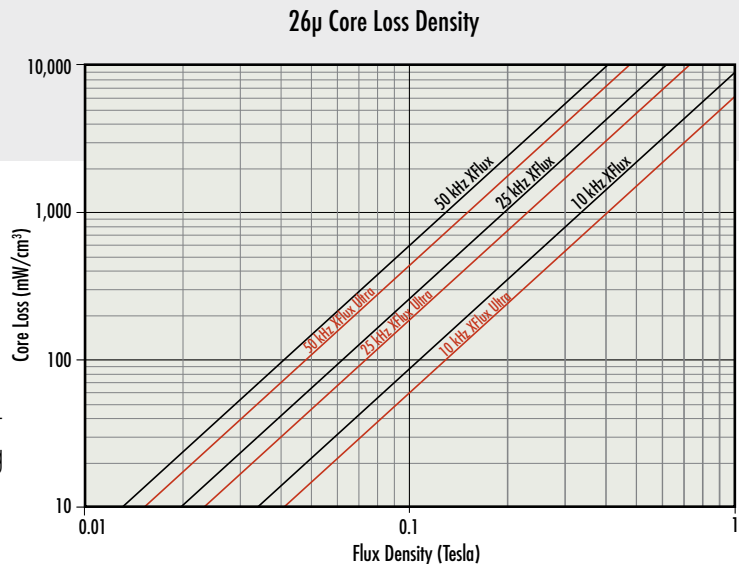
POWDER CORES

Same great DC Bias and high saturation found in XFlux while providing a 20% improvement in core loss.



VISIT US AT PCIM HALL 9 BOOTH 450

www.mag-inc.com



Power Quality Monitoring Part 2: Design Considerations for a Standards Compliant Power Quality Meter

This article explains how to efficiently design a standards compliant power quality (PQ) measurement instrument using a ready to use platform that accelerates development. It will discuss different solutions for designing a Class A and Class S meter, including a new Class S power quality measurement integrated solution that significantly reduces the development time and costs for power quality monitoring products. The article “Power Quality Monitoring Part 1: The Importance of Standards Compliant Power Quality Measurements” in our April issue provided an understanding of the IEC standard of power quality and its parameters.

By Jose Mendia, Senior Engineer, Product Applications, Analog Devices

Challenges to Implementing a Power Quality Solution

The basic components of an instrument designed for power quality measurement are shown in Figure 1. First, the current and voltage transducers must account for the operational range of the instrument and adapt the input signal to the dynamics of the analog-to-digital converter (ADC) input. Traditional transducers are the first source of uncertainty in the measurement; therefore, correct selection is of great importance. Next, the signal goes to an ADC; its individual characteristics such as offset, gain, and nonlinearity errors create a second source of uncertainty. Selecting the correct ADC for this function is a demanding effort for designing a power quality instrument. Lastly, a series of signal processing algorithms must be produced to get electrical and power quality measurements from the input signals.

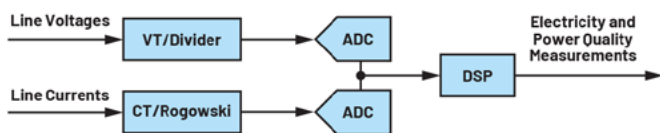


Figure 1: The main components of an instrument for power quality measurements.

Class	Measurement	Conditions	Maximum Error
A	Voltage	$U_M \geq 1\%$ U_{NOM}	$\pm 5\% U_M$
		$U_M < 1\%$ U_{NOM}	$\pm 0.05\% U_{NOM}$
	Current	$I_M \geq 3\% I_{NOM}$ $I_M < 3\% I_{NOM}$	$\pm 5\% I_M$ $\pm 0.15\% I_{NOM}$
S	Voltage	$U_M \geq 3\%$ U_{NOM}	$\pm 5\% U_M$
		$U_M < 3\%$ U_{NOM}	$\pm 0.15\% U_{NOM}$
S	Current	$I_M \geq 10\% I_{NOM}$ $I_M < 10\% I_{NOM}$	$\pm 5\% I_M$ $\pm 0.15\% I_{NOM}$

Table 1: Accuracy Requirements for Current, Voltage, and Power Measurements Specified by IEC 61000-4-7 Standard

Voltage and Current Transducers

Depending on the location and application of the power quality instrument, the nominal supply voltage (UNOM), nominal current (INOM), and frequency varies. Independently of the nominal values that the instrument measures, the IEC 61000-4-7 standard requires power quality measurement instruments to reach the accuracies presented in Table 1; therefore, the transducers must be selected such that the instrument fulfills the accuracy requirements.

I_{NOM} : Nominal current range of the measurement instrument
 U_{NOM} : Nominal voltage range of the measurement instrument
 U_M , I_M , and P_M : Measured values

The IEC61000-4-71 standard recommends designing the input circuitry following these nominal voltages (U_{NOM}) and nominal currents (I_{NOM}):

- ▶ For 50 Hz systems: 66 V, 115 V, 230 V, 400 V, 690 V
- ▶ For 60 Hz systems: 69 V, 120 V, 240 V, 277 V, 347 V, 480 V, 600 V
- ▶ 0.1 A, 0.2 A, 0.5 A, 1 A, 2 A, 5 A, 10 A, 20 A, 50 A, 100 A

Additionally, the transducers selected for measuring voltage and current must keep their characteristics and accuracy unchanged when a 1.2x UNOM and INOM are applied continuously. A signal four times the nominal voltage or 1 kV rms, whichever is less, applied for 1 second to the instrument must not lead to any damage. Likewise, a 10x INOM current for 1 second shall not produce any damage.

Analog-to-Digital Converter

Even though the IEC 61000-4-30 standard does not specify a minimum requirement for sampling rate, the ADC must have enough sampling rate to measure some oscillatory and fast power quality phenomena. An insufficient sampling rate could result in the misclassification of a power quality event or the failure to detect one. The IEC 61000-4-30 standard states that the instrument voltage and current sensors should be appropriate for up to 9 kHz. Thus, the sampling frequency of the ADC must be selected following the rules of signal analysis to perform a measurement of frequency components up to 9 kHz included. Figure 2 illustrates the consequences of when the sampling rate is not sufficient. The top left waveform contains 64 samples per 10 cycles (200 ms) and the top right waveform has 1024 samples per 10 cycles. As shown in Figure 2, the top left graph shows a voltage dip event while the top right graph shows that the dip is transient induced.

DANISENSE



**YOU ASKED FOR IT...WE
MADE IT!**

- 1000A rms
- 41,2mm Aperture
- Linearity better than 1ppm

www.danisense.com



DN1000ID

The IEC standard applies to single-phase and three-phase systems; therefore, the selected ADC must be able to sample the required number of voltage and current channels simultaneously. Having measurements for all the voltage and current channels on the instrument at the same time allows all parameters to be examined and immediately triggered when a power quality event occurs.

Digital Signal Processing (DSP)

Even though selecting the transducers and ADC for power quality measurements requires a comprehensive engineering effort, developing the algorithms for processing the raw ADC measurements is undoubtedly the task that demands most of the time and resources to make a power quality instrument. To implement a standard compliant instrument, the right DSP hardware must be chosen and the algorithms to calculate the power quality parameters from the waveform samples have to be developed and properly tested. The standard not only requires calculations but also different time dependent aggregations with time accuracies less than ± 1 seconds per 24-hour period for Class A and ± 5 seconds per 24-hour period for Class S. These algorithms must perform harmonic analysis. Additionally, power quality parameters rely on fast Fourier transform (FFT) analysis (harmonics, interharmonics, mains signaling voltage, unbalance), which are challenging to implement. The FFT analysis requires the waveforms to be sampled at 1024 samples per 200 ms (10 cycles) minimum. Performing resampling of the raw waveforms from the ADC to the required rate requires care to avoid harmonic distortion and aliasing.

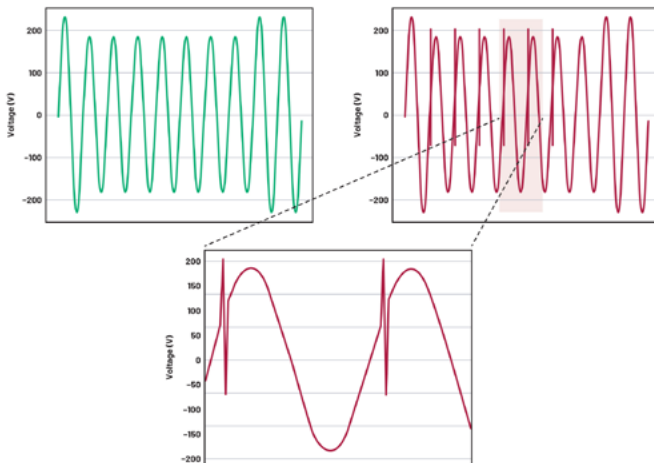


Figure 2: ADC sampling rate effect on power quality measures.

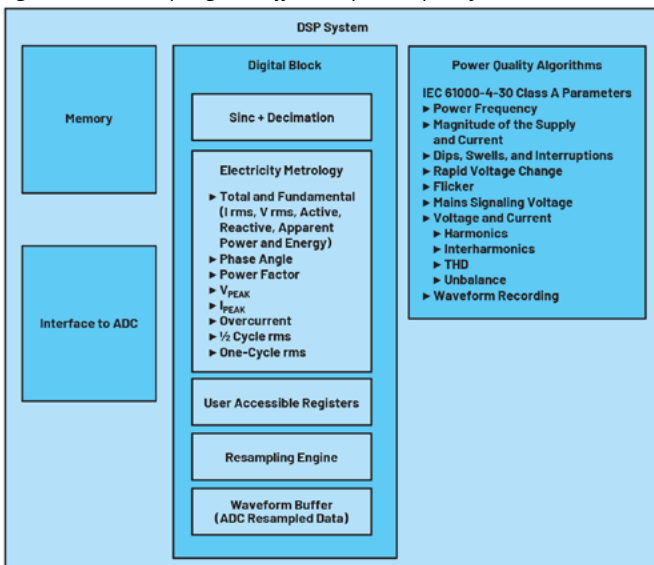


Figure 3: Block diagram: relevant functions of a DSP power quality system.

After the algorithms are developed, the IEC standard requires a comprehensive list of more than 400 tests that the instrument must pass to be fully certified. Figure 3 shows a block diagram with the most relevant functions a DSP system needs for producing power quality measurements.

Analog Devices Power Quality Measurements Solutions

Multichannel Simultaneous Sampling ADCs for IEC 61000-4-30 Class A

Considering the accuracy, number of channels, and sampling rate requirements to develop a Class A PQ instrument, the AD777x and AD7606x family of products are recommended for the ADC conversion of the signal chain/system. Note that these solutions provide just the raw digitized data from the input signals. A DSP system must be developed to get certified PQ measurements.

AD777x Family Sigma-Delta ADC

The AD777x is an 8-channel, 24-bit simultaneous sampling ADC family of devices. Eight full sigma-delta ($\Sigma\Delta$) ADCs are on-chip providing sampling rates of 16 kSPS/32 kSPS/128 kSPS. The AD777x provides a low input current to allow direct sensor connection. Each input channel has a programmable gain stage allowing gains of 1, 2, 4, and 8 to map lower amplitude sensor outputs into the full-scale ADC input range, maximizing the dynamic range of the signal chain. The AD777x accepts a VREF voltage from 1 V up to 3.6 V and analog input range: 0 V to 2.5 V or ± 1.25 V. The analog inputs can be configured to accept true differential, pseudo differential, or single-ended signals to match different sensor output configurations. A sample rate converter is provided to allow fine resolution control over the AD7770 and it can be used in applications where the ODR resolution is required to maintain coherency with 0.01 Hz changes in the line frequency. The AD777x also provides large signal input bandwidth 5 kHz (AD7771 10 kHz). A data output and SPI communications interfaces are provided although the SPI can also be configured to output the sigma-delta conversion data. The temperature range is from -40°C to $+105^{\circ}\text{C}$, functional up to $+125^{\circ}\text{C}$ with a power supply of 3.3 V or ± 1.65 V.

Figure 4 shows a 3-phase typical applications system diagram for the AD777x family of ADCs for a PQ instrument using current transformers as current transducers and resistor dividers for voltage.

AD7606x Family 16-/18-Bit ADC Data Acquisition System

The AD7606x provides a 16-/18-bit, simultaneous sampling, analog-to-digital data acquisition system (DAS) with eight channels. Each channel contains analog input clamp protection, a programmable gain amplifier (PGA), a low-pass filter, and a 16-/18-bit successive approximation register (SAR) ADC. The AD7606x also contains a flexible digital filter, low drift, 2.5 V precision reference and reference buffer to drive the ADC, and flexible parallel and serial interfaces.

The AD7606B operates from a single 5 V supply and accommodates ± 10 V, ± 5 V, and ± 2.5 V true bipolar input ranges when sampling at throughput rates of 800 kSPS (AD7606B)/1 MSPS (AD7606C) for all channels. The input clamp protection tolerates different voltages with user selectable analog input ranges (± 20 V, ± 12.5 V, ± 10 V, ± 5 V, and ± 2.5 V). The AD7606x requires a single 5 V analog supply. The single-supply operation, on-chip filtering, and high input impedance eliminate the need for external driver op amps, which require bipolar supplies.

In software mode, the following advanced features are available:

- Additional oversampling (OS) options, up to $\text{OS} \times 256$
- System gain, system offset, and system phase calibration per channel
- Analog input open circuit detector
- Diagnostic multiplexer
- Monitoring functions: SPI invalid read/write, cyclic redundancy check (CRC), overvoltage and undervoltage events, busy stuck monitor, and reset detection



Simplicity Powers Reliability

Maximize Power Conversion in Solar Applications

Our high-speed, high voltage current sensors help you achieve more reliable, and efficient power conversion in a smaller footprint

- Our sensors enable fast, and robust out of range detection and reporting – keeping your equipment, and people safe
- Improve the reliability of your solar application by choosing from the widest portfolio of 150°C rated current sensors.

Innovative current sensors and high voltage GaN drive solutions are smaller and easier to design-in – getting you to market faster

allegromicro.com/solar

INNOVATION WITH PURPOSE
 **ALLEGRO**
microsystems

Figure 4 shows a 3-phase typical applications system diagram for the AD7606x family of ADCs for a power quality instrument using current transformers as current transducers and resistor dividers for voltage.

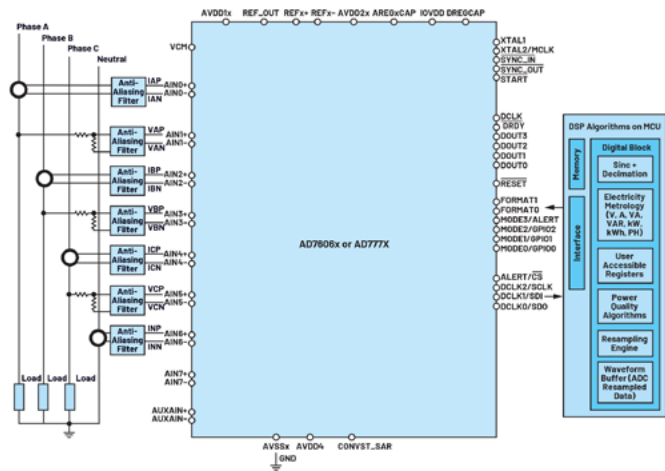


Figure 4: A power quality 3-phase applications system diagram for the AD777X and AD7606x families of ADCs.

Analog Devices Precertified IEC Class S Power Quality Solution

The ADE9430, a highly accurate, fully integrated, polyphase energy metering IC combined with the ADSW-PQ-CLS software library running on a host microcontroller, is a complete solution that is IEC 61000-4-30 Class S standard compliant. This integration significantly reduces the development time and costs for PQ monitoring products. The ADE9430 + ADSW-PQ-CLS solution simplifies the implementation and certification of energy and PQ monitoring systems by providing a tight integration of acquisition and calculation engines. Figure 5 shows a 3-phase applications system diagram for the ADE9430 + ADSW-PQ-CLS solution for a power quality instrument using current transformers as current transducers and resistor dividers for voltage.

ADE9430 Class S Power Quality Analog Front End

With seven input channels, the ADE9430 can be used on a 3-phase system or up to three single-phase systems. It supports current transformers (CTs) or Rogowski coils with an external analog integrator for current measurements. It provides an integrated analog front end for power quality monitoring and energy measurement. The ADE9430 is pin-compatible with the ADE9000 and ADE9078 with equivalent analog and metrology performance. Its features include:

- Seven high performance 24-bit sigma-delta ADCs
- 101 dB SNR
- Wide input voltage range: ±1 V, 707 mV rms, full-scale at gain = 1
- Differential inputs
- Class 0.2 accuracy metrology
- One cycle rms, line frequency, zero crossing, advanced metrology
- Waveform buffer
- Continuous resampled data: 1024 points per 10/12 line cycle
- Advanced metrology covering 50 Hz and 60 Hz fundamental frequencies
- Support of active energy standards: IEC 62053-21 and IEC 62053-22; EN 50470-3 OIML R46; and ANSI C12.20
- Support of reactive energy standards: IEC 62053-23, IEC 62053-24
- A high speed communication port: 20 MHz serial port interface (SPI)

ADSW-PQ-CLS Software Library

The ADSW-PQ-CLS software library is designed specifically to be integrated with the ADE9430 to generate standard compliant IEC 61000-4-30 Class S PQ measurements. It implements all parameters defined in IEC 61000-4-30 for Class S instruments. Users can decide which PQ parameters to use. This library needs low CPU/RAM resources and is core/OS agnostic (Arm® Cortex®-M mini-

Supported MCU architectures include Arm Cortex-M0, Cortex-M0+, Cortex-M1, Cortex-M3, and Cortex-M4. For distribution to end users, the library is provided as a CMSIS-PACK file (.pack) compatible with Keil Microvision, IAR Embedded Workbench version 8.x, or Analog Devices CrossCore® Embedded Studio. The license for software library is included with the purchase of the ADE9430. A PC serial command line interface (CLI) example is provided to evaluate the library and its features. Figure 6 shows how PQ parameters are displayed by this CLI.

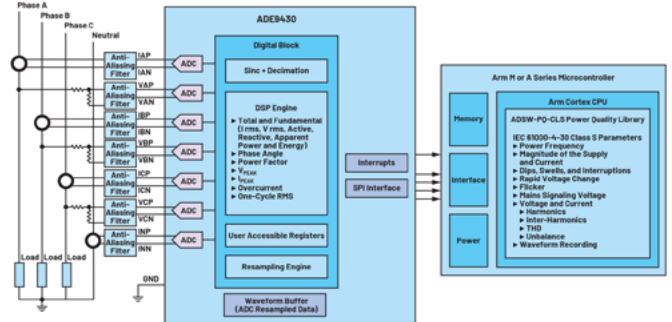


Figure 5: An ADE9430 and ADSW-PQ-CLS PQ 3-phase system diagram.

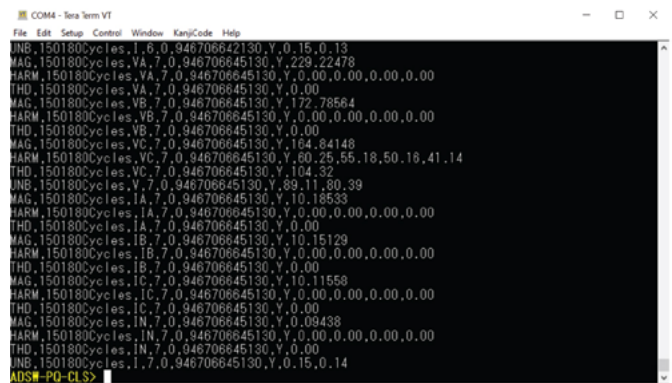


Figure 6: ADSW-PQ-CLS software library serial CLI interface.

ADE9xxx Family Power Quality Features Summary

Table 2: Energy and Power Quality features of the ADE9xxx Family of Energy Metering ICs; Class S Value Indicates Feature Is Standards Compliant with IEC 61000-4-30 Class S

Parameter	ADE9078 Utility Metering	ADE9000 Power Quality	ADE9430 + ADSW-PQ-CLS
Watt, Watt-hr	✓	✓	✓
I rms, V rms, VA, VA-hr	✓	✓	✓
Total VAR, VAR-hr	✓	✓	✓
Fundamental VAR, VAR-hr	✓	✓	✓
Power Factor	✓	✓	✓
Current Phase Angle	✓	✓	✓

POWER ELECTRONICS CAPACITORS



DC link capacitors ■ AC filter capacitors ■ Snubber capacitors ■ Energy storage capacitors



www.zez-silko.com



pcim
EUROPE
Hall 7, Stand 202



AN EVOLUTION IN POWER MAGNETICS

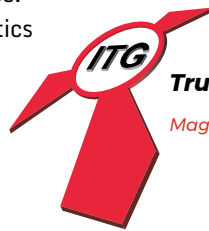
HIGH CURRENT, DENSITY, & POWER FOR EV POWER CONVERSION APPLICATIONS

The proper magnetics will help in improving vehicle efficiencies, offer lower losses and increase overall system and vehicle performance.

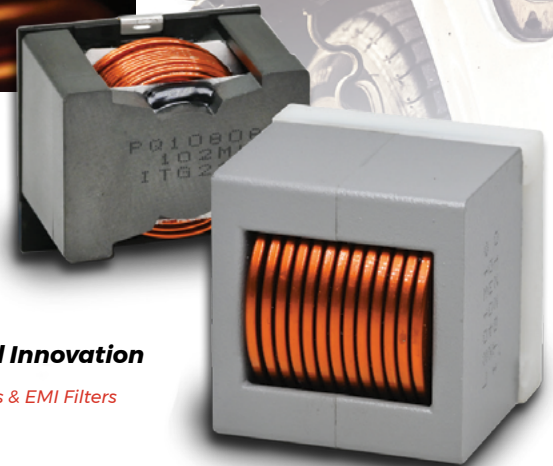
ITG offers a wide variety of high-current, low-power loss magnetics for the electronic vehicle industry. You'll get quick turnarounds, custom solutions, and one-on-one support from the industry's top, high-volume magnetics manufacturer.

www.ITG-Electronics.com

Engineering Electronics Partnership since 1963



Trusted Innovation
Magnetics & EMI Filters



Visit us from 09.05. – 11.05.23 in Nuremberg

pcim

EUROPE

booth 6-410

smtconnect

booth 4-341

PiNK[®]

Vacuum assisted, small scale sintering system SIN 20 For R&D and small series production



Target applications:

- Die attach on substrate and lead frame
- Attach of substrate to baseplate
- Die top sinterconnect
- High power LED attach

Customer benefits:

- Sintering of different layouts without changing the top tool
- Sintering of Cu substrates without oxidation
- Multilayer sintering
- Hermetically sealed, gas tight process chamber

Parameter	ADE9078 Utility Metering	ADE9000 Power Quality	ADE9430 + ADSW-PQ-CLS
Voltage Phase Angle	✓	✓	✓
Line Frequency-Three	✓	✓	Class S
Phase Sequence Detection	✓	✓	✓
1/2 Cycle rms	—	✓	—
1 Cycle rms	—	✓	Class S
10/12 Cycle rms	—	✓	Class S
150/180 Cycle rms	—	—	Class S
Dip/Swell	—	✓	Class S
Interruptions	—	—	Class S
Overcurrent	—	✓	✓
Fundamental Watt, Watt-hr, VA, VA-hr	—	✓	✓
Rapid Voltage Change	—	—	Class S
Over/Under Deviation	—	—	Class S
Flicker	—	—	Class S
Voltage/Current	—	—	Class S
Unbalance	—	—	Class S up to 40th
Voltage/Current Harmonics, Interharmonics	—	—	Class S up to 40th
ITHD, VTHD	—	✓	Class S

Parameter	ADE9078 Utility Metering	ADE9000 Power Quality	ADE9430 + ADSW-PQ-CLS
Mains Signaling Voltage	—	—	Class S (<3 kHz)
Fundamental I rms, V rms	—	✓	✓
Data Rate	16 kSPS/4 kSPS	32 kSPS/8 kSPS	32 kSPS/8 kSPS
Resampled Data	64 pts/cycle	128 pts/cycle	128 pts/cycle or 1024 pts/ (10/12 cycles)
Maximum SPI Frequency	10 MHz	20 MHz	20 MHz

ADE9430 Evaluation Kit

The EVAL-ADE9430ARDZ enables quick evaluation and prototyping of energy and Class S power quality measurement systems with the ADE9430 and the ADSW-PQ-CLS Power Quality Library. The power quality library and application example are provided to simplify implementation of larger systems. This kit provides a plug and play type of experience that is easy to use to test the power quality parameters of a 3-phase electrical system.

The kit has the following hardware features:

- ▶ Current transformer inputs
- ▶ High voltage/current inputs
- ▶ 240 V rms nominal (with potential divider)
- ▶ 80 A rms max (with provided CT sensors)
- ▶ 2.5 kV isolation
- ▶ On-board RTC to timestamp measurements
- ▶ Precertified for IEC 61000-4-30 Class S (requires user to calibrate)
- ▶ ADSW-PQ-CLS library and example application running on Arm Cortex-M4 MCU
- ▶ Serial CLI to PC for configuration and logging of power quality parameters

Figure 7 shows the connections required to use the EVAL-AD-E9430ARDZ with a PC.

The EVAL-ADE9430ARDZ consists of a PCB with four current and three voltages + neutral input connectors and on-board ADE9430, isolators, a real-time clock, a Cortex-M4 STM NUCLEO-413ZH development board with an example application of the ADSW-PQ-CLS library, and three current sensors.

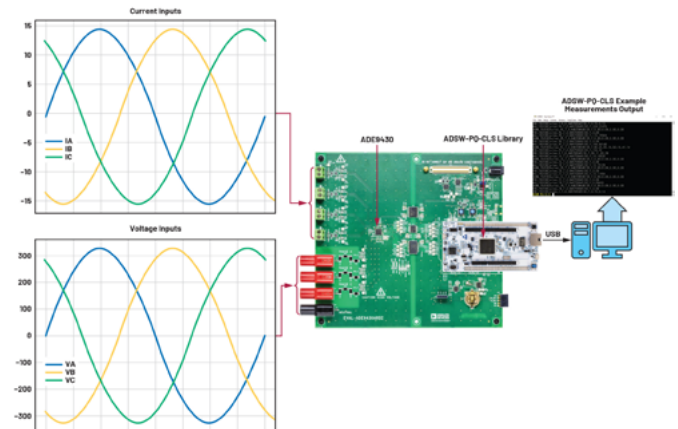


Figure 7: A diagram of the EVAL-ADE9430ARDZ connected to a PC.

Certification

The ADE9430 + ADSW-PQ-CLS solution has been certified to accurately measure power quality parameters following the requirements of the IEC 61000-4-30 Class S standard.

Conclusion

Designing a standards compliant power quality meter is a challenging task. To reduce the time and engineering resources needed to produce an IEC 61000-4-30 Class S standard compliant PQ measurement instrument, the ADE9430 + ADSW-PQ-CLS is a complete go-to solution that enables designers with a ready to use platform to accelerate development and solve for many critical design challenges.

Reference

- 1 “IEC 61000-4-30:2015: Electromagnetic Compatibility (EMC)-Part 4-30: Testing and Measurement Techniques-Power Quality Measurement Methods.” International Electrotechnical Commission, February 2015.



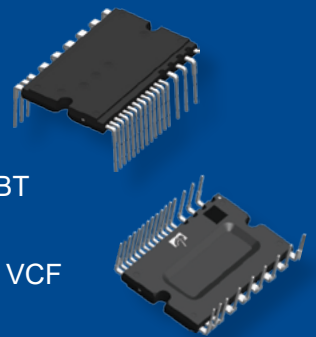
norwe.de | norwe.eu | norwe.com

Intelligent Power Modules IPM3 Series



600V 5A - 30A

- UL Recognized
- 650V Trench Shielded Planar Gate IGBT
- PFC-Diode Integrated (option)
- Full Protection: OT, VOT, UVLO, CSC, VCF
- Isolation Ratings of 2000Vrms/min



ALPHA & OMEGA
SEMICONDUCTOR

Visit us at:
Booth 9-521

pcim
EUROPE

Nuremberg, 9 – 11 May 2023

IPM3 series Intelligent Power Module, integrated AOS' latest TSPG-IGBT and super low Qrr FRD, offering high efficiency, low EMI, and ruggedness for inverter-driven air-conditioners, washing machines, dryers, and fan motors.

Powering a Greener Future™

www.aosmd.com

Mission Critical Power Electronics

Powerex is pleased to announce the expansion of their Steel City Power Module Medium Volume Processing Line located in Youngwood PA, USA.

By Ron Yurko, Chief Operating Officer, Powerex

Due to growing demand for mission critical products and the need to expand capacity and processing technology Powerex has contracted for a 50% expansion of our Class 10000 Clean Room where high-quality power modules are produced for demanding applications.



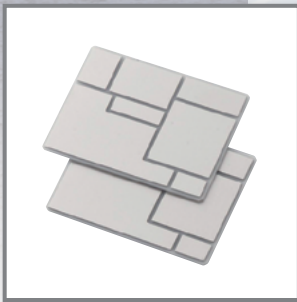
Powerex has proven capabilities and long-term experience to support demanding applications that require mission Critical Power Electronics. Powerex has realized High power density solutions with proven manufacturing methods in an automated clean room processing center named Steel City. The company is located 35 miles from Pittsburgh, Pennsylvania USA in what was once the largest Steel production location in the United States. Powerex Steel City offers a portfolio of power modules intended for power conversion solutions for extreme conditions, found in space, aviation, defense, traction and other mission critical industries. The expansive portfolio includes Rectifiers, Thyristors, Custom Modules, IGBTs, SiC Modules, Assemblies, & Gate drivers/DC-DC Converters. Their IGBT products meet rigid military standards. Powerex is an ITAR registered company with a USA-based manufacturing facility. Silicon IGBT and MOSFET and Silicon Carbide MOSFET Technology in Full SiC modules or Si/SiC hybrid solutions are made to exacting customer specifications as needed. Isolated diode and scr modules are produced in this automated packaging center. These hermetic and near hermetic plastic packaged semiconductors are designed to meet low stray inductance and provide high current carrying capability in SWaP solutions.

This expansion involves improved processing methods including Sintered Die attach technology for improved power cycling and durability and Ultrasonic Copper Bond of power terminals for long term reliability. For higher temperature applications and to utilize WBG junction temperature full capability the sintered die attach will be qualified. The demand for SWaP lightweight form factors for increased system Efficiency, due to low Switching and Conduction Losses of SiC. and options for elevated temperature capability and liquid cooling can be discussed with the design team. The smaller, lighter solutions allow for the downsizing of the inverter, saving costs. Rapid Prototyping equipment is used to accelerate design time and approval process at a lower cost which will allow a transition to automated mass production Powerex has found solutions to 15kV in Silicon Carbide. GaN based transistors (GaN on Silicon) devices to support 400v and 800v bus systems commonly used in today's electric vehicles requires state of the art packaging that Powerex designers perform in house for all mission critical applications.

www.pwr.com



Superior & Innovative Substrates and Baseplates for your Power Modules



AIN-AMB Substrates

Thin AIN-AMB substrates with lowest thermal resistance and cost efficiency in comparison to Si₃N₄ AMB substrates.



New

Almic with Integrated Fins

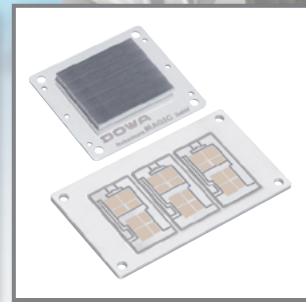
DAB substrates (Almic) with excellent reliability and PD properties in comparison to DBC or AMB substrates. Superior direct cooling by integration of fins.



New

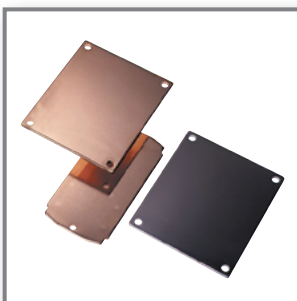
Almic with Integrated Terminals

Higher current and joining reliability by integration of terminals. Various thicknesses on front and back side for combination of power and logic.



Integrated Substrates

High innovative substrates, embedded in Al-baseplate or Al-heatsink, enabling >25% improved power capacity increase and >70% reduction in weight on module level.



Cu Baseplates

Balanced material combination for high thermal conductivity and minimized warpage for high reliability in comparison to conventional Cu baseplates (SE-Cu, SF-Cu).



New

Cu-Diamond Baseplates*

Innovative Cu-diamond composite baseplates with highest thermal conductivity of 1,000 W/mK for high power density applications.

*Co-Development with The Goodsystem Corp.

for generations

DOWA

DOWA HD Europe GmbH

info@dowa-europe.com

www.dowa-europe.com

Microcontroller with Smart Charge Logic Maximises Battery Cell Performance

Mascot introduces its next-generation lithium-ion battery charger for the 4040LI model. The 4040LI uses a 3-stage charging profile with a microcontroller to maximise battery performance. The charger is also capable of waking up deeply discharged batteries and to soft-start charging with low current until voltage is normalized.

This model is well suited for a wide variety of applications from medical to consumer. Owners of the 4040LI charger will enjoy optimised uptime and turnaround for battery-powered equipment such as medical devices, telecom, energy storage and power-assisted E-Mobility products. The 4040LI is medically certified according to EN 60601-1 ed. 3.2 and Home Healthcare EN



60601-1-11. It is also UL-approved and has 12 standard versions initially available for charging batteries from 3 cells (9.0A/12.6V) to 14 cells (2.0A/58.8V). Custom units are available upon request as well.

Alternative chargers that terminate the charge on reaching the battery's threshold voltage can shorten charging time but always leave some capacity unfilled. The 4040LI's 3-stage charging first restores the full 4.2V/cell battery voltage and then applies the saturation charge needed to fill up the battery completely. This ensures the longest possible battery run-time and charging finishes when the battery is full. The 4040LI also features a single 3-colour LED indicator light for charge, error- or standby status, and a wall-mount bracket is available.

www.mascot.no

Simulation Software for Power Electronics

Powersys announces the arrival of SIMBA, the new generation simulation software for power electronics. SIMBA is a simulation tool that delivers fast power converters design without compromising on accuracy. With SIMBA, users can develop advanced prototypes of Power Converters and Motor Drive, design controllers, perform

thermal and efficiency analysis, taking into account great optimization and reliability.

SIMBA's customized and high-performance power converter design capabilities provide versatility, empowering power electronics designers with the ability to accelerate their projects with precision and efficiency. Designed to be fully integrated into the customer's processes, SIMBA can be used in three ways: as a desktop application, using the Python API, or through a web browser (online version).

SIMBA is a perfect match for Powersys! With Powersys' 20-year extensive expertise in simulation software and a global community of experts spanning over two decades, it aligns seamlessly with SIMBA's innovative technology. SIMBA's solutions are tailored to address the challenges of today's power electronics landscape, offering unparalleled flexibility for extreme usage scenarios and remarkable automation.

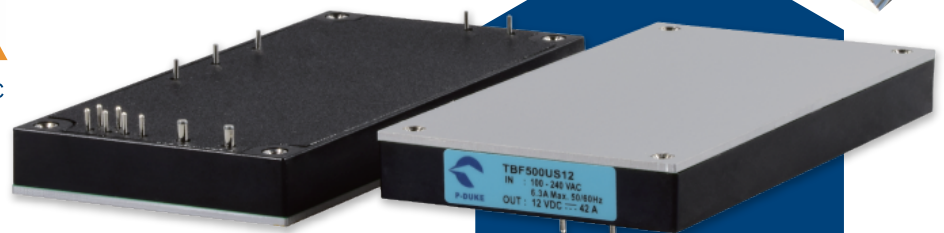
www.simba.io




TBF 500 Series

Full Brick AC-DC Power Supplies
Up to 500 Watts

- Universal Input Range From 85 To 264 Vac
- 12V,15V,24V,28V,48V,54V output
- Full Brick , Conduction Cooled
- Droop Current Sharing
- Applications :
 - 5G Telecomm
 - Factory Automation
 - Defense
 - ESS




 P-DUKE Technology Co., Ltd.
 E-mail: sales@pduke.com
 WEB: www.pduke.com



Charge Measurement Accuracy for Li-ion EV Batteries

To enable designers of Lithium-ion battery management systems (BMSs) in the automotive sector to maximise the autonomy range of electric vehicles (EVs), electrical measurement technology specialist LEM has launched its CAB 1500 current sensor for accurate battery charge level measurement. The CAB 1500 is the latest member of LEM's CAB series of automotive grade design sensors that use the properties of fluxgate transducer technology to deliver the high accuracy and low offset required for reliable coulomb counting – measuring the discharging current of Li-ion batteries to estimate their state of charge (SoC). The CAB series is renowned for compliance with the ISO 26262 functional safety standard (to automotive safety integrity level C) as well as easy application through a controller area network (CAN) interface offering 500 kbps.

Backed by LEM's 50 years' experience in developing electrical measurement solutions, the CAB 1500 open loop fluxgate sensor – equipped with electronic mechanisms and software that guarantee the



levels of reliability required by BMSs – can be busbar or panel mounted and combines resolution up to 0.1% with low offset and highest accuracy.

As well as offering an extended current range up to $\pm 1500A$ and compatibility with 800V applications to the IEC 60664-1 standard, the new sensor boasts non-intrusive measurement for full galvanic isolation up to 2.5kV. Other features include low power consumption VS shunt technology and 0.5% total error over temperatures from $-40^{\circ}C$ to $+85^{\circ}C$.

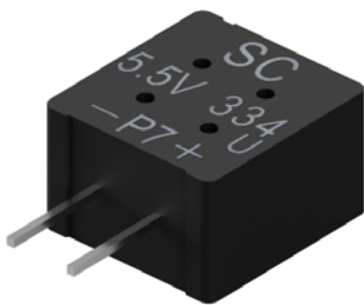
www.lem.com

105°C Supercapacitor for Automotive

KEMET announces its supercapacitor for automotive electronics, FMU Series. This series delivers 1,000 hours at $85^{\circ}C/85\%$ RH-rated voltage and operational temperature ranging from $-40^{\circ}C$ to $105^{\circ}C$. These supercapacitors are qualified to an automotive testing protocol. They are manufactured in an ISO TS 16949 certified plant and are subjected to PPAP/PSW and change control and are ideal for automotive applications needing a main power system backup during a power loss, such as ADAS, autonomous vehicles, and central gateway ECUs. Supercapacitors

are ideal for maintaining the main power system's real-time clock or volatile memory when it is removed, such as during a power failure or when the main power system's battery has been removed for replacement. Additionally, these supercapacitors offer power backup in equipment ranging from IoT devices, smart meters, medical devices, and industrial computing.

Using supercapacitors for automotive electronics enables freedom from the design limits imposed by finite battery lifetimes. The supercapacitor's benign open-circuit failure mode contrasts with typical short-circuit battery failures that may result in outgassing or ignition. Furthermore, supercapacitors are a cost-effective alternative to small backup batteries. Depending on the type of load and current demand, they can store enough energy to provide backup for durations ranging from a few seconds to several hours.

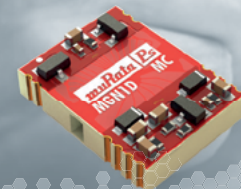


www.kemet.com

Experts on Design-In

Competence in electrified mobility

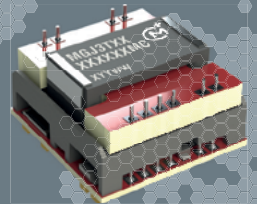
muRata
INNOVATOR IN ELECTRONICS



pcim
Booth 7-676
Hall 7

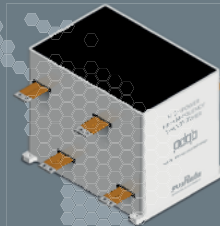
Isolated gate drive

- SiC and GaN
- Single & dual out
- Low coupling C



Multi gate drive

- Isolated SiC Drive
- Dual, Triple, Quad out
- 3W to 6W out



Charging transformer

- Small light weighted
- Low losses
- High frequency, 50kHz



SiC Dual test board

- Isolated data
- Isolated gate
- 400V or 800V bus

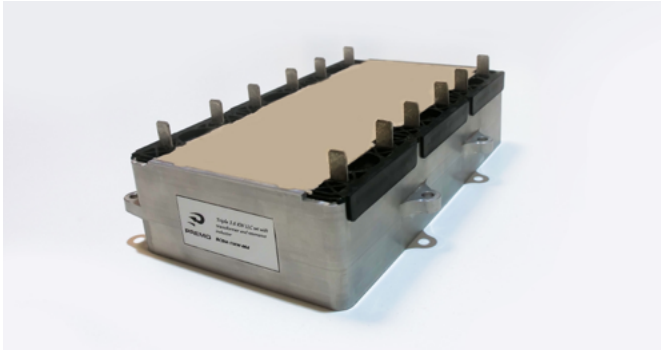


and visit us at Booth 7-676 May 09-11, Nuremberg, Germany

Angst+Pfister Sensors and Power Zurich | Munich
sensorsandpower.angst-pfister.com
sensorsandpower@angst-pfister.com

11 KW LLC Set with Combined Transformer and Resonance Inductor

Premo has developed an efficient triple 3.6 KW LLC (suited for 400V Input) set with transformer and resonance inductor specifically designed for on-board chargers capable of handling up to 11 kilowatts of power. The BCM-11KW-004 series is designed to minimize energy losses during the charging process, which helps to reduce the overall energy consumption of the charging system.



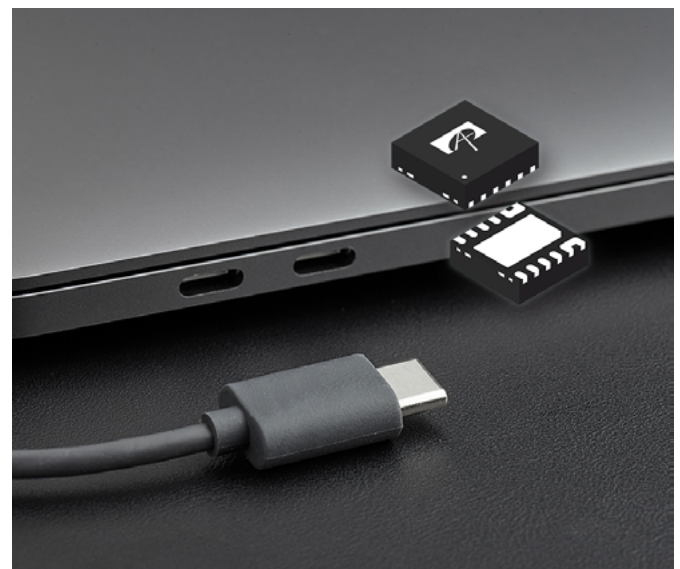
This can be particularly important for electric vehicles, where efficient use of energy can help to maximize the vehicle's range and minimize charging times.

The combined unit features a compact design, 158x98x38cm, and is lightweight, with only 1500g total weight and reduced volume, which makes it well-suited for use in electric vehicles on board chargers where space is at a premium. It is also designed to be highly durable and able to withstand the rigors of daily use in demanding environments. The usage of specific thermal conductive encapsulation material, like Coolmag™, improves the performance capability of the part. During manufacturing, the encapsulation process is made guaranteeing no bubbles or voids inside the part, removing the chances of thermal runaways or failures.

www.grupopremo.com

Protection Switches for Type C EPR 3.1

Alpha and Omega Semiconductor introduced a duo of sink and source switches that can increase the power delivery capability of USB Type-C ports to 140W, paving the way for Type C extended power range (EPR) implementations. The AOZ13937DI is suited for 28V Type C sinking applications while the AOZ15333DI is capable of Type C sourcing applications. These switches are suited for 28V Type C EPR implementations in high-performance laptops, personal computers, monitors, docking, and other applications. The AOZ13937DI features an ultra-low 20mOhm resistance with soft-start, overvoltage, ideal diode reverse-current, shortcircuit, over-current, over-temperature, and ESD and is designed to isolate and protect downstream components from abnormal VBUS voltage and current conditions. The ideal diode fast reverse current protection allows multiple power paths to be connected in parallel without interference. The AOZ15333DI companion source switch IC is capable of sourcing 5V @ 3A while blocking up to 28V. AOZ15333DI is UL 2367 and IEC 62368-1:2018 (3rd Edition) certified as a current limiting switch suited for Type C sourcing applications. The device is protected against numerous fault conditions such as VIN Overvoltage Protection (OVP), Startup Short circuit protection (SCP), Over-temperature (OTP) protection and has a programmable ILIMIT pin.



www.aosmd.com

Advertising Index

Allegro MicroSystems	79	ipTEST	17	Recom	12
Alpha & Omega	83	ITG Electronics	81	RFMW	71
Angst + Pfister	87	J&D Electronics	53	Ridley Engineering	41
CISSOID	73	LEM	5	ROHM	7
COMSOL	37	Magnetics	75	Semikron Danfoss	47
Cornell Dubilier	35	MERSEN	55	SIRIO ELETTRONICA	10
Danisense	77	Mitsubishi Electric	19	TAMURA	21
Dean Technology	61	MJC Elektrotechnik	8	Texas Instruments	39
DOWA	85	NORWE	83	TRACO POWER	17
ed-k	C2	opSens Solutions	15	University of Applied Sciences Kiel	67
Electronic Concepts	1 + 25	P-Duke	86	Vincotech	33
EPC	C4	Payton Planar	75	VisIC	59
Finepower	C3	PCIM Asia	43	VMI	21
Fuji Electric Europe	11	PCIM Europe	43	WIMA	63
GvA	23	PEM UK	27	Würth Elektronik eiSos	3
HIOKI	13	Pink	81	Xiamen Sanan IC	29
Hitachi	9	Plexim	31	ZEZ SILKO	81
Hitachi Energy	57	Powerex	69		
Infineon	49 + 65	Qorvo	51		

Invitation to PCIM May 9 –11, 2023

pcim
EUROPE



Finally, it`s time again!

The gates of the important trade fair for power electronics in Germany are opening and we will join!

The entire Finepower team is looking forward to welcome you personally. Since the trade fair management has changed the allocation of free visitor vouchers, unfortunately, we cannot provide you with a code at this point. The number of free codes has also been limited by Mesago, so please don't wait too long. To receive a personal voucher code, please send an email to: marketing_contact@finepower.com

If you need several codes, please indicate this in the mail.

All members of Finepower are looking forward seeing you again and to exciting discussions.

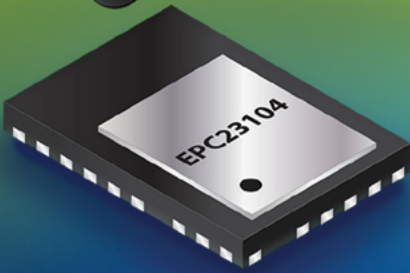
Your Finepower - Team



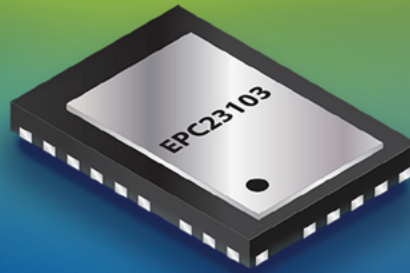
hall 9 / booth 321



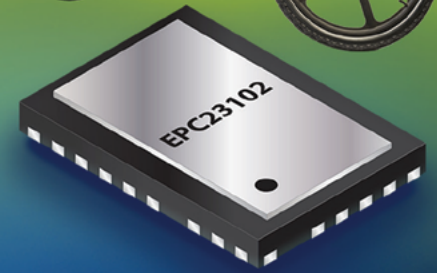
Integrated GaN Power for Every Application



EPC23104
15 A



EPC23103
25 A



EPC23102
35 A



AUTOMOTIVE



MOBILE



ROBOTICS



SERVER



SOLAR



SPACE



TELECOM

Integrated GaN Power

Higher Efficiency • Higher Power Density • Easier Design

ePower™ Stage ICs boost power density and simplify design across power budgets. Integrated devices are easier to design, save space on the PCB, and increase efficiency. Designers can use these devices to make lighter weight and more precise BLDC motor drives, higher efficiency 48 V input DC-DC converters, higher fidelity class-d audio systems, and other industrial and consumer applications.



Note:
Scan QR code to
learn more.
[Lead.me/GaNICSelect](https://www.epccorp.com/Lead.me/GaNICSelect)

pcim
EUROPE
Meet us in Hall 9
Stand 318

EPC 
EFFICIENT POWER CONVERSION

[epc-co.com](https://www.epccorp.com)